AD NUMBER

AD489752

LIMITATION CHANGES

TO:

Approved for public release; distribution is unlimited.

FROM:

**Distribution authorized to U.S. Gov't. agencies and their contractors;
Administrative/Operational Use; SEP 1966. Other requests shall be referred to Air Force Materials Lab., Wright-Patterson AFB, OH 45433.**

AUTHORITY

AFSC/IST USAF ltr 21 Mar 1989

AFML-TR-65-2
Part II, Volume X

TERNARY PHASE EQUILIBRIA IN TRANSITION METAL-BORON-CARBON-SILICON SYSTEMS

Part II. Ternary Systems

Volume X. The Zr-Si-C, Hf-Si-C, Zr-Si-B, and Hf-Si-B Systems

C. E. Brukl
Aerojet-General Corporation

TECHNICAL REPORT NO. AFML-TR-65-2, Part II, Volume X
September 1966

Air Force Materials Laboratory
Research and Technology Division
Air Force Systems Command
Wright-Patterson Air Force Base, Ohio

(6) TERNARY PHASE EQUILIBRIA IN TRANSITION METAL-BORON-CARBON-SILICON SYSTEMS.

Part II. Ternary Systems.

Volume X. The Zr-Si-C, Hf-Si-C, Zr-Si-B, and Hf-Si-B Systems.

(9) Technical rpt.

(10) C. E. Brukl

(11) Sep 62

(12) 15 p.

(15) AF [illegible] (617)-1041

(16) AF-[illegible]

(17) [illegible]

FOREWORD

The work described and illustrated in this report was performed at the Materials Research Laboratory, Aerojet-General Corporation, Sacramento, California, under USAF Contract No. AF 33(615)-1249. The contract was initiated under Project No. 7350, Task No. 735001. The work was administered under the direction of the Air Force Materials Laboratory, Research and Technology Division with Captain R. A. Peterson and Lt. P. J. Marchiando acting as Project Engineers, and Dr. E. Rudy, Aerojet-General Corporation, as Principal Investigator. Professor Dr. Hans Nowotny, University of Vienna, Austria, served as consultant to the project.

The project, which includes the experimental and theoretical investigation of selected refractory ternary systems in the system classes Me_1-Me_2-C, Me-B-C, Me_1-Me_2-B, Me-Si-B and Me-Si-C, was initiated on 1 January 1964.

The experimental program was laid out by E. Rudy, and the author wishes to acknowledge the assistance given by Dr. E. Rudy, D.P. Harmon, and J. Hoffman. R. Cobb, J. Pomodoro, and R. Taylor were of valuable assistance in the preparation of the experimental work.

Chemical analyses of the alloys were carried out under the supervision of Mr. W. E. Trahan, Metals and Plastics Chemical Testing Laboratory, Aerojet-General Corporation. The writers also wish to thank Mr. R. Cristoni, who prepared the many drawings, and Mrs. J. Weidner who typed the report.

The manuscript of this report was released by the author February 1966 for publication as an RTD Technical Report.

Other reports issued under USAF Contract AF 33(615)-1249 have included:

Part I. Related Binaries

Volume I.	Mo-C System
Volume II.	Ti-C and Zr-C Systems
Volume III.	Mo-B and W-B Systems
Volume IV.	Hf-C System
Volume V.	Ta-C System. Partial Investigations in the systems V-C and Nb-C
Volume VI.	W-C System. Supplemental Information on the Mo-C System
Volume VII.	Ti-B System
Volume VIII.	Zr-B System
Volume IX.	Hf-B System
Volume X.	V-B, Nb-B, and Ta-B Systems

Part II. Ternary Systems

Volume I.	Ta-Hf-C System
Volume II.	Ti-Ta-C System
Volume III.	Zr-Ta-C System
Volume IV.	Ti-Zr-C, Ti-Hf-C, and Zr-Hf-C Systems
Volume V.	Ti-Hf-B System

FOREWORD (Cont'd)

Volume VI. Zr-Hf-B System
Volume VII. Ti-Si-C, Nb-Si-C and W-Si-C Systems
Volume VIII. Ta-W-C System
Volume IX. Zr-W-B System, Pseudobinary System TaB_2-HfB_2

Part III. Special Experimental Techniques

Volume I. High Temperature Differential Thermal Analysis

Part IV. Thermochemical Calculations

Volume I. Thermodynamic Properties of Group IV, V, and VI Transition Metal Carbides
Volume II. Thermodynamic Interpretation of Ternary Phase Diagrams.

This technical report has been reviewed and is approved.

W.G. RAMKE
Chief, Ceramics and Graphite Branch
Metals and Ceramics Division
Air Force Materials Laboratory

ABSTRACT

Phase equilibria and mutual solubilities in the Zr-Si-C, Hf-Si-C, and Hf-Si-B ternary systems have been determined at 1300°C. The general melting behavior and high temperature mutual solubilities in the Zr-Si-C, Hf-Si-C, Zr-Si-B, and Hf-Si-B systems have been studied; minimum melting temperatures along various pseudo-binary sections are given. All four systems are characterized by the formation of a ternary $D8_8$-Nowotny phase.

Most melting temperatures in the ternary systems are governed by the lower melting binary silicide compounds. Guidelines for feasible high temperature applications are given.

TABLE OF CONTENTS

		PAGE
I.	INTRODUCTION AND SUMMARY	1
	A. Introduction	1
	B. Summary	3
	1. Binary Silicide Systems	3
	2. Ternary Silicocarbide Systems	3
	3. Ternary Silicoboride Systems	5
II.	LITERATURE REVIEW	6
	A. Binary Systems	6
	1. The Zirconium-Carbon System	6
	2. The Hafnium-Carbon System	9
	3. The Silicon-Carbon System	10
	4. The Zirconium-Boron System	12
	5. The Hafnium-Boron System	14
	6. The Silicon-Boron System	16
	7. The Zirconium-Silicon System	18
	8. The Hafnium-Silicon System	21
	B. Ternary Systems	24
	. The Zirconium-Silicon-Carbon System	24
	2. The Hafnium-Silicon-Carbon System	26
	3. The Zirconium-Silicon-Boron System	26
	4. The Hafnium-Silicon-Boron System	27
III.	EXPERIMENTAL PROGRAM	27
	A. Experimental Procedures	27
	1. Starting Materials	27

TABLE OF CONTENTS (Cont'd)

PAGE

2. Alloy Preparation and Heat Treatment 31

3. Melting Point Determinations 33

4. X-ray Analysis 33

5. Chemical Analysis 34

6. Metallography 35

B. Experimental Results 36

1. The Zirconium-Silicon-Carbon System 36

2. The Hafnium-Silicon-Carbon System 50

3. The Zirconium-Silicon-Boron System 65

4. The Hafnium-Silicon-Boron System 73

IV. DISCUSSION 89

References 92

LIST OF ILLUSTRATIONS

FIGURE		PAGE
1.	Zr-C: Constitution Diagram	7
2.	Zr-C: Lattice Parameters of the Monocarbide Phase	8
3.	Hf-C: Constitution Diagram	10
4.	Si-C: Possible Constitution Diagram	11
5.	Zr-B: Constitution Diagram	13
6.	Hf-B: Constitution Diagram	15
7.	Si-B: Hypothetical Constitution Diagram	17
8.	Zr-Si: Constitution Diagram	20
9.	Hf-Si: Hypothetical Constitution Diagram	23
10.	Zr-Si-C: Schematic Section	24
11.	Zr-Si-C: Phase Equilibria near Central Region of the Zr-Si Binary	25
12.	Zr-Si-B: Section at 1400°C	26
13.	Zr-Si-C: Location and Qualitative X-ray Analysis of 1300°C Samples	37
14.	Zr-Si-C: Section at 1300°C	38
15.	Zr-Si-C: Location of Melting Point Samples	42
16.	Zr-Si-C: 90/7/3, Arc Melted	43
17.	Zr-Si-C: 94/3/3, Arc Melted	43
18.	Zr-Si-C: 56/33/11, Quenched from 2400°C	44
19.	Zr-Si-C: 30/65/5, Quenched from 1555°C	46
20.	Zr-Si-C: 20/60/20, Quenched from 1571°C	46
21.	Zr-Si-C: 40/50/10, Quenched from 1750°C	47
22.	Zr-Si-C: 54/2/44, Quenched from 2800°C	47
23.	Zr-Si-C: 63/2/35, Quenched from 3300°C	48

LIST OF ILLUSTRATIONS (Cont'd)

FIGURE		PAGE
24.	Hf-Si-C: Location and Qualitative X-ray Analysis of 1300°C Samples	50
25.	Hf-Si-C: Section at 1300°C	52
26.	Hf-Si-C: Location of Melting Point Samples	54
27.	Hf-Si: 15/85, Quenched from 1340°C	55
28.	Hf-Si: 10/90, Quenched from 1340°C	56
29.	Hf-Si: 90/10, Quenched from 1830°C	57
30.	Hf-Si-C: 90/5/5, Quenched from 1908°C	58
31.	Hf-Si-C: 54/27/19, Quenched from > 2600°C	59
32.	Hf-Si-C: 59/3/38, Quenched from 3581°C	59
33.	Hf-Si-C: 62/3/35, Quenched from 3302°C	60
34.	Zr-Si-B: Location of Melting Point Samples	65
35.	Zr-Si-B: 60/10/30, Arc Melted	66
36.	Zr-Si-B: 72/13/15, Arc Melted	67
37.	Zr-Si-B: 54/31/15, Arc Melted	68
38.	Zr-Si-B: 31/67/2, Quenched from 1630°C	69
39.	Zr-Si-B: 9/73/18, Quenched from 1374°C	70
40.	Zr-Si-B: 3/90/7, Quenched from 1374°C	71
41.	Zr-Si-B: 36/4/60, Quenched from 2847°C	72
42.	Zr-Si-B: 31/1/68, Quenched from 3012°C	72
43.	Hf-Si-B: Location and Qualitative X-ray Analysis of 1300°C Samples	76
44.	Hf-Si-B: Section at 1300°C	77
45.	Hf-Si-B: Location of Melting Point Samples	80
46.	Hf-Si-B: 67/20/13, Arc Melted	80

LIST OF ILLUSTRATIONS (Cont'd)

FIGURE		PAGE
47.	Hf-Si-B: 87/3/10, Arc Melted	81
48.	Hf-Si-B: 54/6/40, Arc Melted	81
49.	Hf-Si-B: 52/28/20, Arc Melted	82
50.	Hf-Si-B: 52/28/20, Arc Melted	83
51.	Hf-Si-B: 3/91/6, Quenched from 1400°C	84
52.	Hf-Si-B: 30/68/2, Quenched from 1571°C	85
53.	Hf-Si-B: 34/5/61, Quenched from 2800°C	86

LIST OF TABLES

TABLE		PAGE
1.	Lattice Parameters and Crystal Structures of Intermediate Zr-B Compounds	14
2.	Lattice Parameters and Crystal Structures of Intermediate Hf-B Compounds	16
3.	Lattice Parameters and Crystal Structures of Intermediate Si-B Compounds	18
4.	Lattice Parameters and Crystal Structures of Intermediate Zr-Si Compounds	21
5.	Lattice Parameters and Crystal Structures of Intermediate Hf-Si Compounds	23
6.	Heats of Formation of Binary Zirconium Silicides	25
7.	Heat Treatment Conditions for Solid State Samples	32
8.	Lattice Parameters of the Zr-Si-C $D8_8$ Phase	39
9.	Minimum Melting Temperatures of Various Pseudo-binary Sections in the Zr-Si-C System	48
10.	Melting Temperatures, Melting Behavior and Qualitative X-ray Analysis of Zr-Si-C Alloys	49
11.	Lattice Parameters of the Cubic HfC_{1-x} Phase in Both Silicon-Containing and Silicon-Free Alloys	60
12.	Minimum Melting Temperatures of Various Pseudo-binary Sections in the Hf-Si-C System	61
13.	Melting Temperatures, Melting Behavior, and Qualitative X-ray Analysis of Hf-Si-C Alloys	62
14.	Minimum Melting Temperatures of Various Pseudo-binary Sections in the Zr-Si-B System	73
15.	Melting Temperatures, Melting Behavior, and Qualitative X-ray Analysis of Zr-Si-B Alloys	74
16.	Lattice Parameters of the Hf-Si-B $D8_8$ Phase	76
17.	Lattice Parameters of Binary Hf-Si and Hf-B Phases Measured in Binary and Ternary Alloys.	78

LIST OF TABLES (Cont'd)

TABLE		PAGE
18.	Minimum Melting Temperatures of Various Pseudo-binary Sections in the Hf-Si-B System	86
19.	Melting Temperatures, Melting Behavior, and Qualitative X-ray Analysis of Hf-Si-B Alloys	87

I. INTRODUCTION AND SUMMARY

A. INTRODUCTION

It has been known for quite a while that the silicides of some of the refractory metals of the IVa-VIa periodic group possess rather good oxidation resistant properties; in addition, it has been proven that some of the borides of this same refractory metal group, in particular zirconium and hafnium diboride, also have high temperature oxidation resistant properties. The refractory carbides, and borides are known to have very high hardnesses in addition to their extremely high melting points. These properties along with those of the refractory silicides, strongly suggest the possibility of the use of such composite materials in high temperature oxidizing environments. Application feasibility of such silicoboride and silicocarbide combinations requires the basic knowledge of possible phase interactions and phase equilibria of individual refractory silicoboride and silicocarbide ternary systems.

In continuing our basic research on the high temperature interactions and phase equilibria of refractory borides, carbides, silicides, and their various combinations; the silicocarbide and silicoboride systems of zirconium and hafnium have been investigated.

In recent times, a great deal of new knowledge concerning the structures and phases present in the Hf-Si and Zr-Si systems has been published; however, in spite of the fact that so much is known about the individual phases and structures of these silicide systems, no new recent work has been undertaken to confirm some of the older investigations and to accurately investigate the exact characteristics of these two silicide systems.

The state of knowledge of the binary Si-C and Si-B systems is virtually at the same level as the above mentioned two refractory metal silicide systems. Fortunately, the Si-C binary system is the least complicated of all in the number of occurring phases, when the multitude of crystal structure

variations of SiC are disregarded; however, the general constitution of the Si-C system along with the nonvariant reactions involved is still uncertain, for there have been conflicting data published. Not even the exact number of intermediate phases occurring in the Si-B system is known; a hypothetical constitution diagram has been published, but it is evident a great deal of additional experimental work is necessary to firm up knowledge of this system.

It is unfortunate that such great holes are present in the knowledge concerning the binary systems of primary importance in the interpretation of the high temperature constitution of the refractory silicoboride and silicocarbide ternary systems. Complete clarification and description of the high temperature characteristics of these ternary systems is not possible without recourse to known features of the respective binary systems. It was therefore necessary to restrict these investigations to solid state studies and general interpretations of the melting behavior of these ternary systems and to merely report the interphase melting temperatures, which are in themselves a valuable contribution to the high temperature characteristics needed for choice and selection feasibility of these high temperature refractory silicoboride and silicocarbides. Differential thermal analytical techniques could not be employed in studies on these silicon and silicide containing ternary systems due to the lack of any adequate DTA sample-container materials for these extremely reactive silicides. Solid state as well as liquid-solid reactions of the silicon-containing alloys with the DTA sample containers would thoroughly mask the reactions of the sample itself and would seriously hamper the possibility of success in interpreting the results of appropriate DTA experiments. With the advent of newer and better techniques, the container problem for high temperature DTA experiments with reactive materials will be solved.

When the exact constitution of the binary Zr-Si, Hf-Si, Si-C, and Si-B systems is known, detailed high temperature reactions and equilibria present in these silicocarbide and silicoboride systems will be able to be fully interpreted.

B. SUMMARY

1. Binary Silicide Systems

a. The Zirconium-Silicon System

Partial investigations on sintered as well as on melted samples in the Zr-Si system confirmed the presence of the following crystal structures: Zr_2Si, Zr_3Si_2, ZrSi, and $ZrSi_2$; it was also confirmed that the $D8_8$ hexagonal phase previously reported at the concentration "Zr_5Si_3" does not exist[1] in the binary Zr-Si system. Traces of a recently reported phase[2] in the vicinity of 43 At% Si were observed; no evidence of a Zr_4Si[3] or Zr_3Si[4] was found in sintered samples. Only exceeding small traces of the Zr_6Si_5[5] phase with the CrB-type structure were observed.

b. The Hafnium-Silicon-System

Partial investigations of this binary system confirmed the presence of the following crystal structures: Hf_2Si, Hf_3Si_2, HfSi, and $HfSi_2$. Only traces of a recently reported[2] phase near 43 At.% Si were observed; the $D8_8$ structure does not occur in the Hf-Si binary in samples sintered at 1300°C. There is a eutectic between $HfSi_2$ and Si at about 9 At.% hafnium; the eutectic temperature is about 1330°C. Another eutectic, between Hf_2Si and β-Hf, is located between 12 and 16 At.% silicon; this eutectic temperature is 1806°C.

2. Ternary Silicocarbide Systems

a. The Zirconium-Silicon-Carbon System

A ternary phase with $D8_8$ structure is present at a composition of $Zr_{61}Si_{36}C_3$. At 1300°C the following main two-phase equilibria exist (Figure 14): $ZrSi_2$-SiC, ZrSi-SiC, ZrSi-ZrC_{1-x}, $D8_8$(ternary)-ZrC_{1-x}, Zr_2Si-ZrC_{1-x}, and ZrC_{1-x}-SiC. There is virtually no mutual solubility between the silicides and carbides. At a temperature between 1300° and about

1570°C, the ZrSi-SiC equilibria is replaced by a $ZrSi_2$-ZrC_{1-x} two-phase field.

A phase having the CrB-type crystal structure was found in varying amounts in melted ternary alloys; it is suspected that this phase does not exist as a true binary zirconium silicide phase.

At higher temperatures the ternary $D8_8$ phase increases to homogeneous range to encompass the following composition range: Zr: 56-65, Si: 32-37, C: 0.3-8 At.%. The highest observed melting point of the $D8_8$ phase, which melts with a rather broad maximum, is 2385°C.

The melting temperatures of ternary Zr-Si-C alloys are governed in general by the melting points of the lower melting silicides (Table 9). Ternary alloys containing silicon carbide showed extremely heterogeneous melting behavior owing to the decomposition of SiC.

b. The Hafnium-Silicon-Carbon System.

A ternary $D8_8$ phase at the composition Hf_5Si_3C is found in this system. At higher temperatures it increases its homogeneous range to encompass the following region: Hf: 62-55, Si:33-37, C: 3-11 At.%. This phase melts with a broad maximum; the highest melting temperature observed for this phase was 2467°C. The main equilibria present at 1300°C (see Figure 25) are: $HfSi_2$-SiC, HfSi -HfC_{1-x}, HfSi-HfC_{1-x}, HfSi-$D8_8$ (ternary), $D8_8$ (ternary)-HfC_{1-x}, Hf_2Si-HfC_{1-x}, and HfC_{1-x}-SiC.

There is virtually no mutual solubility of silicides and carbides at 1300°C or at higher temperatures in this system.

A ternary eutectic consisting of Hf_2Si, β-Hf, and HfC_{1-x} is present in the metal-rich portion of the ternary system; the eutectic temperature is probably quite close to the Hf-Si binary eutectic temperature of 1806°C.

Again, the lower melting points of the silicides govern the general melting behavior (Table 12) of the ternary Hf-Si-C system.

3. Ternary Silicoboride Systems

a. The Zirconium-Silicon-Boron System

The basic equilibrium at 1400°C as described in a previous publication[6] (Figure 12) also exists at higher temperatures. A ternary eutectic consisting of β-Zr, Zr_2Si, and ZrB_2 exists in the metal-rich portion of the ternary system; the eutectic temperature is about 1536°C. There are also eutectics between ZrB_2 and silicon as well as between ZrB_2 and the ternary $D8_8$ phase; the ternary $D8_8$ phase showed a maximum melting point of 2343°C; this phase expands its homogeneous region to encompass the following range at temperatures close to melting: Zr: 63-55, Si: 30-38, B: 5-11 At.%. The presence of a phase with the CrB-type crystal structure was observed in melted ternary alloys lying in the vicinity of the Zr-Si binary; as in the Zr-Si-C system it is suspected that this phase is a stabilized ternary crystal structure. Zirconium silicides and borides have practically no mutual solubility at high temperatures.

As is apparently the rule in the carbide and boride containing ternary silicide systems, the melting behavior of ternary alloys in the Zr-Si-B system is governed by the lower melting behavior of the binary silicides (Table 14).

b. The Hafnium-Silicon-Boron System

At 1300°C the most stable phase in this system, HfB_2, forms two-phase equilibria with all other binary phases (Figure 44), including a ternary $D8_8$ phase which is formed in a small homogeneous region near the composition $Hf_{52}Si_{38}B_{10}$. At 1300°C as well as at temperatures near melting, there is practically no mutual solubilities between hafnium silicides and hafnium borides.

There is a ternary eutectic formed among β-Hf, Hf_2Si, and HfB in the metal-rich portion of the ternary system. There are also eutectics formed between HfB_2 and silicon as well as between HfB_2 and $D8_8$ (ternary). The ternary $D8_8$ phase increases its homogeneous range moderately at temperatures near melting to encompass the following region: Hf: 60-67, Si:32-37, B: 6-13 At.%; the highest melting point observed for the $D8_8$ phase was 2425°C. The melting temperatures of ternary Hf-Si-B alloys are governed by the lower melting silicides (Table 18).

II. LITERATURE REVIEW

A. BINARY SYSTEMS

1. The Zirconium-Carbon System

As part of the general theme of the investigation of ternary refractory alloy systems, the binary zirconium-carbon system was studied in this laboratory[7] to provide a valid starting point for the ternary investigations.

A listing of the many older papers is found in Kieffer and Benesovsky's Hartstoffe[8].

Preliminary investigations in this laboratory agreed quite well with the results of recent study of the zirconium-carbon system by R. Sara, et al.[9,10].

Figure 1 shows the zirconium-carbon system which resulted from the investigation in the laboratory[7]. The α-β-Zr transformation temperature in the two-phase region, $Zr-ZrC_{1-x}$, was found to be approximately 885°C [10] and 875°C [7]; a peritectoid decomposition of the α-phase is most likely to occur in view of the results obtained in the Ti-C and Hf-C systems[7,11].

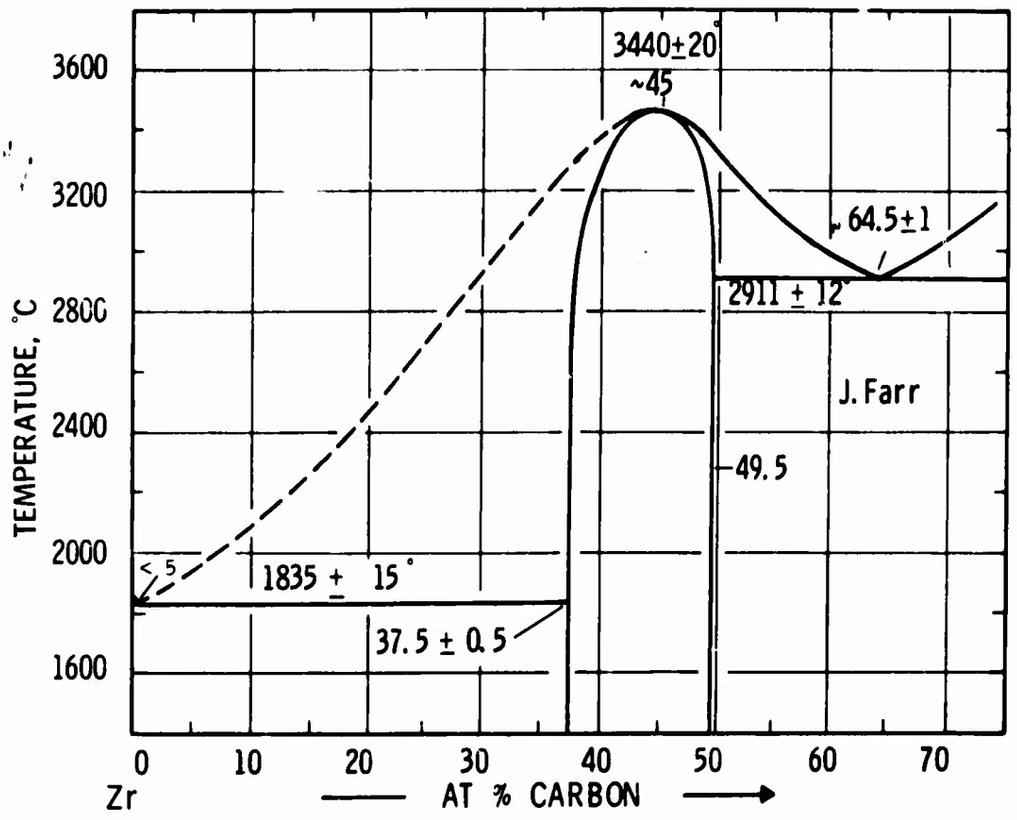

Figure 1. Zr-C: Constitution Diagram
(E. Rudy, D.P. Harmon, and C.E. Brukl, 1965).

The monocarbide phase, (f.c.c.-NaCl type structure[12]) is found to have an extended range of homogeneity. The most recent determinations of the limits are: (lower): 35.4 At.% C[13,14], 38.5 At.% C[10], and 37.5 At.% C[7]; (upper): in each case the upper limit was defined as 49.4 At.% C using the value determined by J. Farr[13,14]. Figure 2 gives a lattice parameter plot of samples quenched from above 2800°C[7]; the anomalous maximum has also been observed by Sara[10] in alloys heat-treated at high-temperatures (3300°C).

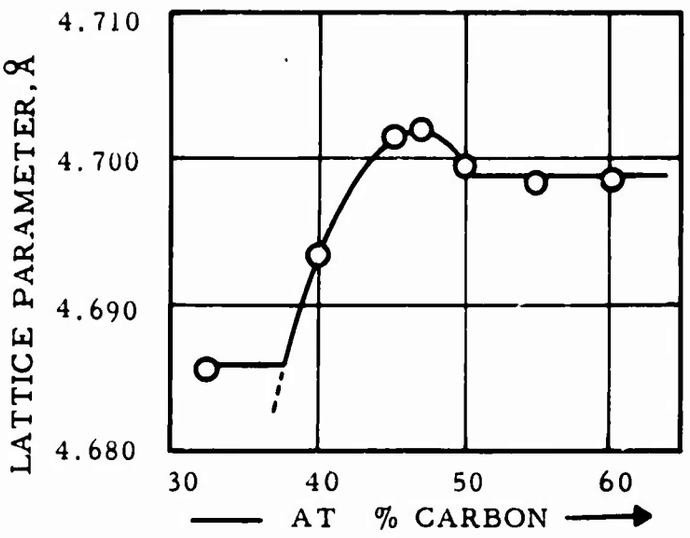

Figure 2. Zr-C: Lattice Parameters of the Monocarbide Phase. (E. Rudy, D.P. Harmon, and C.E. Brukl, 1965).

The monocarbide phase melts congruently at a sub-stoichiometric composition of approximately 45-46 At.% carbon[7,10,13,14], and at a temperature of 3400 - 3440°C[7,10,13,14].

The eutectic temperature between the metal and monocarbide has been indicated to be 1830°C[15], 1810°C[13,14], 1860°C[10], and 1835°C[7]; Sara[10] locates the eutectic composition at approximately 1 At.% carbon.

For the ZrC-C eutectic temperature, literature values are 2850°C[10], 2850 ± 50°C[13,14], 2911 ± 12°C[7], and 2920 ± 50°C[17]; the eutectic is located at a carbon concentration of approximately 65 atomic percent[7,10].

2. The Hafnium-Carbon System

Similar to the occurrences in the Ti-C and Zr-C binary systems, only a single intermediate phase, HfC_{1-x}, is formed in the Hf-C system; however, unlike the other two group-IVa metal-carbon systems, the α-Hf phase is stabilized to much higher temperatures and carbon concentrations by incorporating carbon atoms into interstitial lattice sites[18]. The α-Hf phase decomposes peritectically into HfC_{1-x} and liquid at 2360°C and forms a eutectic with the β-Hf phase at 2180°C at approximately 1.5 At.% carbon[11].

The monocarbide phase (NaCl) type structure[19] has a homogeneity range between 34 At.% C (a = 4.608 Å)[11] and 49.5 At.% C (a = 4.640 Å)[11] at the peritectic and eutectic temperatures respectively. The lower boundary is strongly temperature dependent below the peritectic isotherm[11,20]. At 1500°C the boundary is located at a carbon concentration of 37.5 atomic percent[15]. As early as 1930, the HfC_{1-x} phase was reported to have an extremely high melting point. Agte and H. Alterthum[16] found that the phase melted at 3890°C. Subsequent measurements have resulted in values 3895°C[18], 3830°C[20] and 3928°C[11] for the melting point of HfC_{1-x}; the melting point maximum is located at approximately 48.5 At.% carbon[11].

The eutectic between the monocarbide phase and carbon is located at a carbon concentration of 65-66 atomic percent; the eutectic temperature has been measured on several occasions; the following values have been published: 2800°C[18], 2915°C[21], 3150°C[20], 3180°C[11], and 3260°C[17].

Figure 3 presents the constitution diagram as determined by investigations in this laboratory[11].

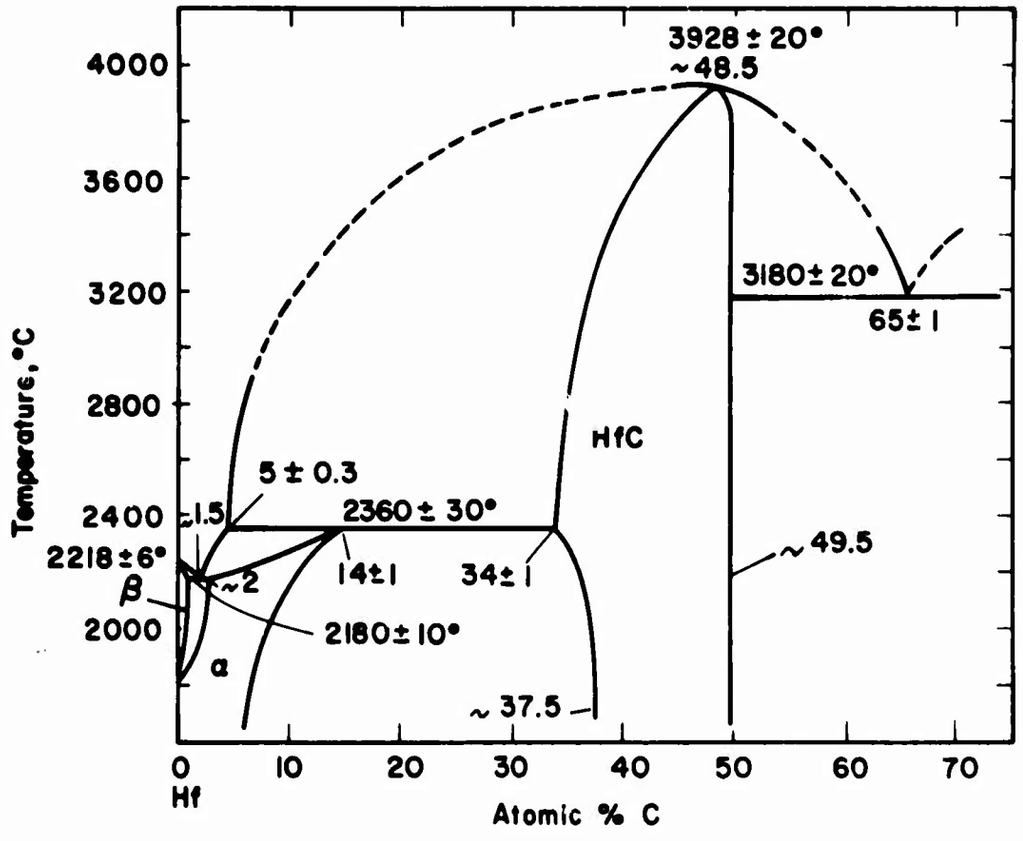

Figure 3. Hf-C: Constitution Diagram.
(E. Rudy, 1965)

3. The Silicon-Carbon System

In spite of the fact that silicon monocarbide is the basis of many commercial abrasive items by virtue of its high hardness, as well as being used in many high temperature applications, the constitution diagram of the silicon carbon system has never been completely established.

Many different, but closely related, crystal polymorphs of SiC, (apparently the only intermediate compound observed in this system) have been observed, isolated, and their crystal structures determined[22]. The so called α-forms have either hexagonal or rhombohedral symmetry, and the various polymorphs are based on different atom stacking sequences[23].

A lengthy listing of the many works is given in Constitution of Binary Alloys[22]. A face-centered cubic form, the β-SiC (B3-type), a low temperature modification with a lattice parameter of 4.349 Å has also been observed[23].

H. Nowotny and co-workers[24] performed exploratory investigations in the silicon-carbon system using X-ray, chemical, and thermal analyses. On the basis of these experiments, two possible phase diagrams for the silicon-carbon systems were developed. Figure 4 presents the version containing peritectic-similar reaction involving liquid silicon (with carbon in solution), solid SiC, and vapor. The other version proposes a

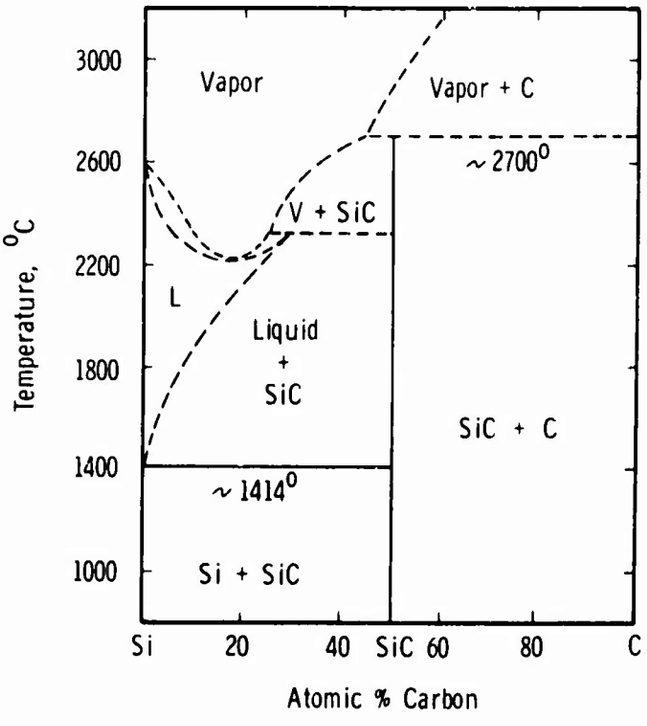

Figure 4. Si-C: Possible Constitution Diagram.
(H. Nowotny, et al., 1954)

eutectic-similar decomposition of liquid silicon (with carbon in solution) into solid SiC and vapor. Due to the small temperature difference between the melting point of pure silicon and silicon-carbon alloys lying between Si and SiC, it was not possible to determine whether a eutectic or peritectic reaction

is present at lower temperatures. Both proposed diagrams display the decomposition of SiC into graphite and vapor at about 2700°C. The decomposition temperature of SiC has also been independently reported by O. Ruff[25].

Recently, R. Scarce and G. Slack[26] as well as R. Dolloff[27] have investigated the silicon-carbon system and have concluded that SiC decomposes peritectically into liquid Si and graphite. There is, however, a vast discrepancy in the reported peritectic decomposition temperatures. Scarce[26] reports 2830°C while Dolloff[27] reports 2540°C; the latter author further reports that silicon and SiC form a eutectic at .75 At.% C and 1402°C. It seems quite apparent that the exact constitution of the silicon-carbon-diagram — excluding the many crystallographic modifications of SiC — is not known, and additional investigations are indeed necessary.

4. The Zirconium-Boron System

There have been numerous investigations in the zirconium-boron system, and many of the results have been conflicting. Recent work in this laboratory[28] confirm some of the earlier published results.

Two phases are present in the zirconium-boron system: ZrB_2 and ZrB_{12}. Zirconium diboride crystallizes in a hexagonal C 32 type structure[29,30] and has a very narrow homogeneous range[30,31]. The reported melting temperatures of the diboride phase are 3040°C[32] and 2990 ± 50°C[33]. More recent determinations by F. Glaser and co-workers[34,35] are difficult to assess since no experimental details on the techniques used were given.

ZrB_{12}, a high temperature phase, has a face-centered cubic, D2f, UB_2-type structure[36,37], is unstable at temperatures below about 1600°C[34], and melts congruently at 2680°C[34,38]. Post and Glaser[34,36,37] as well as Schedler[38] have reported the existence of a face-centered cubic ZrB phase. Other investigations[30,31,39], however, have proven that this phase does not exist in the true binary system but is apparently stabilized by small quantities of carbon, oxygen, and nitrogen.

For other details and information concerning the preparation of zirconium borides, the excellent compilation in Hartstoffe[40] should be consulted.

A complete investigation of the Zr-B system was undertaken at this laboratory[28]. Figure 5 portrays the results of these studies.

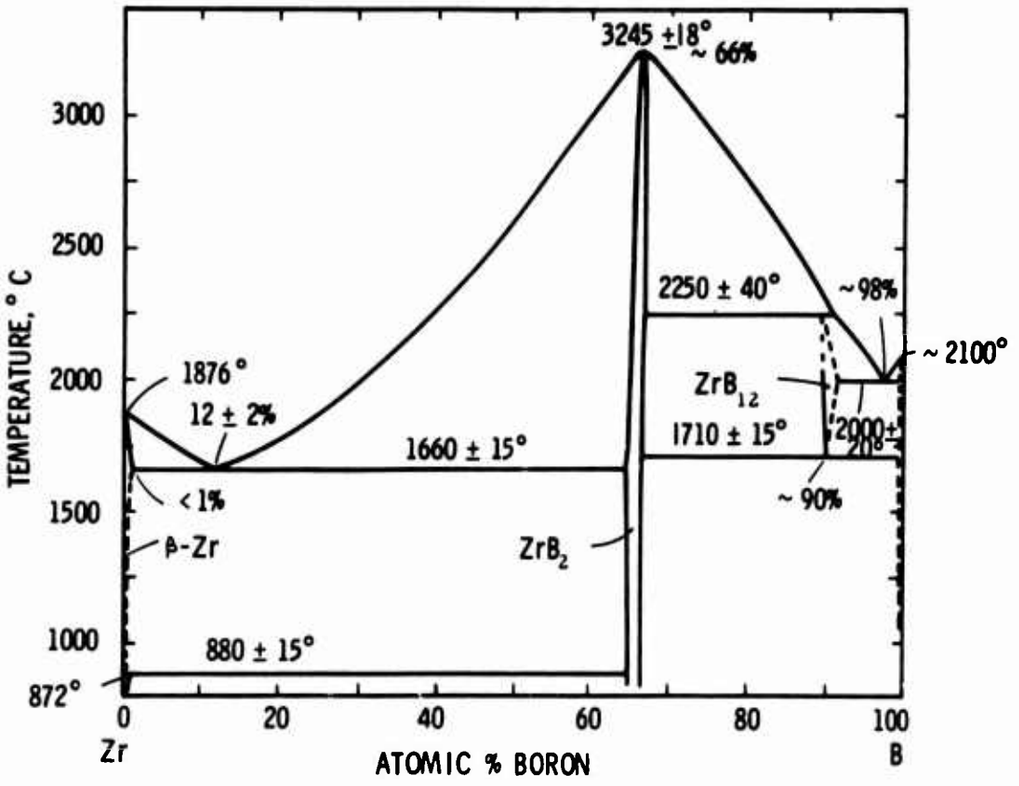

Figure 5. Zr-B: Constitution Diagram.
(E. Rudy and St. Windisch, 1965)

The solubility of boron in zirconium is less than 1 At.%; the temperature of the eutectic formed between zirconium and ZrB_2 is 1660°C; this eutectic is located at about 12 At.% B. Zirconium diboride has a narrow homogeneous range and melts at 3245°C. ZrB_{12} melts peritectically at 2250°C and

decomposes in a eutectoid reaction into ZrB_2 and boron at 1710°C. A eutectic, whose temperature is 2000°C, is formed between ZrB_{12} and B at about 98 At.% B.

Table 1 lists the intermediate phases present in the Zr-B system along with their crystal structures and lattice parameters.

Table 1. Lattice Parameters and Crystal Structures of Intermediate Zr-B Compounds.

Phase	Crystal Structure	Lattice Parameter	Literature
ZrB_2	hexagonal, C-32 type	a = 3.169 Å c = 3.530 Å	30
ZrB_{12}	cubic, UB_{12}-type ($D2_f$)	7.408 Å	28

5. The Hafnium-Boron System

Two intermediate phases are formed in the Hf-B system. HfB_2, which crystallizes in a hexagonal lattice structure, has a negligible homogeneous range and has been reported to melt in the temperature range 3060°-3240°C[32, 41-43].

Early investigations[41] indicated that a monoboride with a face-centered cubic structure was formed in the Hf-B system. However, it was later shown by E. Rudy and F. Benesovsky[44] that the true structure of the monoboride is an orthorhombic B-27 type; the formation of the monoboride in the face-centered cubic structure is attributed to impurities such as carbon, nitrogen, and oxygen.

Proposed phase diagrams[45, 46] for the Hf-B system have been based mainly on estimates. A recent publication by Kaufman and

Clougherty[47] has reported a Hf-HfB eutectic temperature of 1960°C as well as a peritectic decomposition temperature of greater than 2400°C for HfB. (48 For earlier details, including the preparation of hafnium borides, Hartstoffe by Kieffer and Benesovsky should be consulted. A complete investigation of the hafnium-boron system was carried out in this laboratory[49]. The results are depicted in Figure 6. The solubility of boron in β-hafnium is less than

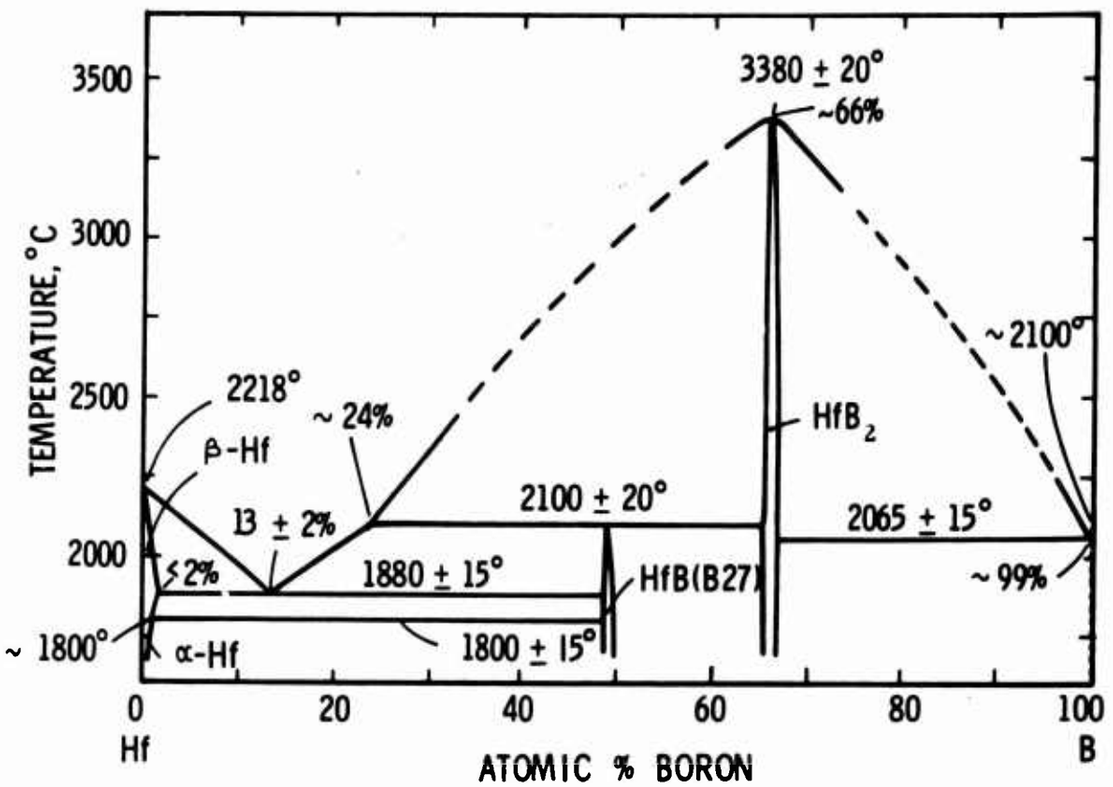

Figure 6. Hf-B: Constitution Diagram.
(E. Rudy and St. Windisch, 1966)

2 At.% B; the eutectic, whose temperatures is 1880°C, formed between HfB and β-Hf lies at about 13 At.%.

HfB, with an orthorhombic unit cell, decomposes peritectically into melt and HfB_2 at 2100°C. HfB_2 melts congruently at 3380°C and forms a eutectic with boron at about 99 At.% B. The eutectic temperature is 2065°C.

Table 2 gives the intermediate phases and crystal structures of the Hf-B compounds.

Table 2. Lattice Parameters and Crystal Structures of Intermediate Hf-B Compounds.

Phase	Crystal Structure	Lattice Parameters	Literature
HfB_2	hexagonal (C-32 type)	a = 3.142 Å c = 3.477 Å	49
HfB	orthorhombic (B-27 type)	a = 6.51_7 Å b = 3.21_8 Å c = 4.92_0 Å	49

6. The Silicon-Boron System

This system has not yet been completely investigated; in fact, there are a great deal of discrepancies concerning whether or not there are intermetallic phases present, and if so, what their compositions and structures are. It is quite evident that a considerable amount of work is still needed to clarify the silicon-boron system.

As early as 1900, H. Moissan[50] reported the finding of the compounds SiB_3 and SiB_6. G. V. Samsonov[51] was to have found a SiB_3, while recently, J. Adamsky[52] and C. Cline[53] have reported finding a SiB_6 possessing an orthorhombic unit cell. C. Cline[54], E. Colton[55], V. Matkovish[56], H. Rizzo[57], and C. Brosset[58] have published data on a new silicon boride, SiB_4, which is isomorphous with B_4C. L. Brewer[59] et al. reports, however, that no evidence of intermediate silicoborides was found.

C. Brosset[58] has determined that a eutectic minimum exists at 7.4 At.% B and 1403°C; the solubility of boron in silicon[60] is

2.9 At.% at 1300°C, 1.45 At.% at 1200°C, and 1.25 At.% at 1100°C, while the solubility of silicon in boron[61] is approximately 9.7 At.% at 1750°C.

Recently, G.V. Samsonov and V. Sleptsov[62] have investigated the silicon-boron system using metallographic, X-ray, and thermal analysis techniques. With their results and other previous literature, they have established a hypothetical phase diagram of the silicon-boron system; this diagram is reproduced in Figure 7.

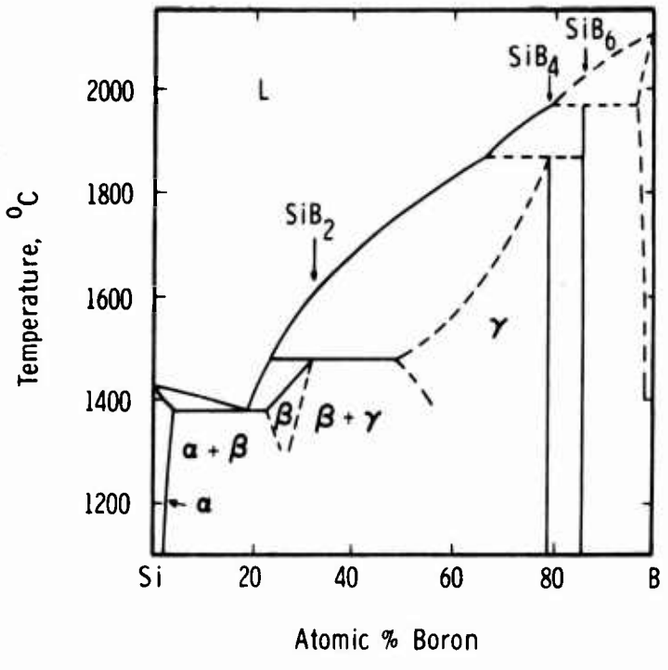

Figure 7. Si-B: Hypothetical Constitution Diagram.
(G.V. Samsonov and V. Sleptsov,1962)

In the diagram by the Russian authors, three intermediate compounds, Si_2B, SiB_4, and SiB_6 are indicated. Si_2B forms peritectically at about 1450°C from melt and SiB_{4-x}. SiB_4 also forms peritectically from SiB_6 and melts at about 1830°C; SiB_4 possesses a wide homogeneous range at lower temperatures. SiB_6 forms peritectically at about 1950°C and is essentially a line compound.

Table 3 lists the intermediate phases and the crystal structures of the silicon-boron system.

Table 3. Lattice Parameters and Crystal Structures of Intermediate Si-B Compounds

Phase	Crystal Structure	Lattice Parameters in Angstroms	Literature
SiB_4	rhombohedral (B_4C-type)	a = 6.319 Å c = 12.713 Å	58
SiB_6	orthorhombic	a = 14.39 Å b = 18.27 Å c = 9.88 Å	53
Si_2B	unknown	-	62

In spite of the numerous, recent investigations in the silicon-boron system — these are listed in detail in a new compilation by R. Elliott[63] — it is seen that many discrepancies are still present in the silicon-boron constitution diagram, and additional investigations are still necessary.

7. The Zirconium-Silicon System

In view of past investigations as well as in the light of more recent ones, it may be said that the zirconium-silicon system belongs to the most complicated refractory-metal silicide systems. The majority of the existing discrepancies have been clarified, but some points need considerable additional clarification. There is no doubt about the existence of the phases $ZrSi_2$ and Zr_2Si. The crystal structure of $ZrSi_2$ was first determined in 1928 by Seyfarth[64] and later also investigated by Naray-Szabo[65], Brauer[66,67], and Nowotny[68]. H. Nowotny, et al.[69], P. Pietrokowsky[70], and L. Brewer[71] all determined that Zr_2Si has the tetragonal $CuAl_2$ structure type.

C. E. Lundin, D.J. McPherson, and M. Hansen[3] were the first ones to undertake a complete investigation of the Zr-Si system. These authors listed the following phases as being present: Zr_4Si, Zr_2Si, Zr_3Si_2, Zr_4Si_3, Zr_6Si_5, ZrSi, and $ZrSi_2$. Of these phases, ZrSi was described[3] as having a hexagonal unit cell with a = 12.772 Å and c = 7.005 Å. C. Lundin, et al.[3] also presented a constitution diagram for the Zr-Si System.

In a later investigation of the phases occurring in the Zr-Si-system, H. Nowotny and co-workers[69] found no evidence of the Zr_6Si_5, Zr_4Si_3, and Zr_3Si_2 phases, but were able to identify a Zr_5Si_3 phase with the $D8_8$ structure; the hexagonal indexing of the ZrSi phase was not confirmed. In a later work[68] the ZrSi phase was found to have the orthorhombic FeB type structure. Kieffer, Benesovsky, and Machenschalk[72] investigated the zirconium-silicon system by means of melting point determinations, metallography, and X-ray analysis; they constructed a temporary constitution diagram. The phases Zr_2Si, Zr_5Si_3, ZrSi and $ZrSi_2$ were found.

In renewed investigations of the Zr-Si system, with and without carbon additions, H. Nowotny[1] and co-workers as well as L.Brewer[73] were able to show that the phase previously denoted as Zr_5Si_3 is in reality a ternary $D8_8$ phase, Zr_5Si_3 (C), stabilized by carbon, oxygen, nitrogen, and boron. Furthermore, Brewer and Krikorian[73] state that the phase designated by C. Lundin[3] as Zr_3Si_2 corresponds to the Zr_5Si_3phase, and the Zr_4Si_3 is the Zr_3Si_2 phase which, after Pietrokowsky[74] has the U_3Si_2 type structure. C. H. Dauben[75] later reported that Zr_3Si_2 was isostructural with U_3Si_2. H. Nowotny[1] further confirmed the existence of the Zr_6Si_5 phase[3] and designated it U-II because of its unknown structure and in exact composition; by the same token, another phase which seemed to be at about 40 At.% silicon was designated U-I.

This was the state of the knowledge of the Zr-Si system until the year 1961 when again Nowotny and co-workers[5], in conjunction with work on the Zr-Si-Al system, were able to show that the U-II phase (Zr_6Si_5) was a CrB-structure-type monosilicide which always occurred at zirconium concentrations of somewhat less than 50 At.% Si, i.e. $Zr_{\sim 6}Si_{\sim 5}$. These authors

were further able to confirm the findings of Brewer[73] and Dauben[75] that Zr_3Si_2 is isostructural with U_3Si_2; this Zr_3Si_2 phase is however; not the previously described[1] U-I phase. This U-I phase[1-2] has a σ-similar structure and is isostructural with other unknown phases in the Ti-Si and Hf-Si systems.

Recently, K. Schubert[4] reported finding a Zr_3Si with the Ti_3P type structure; this reported phase has not yet been confirmed, but may be identical to the rather evasive Zr_4Si[3].

The solubility of silicon in zirconium was determined by M. Hansen and co-workers[3]: α-zirconium dissolves a maximum of approximately 0.3 At.% Si whereas β-zirconium dissolves about 0.6 At.% Si.

A constitution diagram (Figure 8) of the Zr-Si system, taken from Hartstoffe[76], shows the basic diagram of C. Lundin et al.[3] modified with some of the more recent findings; the new σ-similar phase[1,2] near 40 At.% Si as well as Schubert's[4] Zr_3Si phase are not depicted. Table 4 contains the established phases and crystal structures of the Zr-Si intermediate phases.

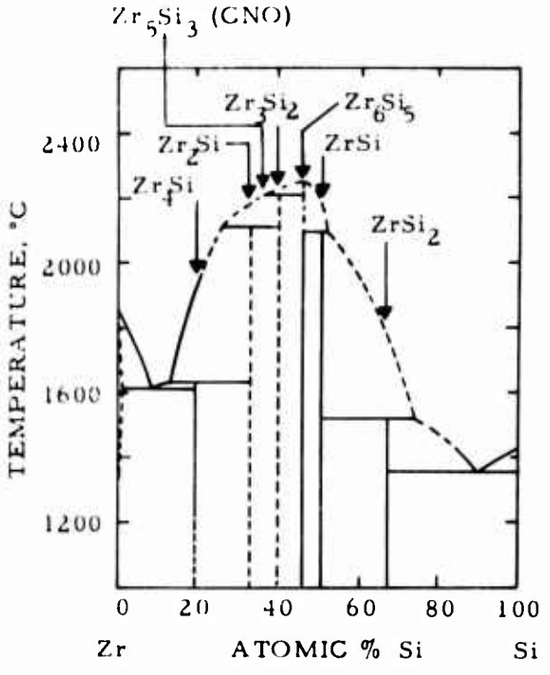

Figure 8. Zr-Si: Constitution Diagram.

(C.E. Lundin, D.J. McPherson, and M. Hansen, 1953 - Modified by R. Kieffer, 1963).

Table 4. Lattice Parameters and Crystal Structures of Intermediate Zr-Si Compounds

Phase	Crystal Structure	Lattice Parameters in Ångstrom	Literature
$ZrSi_2$	orthorhombic C49 type	a = 3.72 Å b = 14.76 Å c = 3.67 Å	68
ZrSi	orthorhombic B-27 (FeB type)	a = 6.98 Å b = 3.78$_6$ Å c = 5.30$_2$ Å	68
$Zr_{\sim 6}Si_{\sim 5}$	orthorhombic B_f (CrB-type)	a = 3.76$_2$ Å b = 9.91$_2$ Å c = 3.75$_3$ Å	5
$Zr_{\sim 3}Si_{\sim 2}$	unknown, but σ-similar	-	2
Zr_3Si_2	tetragonal (U_3Si_2 type)	a = 7.082 Å c = 3.715 Å	
Zr_2Si	tetragonal C 16 ($CuAl_2$ type)	a = 6.6120 Å c = 5.45 Å	70
Zr_3Si	tegragonal DO_e (Ti_3P-type)	a = 11.01 Å c = 5.45 Å	4
Zr_4Si	unknown	-	3

8. The Hafnium-Silicon System

Of all the silicide systems of the refractory metals of the IVa-IVa groups, the hafnium-silicon system has received the least attention; the system has not yet been completely investigated, although the majority of the occurring compounds have been characterized. B. Post,

F. Glaser, and D. Moskowitz[77] found two silicides, $HfSi_2$ and HfSi. $HfSi_2$ has an orthorhombic unit cell; Smith and Bailey[78] determined the exact atomic parameters and found $HfSi_2$ to be isostructural with the analogous zirconium silicide. By analogy, also, B. Post, et al.[77] stated that HfSi crystallizes in a hexagonal structure. It has subsequently been shown, however, by H. Nowotny and co-workers[79] that HfSi has an orthorhombic-FeB type structure. H. Nowotny[79] also prepared and identified the compound Hf_2Si. This compound has the $CuAl_2$-type structure and is isostructural with the zirconium silicon compound. H. Nowotny[79] found traces of a possible Hf_4Si phase, but could not identify the suspected phase more closely. The compound $Hf_5Si_3(C)(B)$ has also been found[79] and characterized as having the $D8_8$-Mn_5Si_3 structure. In strong analogy to the $Zr_5Si_3(C)(B)$ phase it is suspected[79,80] that the $D8_8$ phase is really a stabilized ternary phase and would not be found in the true binary system.

In 1961, H. Nowotny[5] and co-workers discovered two more phases in the Hf-Si system; one of these, Hf_3Si_2 has the tetragonal U_3Si_2 structure while the other phase, lying near 43 At.% Si, was described as having a σ-type similar structure; this phase is isostructural with the other unknown phases in the Ti-Si and Zr-Si systems.

Nowotny, Braun, and Benesovsky[45] presented a hypothetical phase diagram of the hafnium-silicon system based on melting point determinations and analogies with the Zr-Si system. This temporary diagram (Figure 9) does not include the more recent findings concerning the probable absence of the Hf_5Si_3 phase, the presence of the Hf_3Si_2, and the existence of the σ-similar phase .

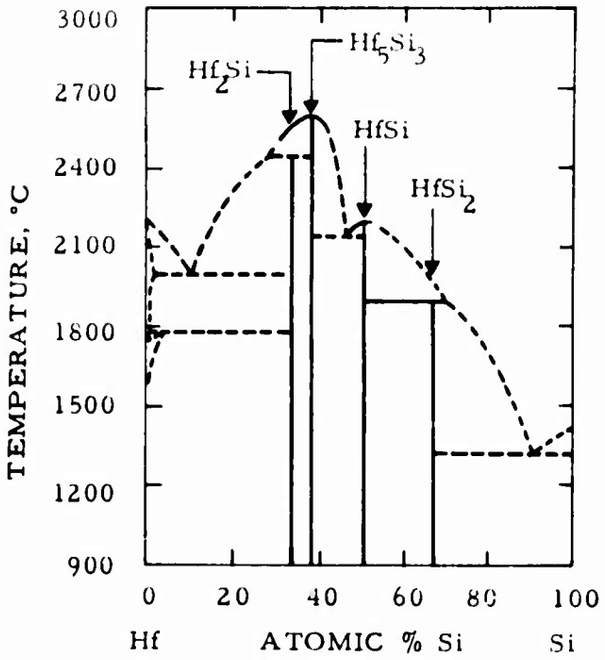

Figure 9. Hf-Si: Hypothetical Constitution Diagram.
(H. Nowotny, H.Braun, and F.Benesovsky, 1960)

Table 5. Lattice Parameters and Crystal Structures of Intermediate Hf-Si Compounds

Phase	Crystal Structure	Lattice Parameters in Angstroms	Literature
Hf_2Si	tetragonal $CuAl_2$-type (C-16)	a = 6.48 Å c = 5.21 Å	79
Hf_5Si_3	hexagonal Mn_5Si_3 type ($D8_8$)	a = 7.89_0 Å c = 5.55_8 Å	79
Hf_3Si_2	tetragonal U_3Si_2 type	a = 7.00_0 Å c = 3.67_1 Å	
$Hf_{\sim 3}Si_{\sim 2}$	unknown, but σ-similar	-	5, 2
HfSi	orthorhombic FeB type (B-27)	a = 6.85_5 Å b = 3.75_3 Å c = 5.19_1 Å	79
$HfSi_2$	orthorhombic $ZrSi_2$ type	a = 3.677 Å b = 14.550 Å c = 3.649 Å	78

B. TERNARY SYSTEMS

1. The Zirconium-Silicon-Carbon System

Cursory investigations were performed by L. Brewer and O. Krikorian[71]. They observed the formation of a ternary $D8_8$-type phase in the region near the Zr-Si side near 40 At.% Si; they indicated, however, that the ternary phase was an extension into the ternary field of the Zr_5Si_3 binary phase observed by C. Lundin[3], et al., although they suspected that the Zr_5Si_3 was not a true binary phase. A schematic diagram (Figure 10) of the phase relationships in the Zr-Si-C system was presented by L. Brewer[71] along with the calculated heats of formation of some silicides (Table 6).

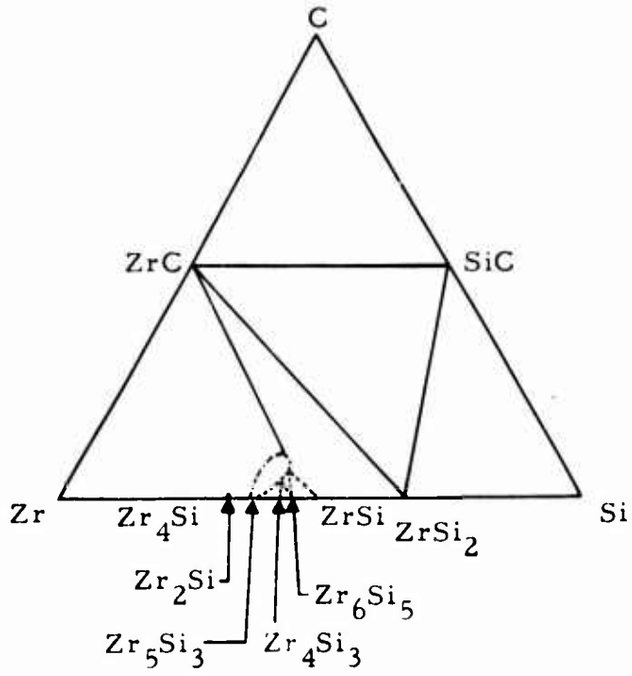

Figure 10. Zr-Si-C: Schematic Section .
(L. Brewer and O. Krikorian, 1954)

Table 6. Heats of Formation of Binary Zirconium Silicides

Phase	ΔH°_{298} of Formation per gram-at. Si in Kcal
$ZrSi_2$	-21 ± 5
ZrSi	-39 ± 10
Zr_6Si_5	-43 ± 10
Zr_4Si_3	-45 ± 10
Zr_5Si_3	-48 ± 10
Zr_2Si	-50 ± 10
Zr_4Si	-53 ± 10

Later, H. Nowotny, B. Lux, and H. Kudielka[1], were able to conclusively show that the Zr_5Si_3 phase observed by C. Lundin[3] and L. Brewer[71] is actually a ternary phase stabilized by small amounts of either carbon, boron, nitrogen, or oxygen. Nowotny[1] and co-workers investigated the central portion of the Zr-Si system with additions of up to 5 At.% carbon and presented the diagram depicted in Figure 11. It is shown that $D8_8$ phase does not occur in the binary Zr-Si system.

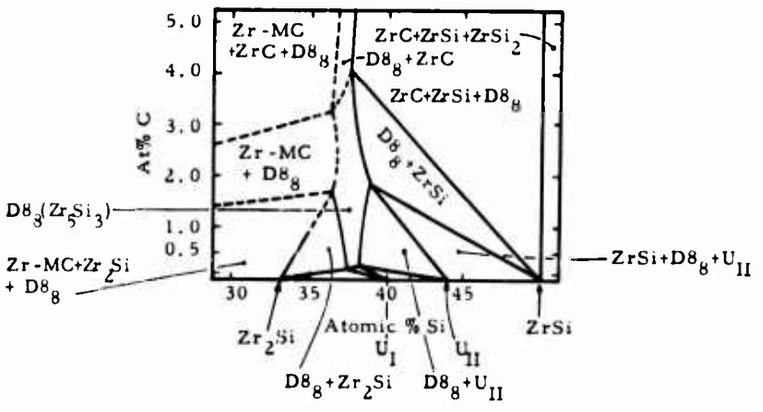

Figure 11. Zr-Si-C: Phase Equilibria Near Central Region of the Zr-Si Binary

2. The Hafnium-Silicon-Carbon System

This system has not yet been completely investigated, although H. Nowotny, E. Laube, R. Kieffer, and F. Benesovsky[79] have observed the formation of a $Hf_5Si_3(C)$ ternary-$D8_8$ phase which forms with less ease than the corresponding zirconium phase. The reported[79] lattice parameters of the $Hf_5Si_3(C)$ phase are: $a = 7.89_0$ Å and $c = 5.55_8$ Å.

3. The Zirconium-Silicon-Boron System

Nowotny[1] and co-workers observed the formation of a ternary $D8_8$ phase at the composition Zr_5Si_3 + 5 At.% B in both sintered and arc melted samples; the reported lattice parameters were: $a = 7.93_6$ Å, $c = 5.57_1$ Å.

An isothermal section of the Zr-Si-B system at 1400°C was presented by E. Parthe and J.T. Norton[6]. This section is reproduced in Figure 12.

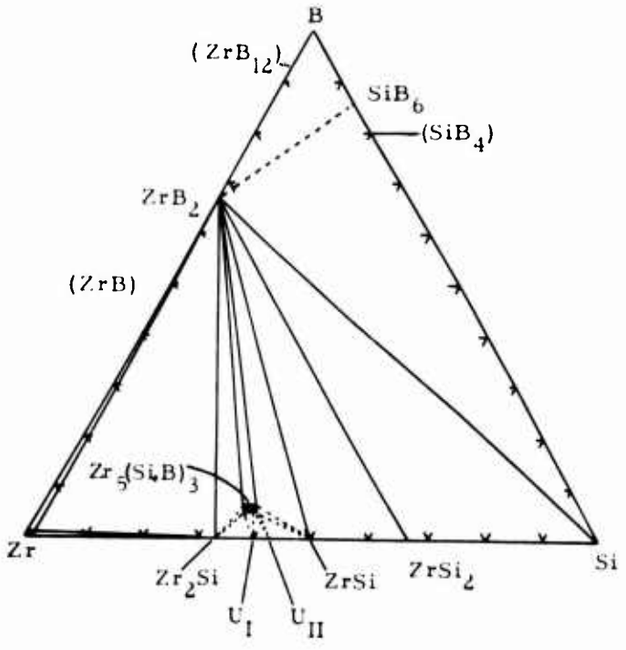

Figure 12. Zr-Si-B: Section at 1400°C.
(E. Parthe and J. T. Norton, 1960)

There are no mutual solubilities in the silicide and boride phases; a ternary $D8_8$-phase with a slight homogeneous range is located on the "Zr_5Si_3"-B section and contains about 5 At.% boron. ZrB_2 is the most stable binary phase and forms equilibria with all the other silicide phases and the $D8_8$-ternary phase as well as with silicon itself.

4. The Hafnium-Silicon-Boron System

A ternary phase, lying on the "Hf_5Si_3"-B section and containing about 5 At.% B, was found by H. Nowotny[79] and co-workers; the ternary phase possesses the $D8_8$, hexagonal structure.

No other work concerning the Hf-Si-B system has been reported.

III. EXPERIMENTAL PROGRAM

A. EXPERIMENTAL PROCEDURES

1. Starting Materials

Elemental, pre-prepared binary monocarbide, diboride, and disilicide as well as zirconium hydride powders were used as starting materials for the alloys investigated.

Zirconium metal powder was obtained from the Wah Chang Corporation, Albany, Oregon, and had the following main impurities (in ppm): C-40, Nb-<100, Fe-315, Hf-67, N-34, O-830, Si-<40, Ta-<200, Ti-<20, and W-<25. The lattice parameters of this starting material were a = 3.232 Å and c = 5.149 Å. The metal powder was sized between 74 and 44 micrometers. Spectrographic analysis performed at the Aerojet Metals and Plastics Chemical Testing Laboratory yielded the following results (in ppm): Si-10, Fe-20, Ta-not detected, and Hf-500.

A second batch of zirconium metal powder, also obtained from the Wah Chang Corporation had the following main impurities as designated by the vendor (in ppm): Al-25, C-40, Nb0<100, Cr-47, Cu-61, Fe-315, H-270, Hf-67, N-34, O-830, Ta-<200, and W-<25. The metal powder had a particle size of less than 74 micrometers; the lattice parameters of this zirconium powder were also a = 3.232 Å and c = 5.149 Å.

Zirconium dihydride, also purchased from the Wah Chang Corporation, Albany,Oregon, had the following main impurities (in ppm): C-320, Nb-<100, Cr-125, Fe-1800, Hf-137, Mg-255, N-116, O-1300, Si-157, Ta-<200, Ti-29, and W-<25. The hydrogen content was 2.1% by weight, and the particle size was less than 44 micrometers.

An overexposed Debye-Scherrer powder diagram of this material showed only the tetragonal-$ZrH_{\sim 2}$-pattern with no other extraneous lines. Spectrographic analysis performed at the Aerojet MPCT Laboratory gave the following results (in ppm): Si-10, Fe-500, Ta-not detected, Hf-<100, and Mg-40.

The hafnium metal powder used was of two different batches; both lots were purchased from the Wah Chang Corporation, Albany, Oregon.

The first batch had the following main impurities in the vendor's analysis (in ppm): Al-20, C-210, Nb-680, Fe-265, H-55, N-200, O-810, Si-<40, Ta-200, and W-235. This hafnium contained 3.2% by weight of zirconium. Spectrographic and vacuum fusion analysis of the hafnium powder by the Aerojet Metals and Plastics Chemical Testing Laboratory yielded the following values (in ppm): Nb-<1000, N-<300, O-<1000, Si-10, and Ta-400. The average particle size was 74 micrometers; lattice parameters of $a = 3.19_6$ Å and $c = 5.05_7$ Å were obtained from a powder diffraction pattern taken with Cu-K_α radiation.

The second batch of hafnium powder had the following main impurities (in ppm): Al-44, C-60, Nb-<100, Fe-99, H-45, N-200, O-660, Ta-<200, Si-<40, and W-<20. 2.5% zirconium by weight was present in this hafnium metal powder whose particle size was less than 74 micrometers.

The boron used was supplied by the United Mineral and Chemical Corporation, New York. The vendor's analysis contained the following values (in ppm): Fe-2500, C-800 ppm; Boron-99.55% by weight. The boron powder was sized between 149 and 44 micrometers. Spectrographic and chemical analyses at the Aerojet Metals and Plastics Chemical Testing Laboratory yielded the following results (in ppm): Mn-1500, Si-2000, Cr-1000, Mo-3000, Fe-500, and B_2O_3- 1.37% by weight.

The silicon used was supplied by the Var-Lac-Oid Chemical Company, New York and had the following vendor's analysis (in ppm): Fe-500, Al-100, Ca-200, Ti-10, Cr-50, Mn-30, Cu-10, Ni-trace. The particles were sized smaller than 44 micrometers. The Aerojet Metals and Plastics Chemical Testing Laboratory's spectrographic analysis of this materials was (in ppm): C-80, Cr-100, Ni-<10, Cu-800, Al-1000, Fe-250, Ti-400, Mg-<10, B-10, and Ca-500. The lattice parameter of this starting material was 5.429$_7$Å.

Carbon was used in two forms. The lampblack powder, supplied by Monsanto Chemical Company, had 99.57% free carbon and the following impurities (in ppm): H_2O-400, benzol extract-3000, ash-300, and volatiles-3600. The particle size was 0.01-0.1 micrometers. Spectrographic analysis at Aerojet gave the following results (in ppm): Si-20, Mg-<10, Cu-<10, Al-10, and Fe-10.

Graphite powder was obtained from the National Carbon Company and had the following typical impurities (in ppm): S-110, Si-46, Ca-44, Fe-40, Al-8, Ti-4, Mg-2, V-trace, and ash-800 max. 99% of the graphite was smaller than 44 micrometers. Highly overexposed X-ray films of these materials showed no traces of any impurities.

The zirconium monocarbide powder was supplied by the Wah Chang Corporation, Albany, Oregon. The main impurities were (in ppm): Nb-100, Fe-<50, Hf-<10, Ta-<200, Ti-38, and W-<25. The monocarbide had a carbon content of 11.54% (49.8 At.%) and a particle size of less than 44 micrometers.

The zirconium disilicide was prepared with a nominal content of 68 At.% Si by cold pressing the mixed powders with a small amount of camphor dissolved in ether as a binder. The bricketts were placed under a vacuum of 30 inches of mercury at a temperature of 110°C for 12 hours to remove the camphor. The compacts were then reacted in a molybdenum boat in a muffle furnace under hydrogen at 1250°C. Subsequent sintering under the same conditions lasted for two hours. The reacted compacts were crushed in an agate mortar and sieved to a particle size of less than 74 micrometers. Chemical analysis on silicon showed 39.6 Wt.%, or 68.2 At.% silicon. A Debye-Scherrer X-ray film of this material showed only the disilicide pattern and very faint lines of silicon metal. The lattice parameters of the disilicide were: $a=3.69_4$, $b = 14.75$, and $c = 3.66_5$ Å. The hafnium disilicide was prepared in the exact same manner as that described above for $ZrSi_2$. Chemical analysis showed 67.6 At.% silicon to be present in the disilicide. The lattice parameters of this starting material taken from an X-ray film which showed only the disilicide pattern and faint traces of silicon metal were: $a = 3.67_5$, $b = 14.56$, $c = 3.63_2$ Å.

The preparation of the silicon carbide master alloy followed the steps outlined above for the preparation of the disilicides, but it was sintered at 1350°C for 1 hour. An X-ray film of this silicon carbide showed only the pattern of the cubic β-SiC; the lattice parameter was 4.35_8 Å; and a carbon analysis showed 47.4 At.% carbon to be present.

Because of the violent exothermic reaction associated with the formation of the zirconium and hafnium diborides, these two materials were prepared in two steps.

For the ZrB_2, the initial reaction involved a mixture whose overall nominal composition was 76.6 At.% B. This mixture was cold compacted with the addition of a camphor-ether solution as a binder. When the ether had evaporated, the compacts were placed in a tantalum container which was placed in the center of the graphite heating element of a carbon pot furnace. Under a vacuum of 1×10^{-2} Torr and a temperature around 200°C the camphor was driven off. After the temperature was allowed to climb slowly to near 900°C, the furnace was flooded with helium; after the exothermic reaction at a slightly higher temperature, the furnace was again placed under vacuum and allowed to cool. The boride was removed and ground to particles smaller than 100 micrometers. The remaining portion of the zirconium metal was mixed with the initially formed boride to yield a diboride composition. The cold pressing and reaction steps were rerun, and the material was given a final heat treatment at 1750°C for 30 minutes under helium.

An X-ray film of the final diboride showed only the pattern of the diboride and some faint lines of the zirconium metal phase. The lattice parameters of this starting material were a = 3.167 and c = 3.530 Å. A boron analysis showed 63.5 At.% B to be present in the starting material.

The same procedure as above for ZrB_2 was followed in the preparation of HfB_2. Chemical analysis of the total boron contained in the HfB_2 starting material showed that 67.6 At.% B was present. The lattice parameters of the diboride, taken from an X-ray film which showed only the diboride pattern, were a = 3.142 and c = 3.477 Å.

2. Alloy Preparation and Heat Treatment

a. Solid State Samples

Solid state samples for the Zr-Si-C, Hf-Si-C, nd Hf-Si-B systems were made by hot pressing the mixed powders using the respective components: Hf, Si, C, $HfSi_2$, B, and ZrH_2. The samples for these solid state investigations were prepared without using the extremely

high melting compounds, i.e., HfC, SiC, HfB_2, ZrB_2, and ZrC, to assure the maximum possible chance for the attainment of equilibrium at the lower heat treating temperatures.

The following table provides the detailed information concerning the heat treatment of the solid state alloys.

Table 7. Heat Treatment Conditions for Solid State Samples

System	Heat Treatment Temperature, °C	Duration of Heat Treatment in Hours	Atmosphere
Zr-Si-C	1300°	63-65	Helium
Hf-Si-C	1300°	64-65	Helium
Hf-Si-B	1300°	66	Helium

b. Melting Point Samples

The majority of the melting point samples for the Zr-Si-C, Hf-Si-C, Zr-Si-B, and Hf-Si-B systems were prepared by hot-pressing in the manner previously described[81]. Again, the use of the extremely high melting compounds — except in those cases where the ternary samples had compositions quite close to the high melting binary compounds — was eliminated in order not to hinder the correct equilibrium formation with these slowly reacting compounds.

A few of the extremely metal-rich melting point samples were cold pressed and given a subsequent low temperature heat treatment for strength; sample preparation in this manner prevented possible undue carbon and air contamination in hot pressing.

3. Melting Point Determinations

Melting points of the alloys in the four ternary systems were determined by direct resistance heating of the samples. Observation of melting was conducted using the Pirani-hole method. The special melting point furnace and the Pirani-technique have been previously described[81] in this series of reports.

The temperature measurements were carried out with a disappearing-filament type micropyrometer which was calibrated against a certified, standard lamp from the National Bureau of Standards. The temperature correction for the absorption in the quartz furnace window, as well as that for deviation due to non-black body conditions have been amply described and validated in a previous report[81].

The melting point experiments were conducted under high purity helium at 2 1/4 atmospheres pressure to prevent undue vaporization of silicon.

Considerable difficulty was encountered in the heating of the silicon and boron-rich alloys. At normal temperatures, these materials have a very low electrical conductance, and it was difficult to initially heat the samples using the direct resistance method. This difficulty was overcome in some cases by rubbing a small amount of molybdenum powder on the ends of the sample to provide a better contact between the sample and the tungsten insulating plate in the melting point furnace. The melting of the sample occurred in the center of the sample in the reduced area at the black body hole, and no contamination of the molten portion of the sample was possible.

4. X-ray Analysis

Debye-Scherrer X-ray photographs were made of all samples in the Zr-Si-C, Zr-Si-B, Hf-Si-C, and Hf-Si-B systems after solid state heat treatment, melting point experiments, and arc melting. Because of the complicated X-ray patterns offered by the many silicide compounds, chromium K_α radiation was used exclusively to spread out the diffraction lines.

Due to the rapid martensitic-like transformation which occurs in both the hafnium and zirconium metals, the high temperature β-form of the metals was never observed in the X-ray patterns of samples which were at high temperatures.

The majority of the structures of the zirconium and hafnium silicides are known, and no difficulty was encountered in indexing and calculating lattice parameters of these phases except in the case of the Zr_3Si_2 and Hf_3Si_2 phases where equilibrium was not obtained and the quality of the Debye-Scherrer patterns was quite poor. Traces of some of the other reported binary silicide phases, whose structure and exact compositions are not known, were observed, and it was possible to only indicate the phase equilibria with uncertainty.

In the few cases (melting point samples) where the complicated high temperature structures of SiC were observed, no attempt was made to identify or index these phases.

5. Chemical Analyses*

Chemical and spectrographic analyses were performed on the majority of starting materials to check the vendor's analyses. In addition, the pre-prepared master silicide and boride alloys were analyzed for their silicon and boron contents. The interstitial impurities of some of the starting metal powders was checked using a vacuum fusion technique in a platinum bath.

Silicon was determined by fusing the sample in a sodium hydroxide-sodium peroxide mixture, dissolving the melt in perchloric acid and volatilizing the silicon as H_2SiF_6 with a hydrofluoric-sulfuric acid mixture.

---

*The chemical analyses were performed under the direction of W.E. Trahan in the Aerojet-General's Metals and Plastics Chemical Testing Laboratory.

Boron was determined by fusing the borides in pre-dried sodium carbonate at 1000°C. The resulting melt was dissolved in water, and the excess carbonate was removed with barium hydroxide. After removal of the precipitates, boric acid was determined by differential titration of the boro-mannitol complex with N/10 sodium hydroxide between pH-values of 5.3 and 8.5.

The spectrographic analyses showed that there was no major metallic impurity present in the starting materials which would seriously affect the high temperature equilibrium. The values of the interstitial contents (O, N, H) of the starting materials were somewhat higher than those indicated by the vendor; this discrepancy, however, is attributed to the time interval between Aerojet's and the vendor's analyses; the metal powders had sufficient time to absorb both water and air.

The prepared silicides held their nominal compositions quite well, although the prepared borides showed up to several atomic percent boron loss owing to the volatilization of B_2O_3.

6. Metallography

Metallographic studies were made of the melted portions of melting point samples as well as of arc melted specimens. The samples were prepared by mounting the alloys in an electrically conductive mixture of diallyl-phthalate-lucite copper base mounting material. The samples were roughly ground on varying grit sizes of silicon carbide paper; the final polishing was performed on a microcloth using a suspension of 0.05 micrometer alumina in Murakami's solution.

The final etching techniques used on the samples varied with the overall alloy composition. The silicon-rich, diboride-rich, and carbide-rich specimens were best dip etched in a aqueous aqua regia-hydrofluoric acid solution (9 parts H_2O - 1 part acid mixture) (60% HCl-20% HNO_3-20% HF). The metal-richer silicides as well as the metal phase, (Hf, Zr), itself responded best to electroetching with 10% oxalic acid solution.

Etchants which would selectively attack only one or more of the many silicide phases could not be discovered. The oxalic acid produced only gradually varying color changes in the silicides depending on metal content. The majority of the silicide phases were differentiated by careful comparison of the metallographic specimen with the corresponding X-ray film. Most of the silicides showed a considerable amount of intragranular cracking produced upon cooling; this in itself was sufficient for identification in many instances.

B. EXPERIMENTAL RESULTS

1. The Zirconium-Silicon-Carbon System

Seventy-nine samples were prepared by hot-pressing for solid state investigations in the Zr-Si-binary and the Zr-Si-C ternary fields. Figure 13 shows the locations and qualitative X-ray analysis of the Zr-Si-C samples heat treated at 1300°C.

a. The Zr-Si-System

The results obtained from the binary Zr-Si samples confirmed the majority of the more recently published results. The zirconium disilicide, with the orthorhombic, C49-type unit cell, had the following lattice parameters: $a = 3.69_4$ Å, $b = 14.75$ Å, and $c = 3.66_6$ Å. Debye-Scherrer films of quite good quality were obtained of the monosilicide with the orthorhombic, B-27 type structure. Lattice parameter measurements of this phase gave: $a = 6.99_2$ Å, $b = 3.78_5$ Å, and $c = 5.30_1$ Å.

Samples containing between about 49 and 44 At.% silicon presented X-ray patterns which were quite complicated; none of the films were sharp, and varying amounts of the phases present were observed seemingly independent of concentration. The reported ZrSi, or better said $ZrSi_{1-x}$, or Zr_6Si_5 was observed in only exceedingly small trace amounts in the binary samples. The majority of material present in these samples consisted of the tetragonal Zr_3Si_2[5] phase mixed with the as yet unknown σ-similar

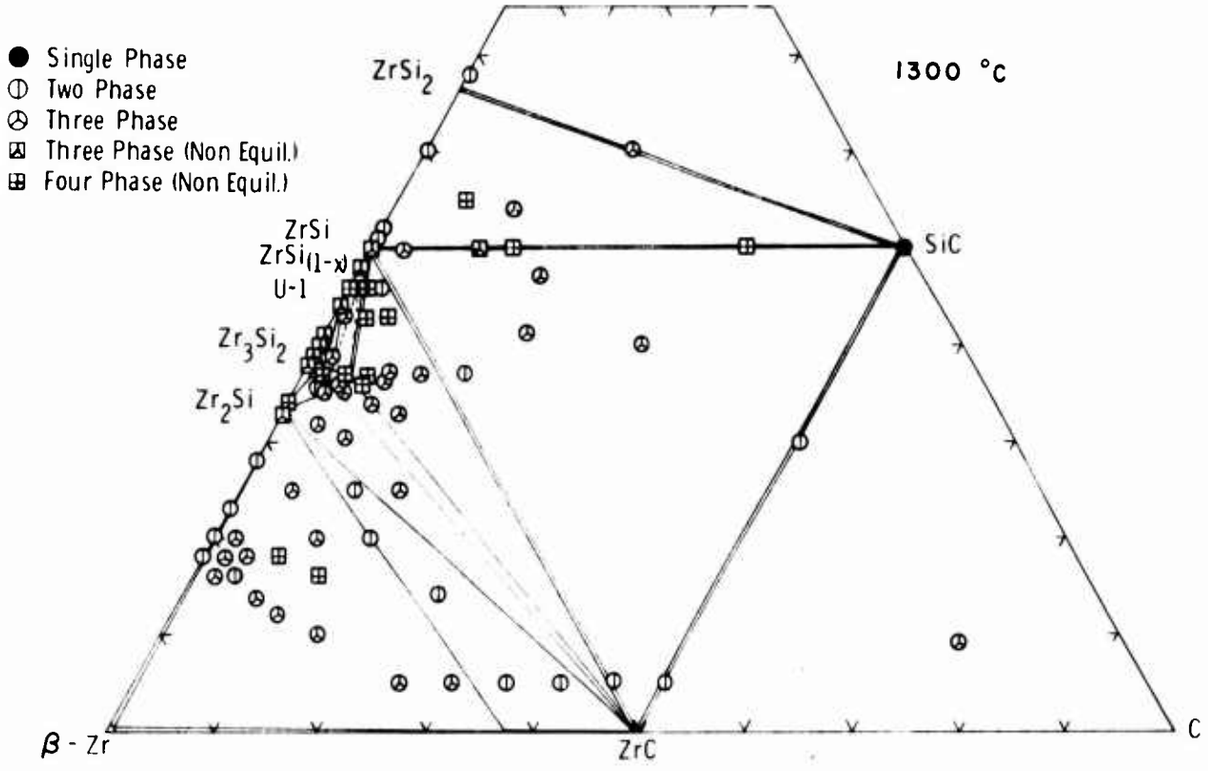

Figure 13. Zr-Si-C Location and Qualitative X-ray Analysis of 1300°C Samples.

U-1[2] phase which also lies near 40 At.% Si. In substantiation of previously reported results[1] the $D8_8$ phase was not observed in binary Zr-Si samples. The tetragonal Zr_2Si phase was never obtained as a single phase, but was always seen in the presence of either zirconium metal or the Zr_3Si_2 phase. The Zr_2Si phase appears to have a slight homogeneous range in the binary even though many of the X-ray films obtained were not sufficiently in equilibrium to permit exact lattice parameter measurements; a sample with 18 At.% silicon showed zirconium metal and the Zr_2Si phase which had lattice parameters of: $a = 6.60_4$ Å and $c = 5.31_6$ Å.

No evidence was seen in these hot pressed samples, which were heat treated at 1300°C, of the reported Zr_4Si[3] or Zr_3Si[4] phases.

b. **The Zr-Si-C Equilibria at 1300°C**

The main equilibria at 1300°C have been established; until the exact nature and characteristics of the binary Zr-Si system are clarified, some uncertainties must remain concerning the equilibria involved near the region of 50 At.% silicon near the Zr-Si binary.

Qualitative X-ray analysis of the many samples prepared showed that the following equilibria exist at 1300°C. $ZrSi_2$-SiC, ZrSi(B-27)-SiC, ZrSi(B-27)-ZrC_{1-x}, SiC-ZrC_{1-x}, $D8_8$(ternary)-ZrC_{1-x}, $D8_8$—U-1, D8 -Zr_3Si_2, $D8_8$-Zr_2Si and Zr_2Si-ZrC_{1-x}. These results are depicted in Figure 14.

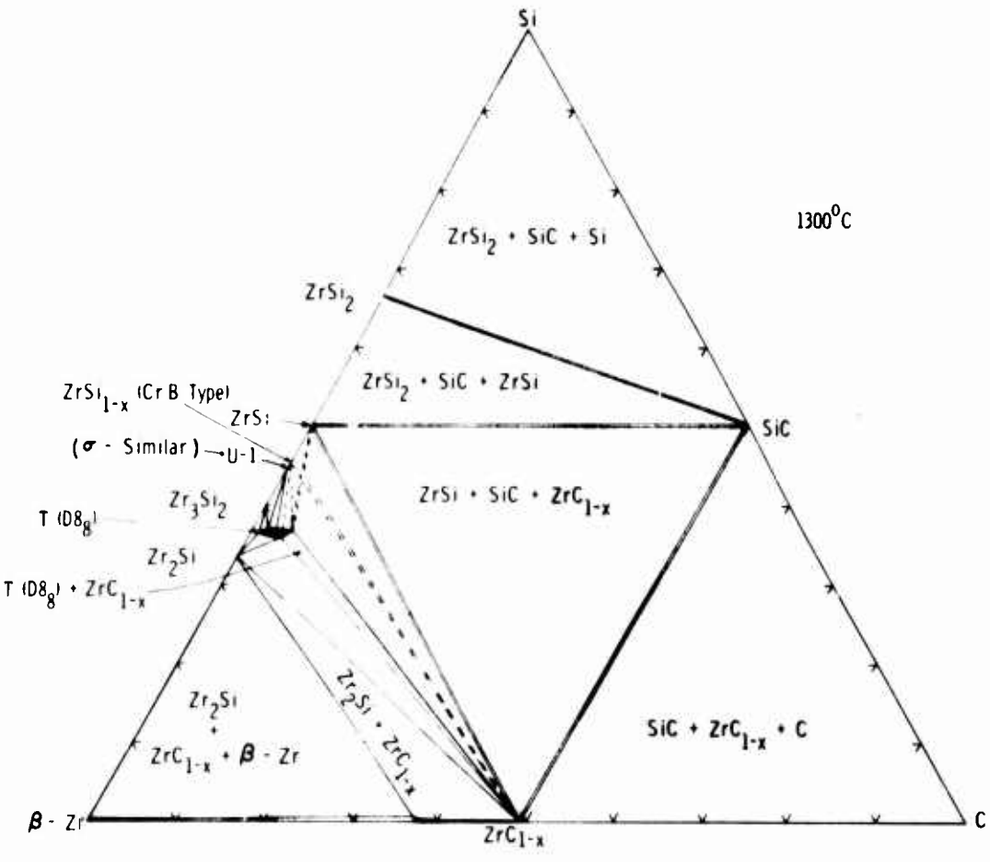

Figure 14. Zr-Si-C: Section at 1300°C.

The $D8_8$ phase, which is formed only in the ternary region, stretches from about 1/2 At.% to about 5 At.% C and lies between 36 and 37 At.% silicon at 1300°C. Table 8 shows the variance in lattice parameters of the $D8_8$ ternary phase as a function of nominal composition. Owing to

Table 8. Lattice Parameters of the Zr-Si-C $D8_8$-Phase

Nominal Composition in Atomic Percent			Lattice Parameters in Angstroms	
Zr	Si	C	a	c
62	35	3	7.92_9	5.56_6
61	37	2	7.93_7	5.57_0
60	25	15	7.93_1	5.60_1
56	36	8	7.91_6	5.60_0

the uncertainties in the binary Zr-Si system near 50 At.% Si, some of the equilibria emanating from the binary Zr-Si edge have been dotted (Figure 14). to indicate uncertainty. Although the Zr_6Si_5 or $ZrSi_{1-x}$ phase with the chromium monoboride structure has been observed[1, 5, 69] in binary Zr-Si samples, it was evident from this investigation that this crystal structure is far more stable in ternary, i.e., carbon containing, samples. It is not inconceivable that the Zr-Si phase with the CrB orthorhombic structure is also a stabilized ternary phase. The lattice parameters of a Zr-Si-C 52/43/5 sample which contained a majority of the Zr-Si phase with the CrB-type structure were a = 3.75_3 Å, b = 9.92_0 Å, and c = 3.75_2 Å. Qualitative X-ray analysis of samples from this region did not yield conclusive evidence as to which equilibrium, ZrC_{1-x}-Zr_6Si_5 or ZrSi(B-27)-$D8_8$ exists at 1300°C. In general, the films of samples from this area showed all four phases ZrC_{1-x}, Zr_6Si_5, $D8_8$, and ZrSi(B-27). In view of the preceding results and the fact that the exact characteristics of the Zr-Si binary are are not accurately known, the phase relationships in this area are indicated with uncertainty.

The majority of the samples from $Zr-Zr_2Si-ZrC_{1-x}$ region indicated the equilibrium as depicted in Figure 14. Two samples, however, had extremely faint lines which could not be either identified or accurately measured; the X-ray findings, showing non-equilibrium conditions in these samples have been indicated in an appropriate manner in Figure 13. These faint lines possibly stem from the reported Zr_4Si[3] or Zr_3Si[4], but since other evidence of the presence of these phases was not found, these crystal structures and their possible equilibria are not depicted in any of the drawings.

The lattice parameters of the $ZrSi_2$ phase as taken from ternary, carbon-containing samples showed no change compared with those of the binary disilicide; there is no carbon or carbide solubility in $ZrSi_2$. The above statements hold true for the monosilicide with the orthorhombic B-27 type structure. There appears to be no lattice parameter change in the Zr_6Si_5, U-1, and Zr_3Si_2 phases present in carbon-containing samples, although exact measurement of lattice parameters was not possible because of the diffuse nature of the Debye-Scherrer patterns.

A slight variation of the lattice parameters of the Zr_2Si phase was observed: a Zr-Si-C sample, 70/25/5 had $a = 6.59_9$ Å and $c = 5.30_6$ Å whereas the sample 80/18/2 had $a = 6.60_3$ Å and $c = 5.30_7$ Å. In view of the observed lattice parameter variance of the Zr_2Si phase in binary samples, this slight change in lattice parameters observed in ternary, carbon-containing samples is most probably due to a homogeneous range of this phase in the binary Zr-Si system rather than a solubility of carbide in the Zr_2Si phase. Final clarification of this point must await exact investigations in the binary Zr-Si system.

The lattice parameters of the SiC cubic phase, which were measured on films taken from samples lying in the two and three phase fields in equilibrium with ZrC_{1-x}, showed a slight enlargement to 4.36_0 Å as compared to 4.35_8 Å for a binary SiC pattern. This observation speaks for an ever so slight solubility of ZrC_{1-x} in SiC at 1300°C.

At 1300°C the cubic, B-1 structure of the ZrC_{1-x} phase has a lattice parameter of 4.69_7 Å at 49.5 At.% C or greater in the Zr-C binary[7]. On the other hand, the lattice parameters of the ZrC_{1-x} phase taken from samples which showed this phase in equilibrium with SiC, SiC and graphite, SiC and ZrSi(B-27); and $D8_8$ varied between 4.69_7 and 4.69_5Å. These findings prove that there is no solubility of silicides in the least carbon defect part of the homogeneous range of ZrC_{1-x}; furthermore, the only slight variation in lattice constant of silicon-containing samples from the value exhibited by the binary $ZrC_{\sim 1}$ phase indicates that the ZrSi, SiC, and $D8_8$ phases are in equilibrium with an almost stoichiometric ZrC_{1-x}.

The solubility of carbon and silicon in zirconium was not specifically investigated; the values used in the isothermal section (Figure 14) were taken from the literature[7, 3].

c. Melting Point Results and High Temperature Equilibrium

Owing to the uncertainties of the characteristics of the binary Zr-Si and Si-C systems, no attempt can be made to completely describe, elucidate, and depict the various complicated high temperature solid-liquid equilibria in the Zr-Si-C system. The investigations, therefore, were limited to the obtainment of melting point data showing the interphase melting temperatures of the various sample compositions. Closer interpretations of ternary solid-melt equilibria were possible in a few cases.

Figure 15 shows the compositional location of the ternary Zr-Si-C samples whose melting points were determined. There is a eutectic in the Zr-Si binary between β-Zr and Zr_2Si at approximately 9 At.% Si[3]; the eutectic temperature is about 1610°C[3]. In the binary Zr-C system, there is a eutectic between β-Zr and ZrC_{1-x} at less than about 2 At.% C[7] ($T_{eut.}$ = 1835°C). A ternary eutectic consisting of Zr_2Si, ZrC_{1-x} and β-Zr is most probably present in this region but due to the vanishingly small amount of carbide present, this ternary eutectic was not observed metallographically; no decided temperature minimum was observed which would indicate the exact melting point of the ternary eutectic; the ternary eutectic must

be quite close both in temperature and composition to the β-Zr-Zr_2Si eutectic at 1610°C.

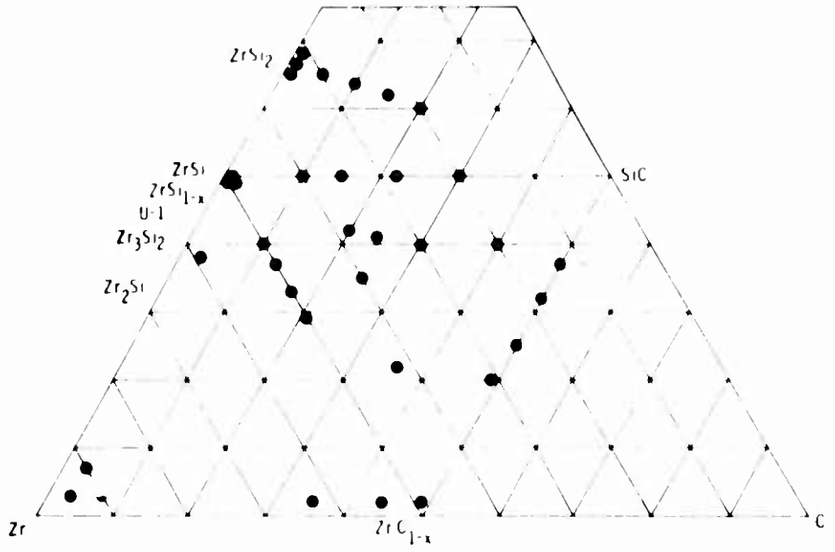

Figure 15. Zr-Si-C: Location of Melting Point Samples.

Figures 16 and 17 show the metallographic findings in this metal rich region. The $D8_8$ phase increases its homogeneous range with increasing temperature in the ternary region. The compound melts with a large, flat maximum at temperatures near 2400°C in the ternary region (Table 10). Near its melting point, the homogeneous region of the $D8_8$ phase encompasses the approximate compositional region; Zr: 56-65, Si: 32-37, and C: 0.3-8 At.%.

There is probably a eutectic between the $D8_8$ ternary phase and ZrC_{1-x}; because of the great difference in melting points of these two phases, the eutectic point lies very close to the $D8_8$ phase in both temperature and composition. Due to the relatively small percentage of the ZrC_{1-x} phase present in the eutectic, a eutectic structure was not observed. Figure 18 shows a metallographic picture of a small amount of ZrC_{1-x} in a $D8_8$ matrix.

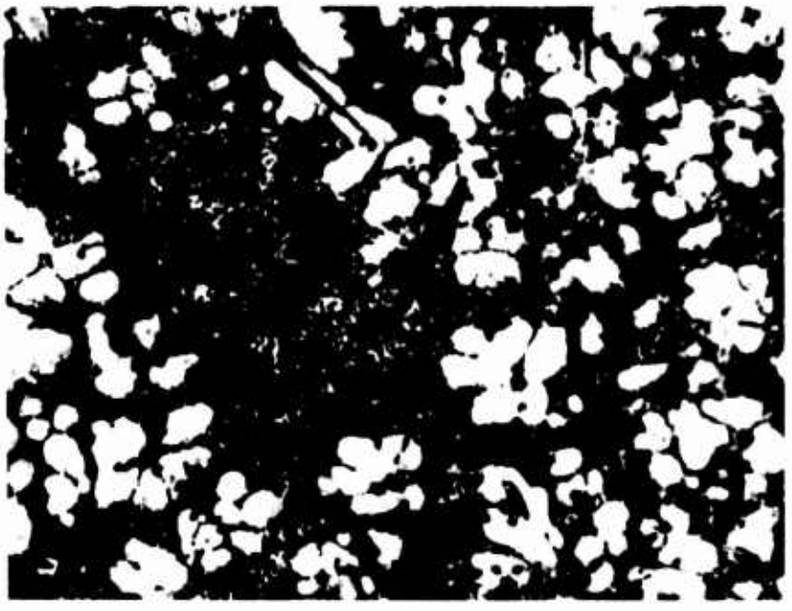

Figure 16. Zr-Si-C: 90/7/3, Arc Melted X1000

Primary β(transformed)-Zr (White) in β-Zr-Zr_2Si-ZrC_{1-x} Matrix (ZrC_{1-x} Unresolved).

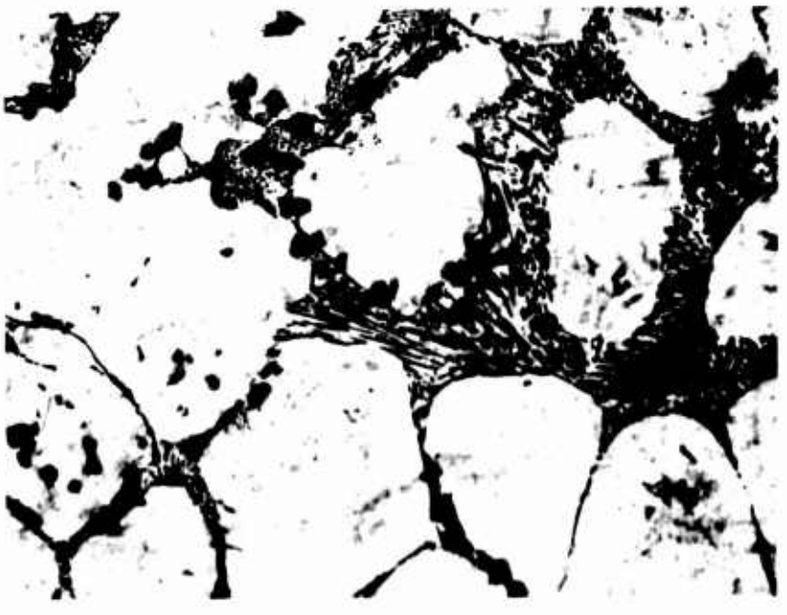

Figure 17. Zr-Si-C: 94/3/3, Arc Melted X600

Primary β(transformed)-Zr (White), Secondary Zr_2Si (Grey) in β(α)-Zr-Zr_2Si-ZrC_{1-x} Matrix (ZrC_{1-x} Unresolved).

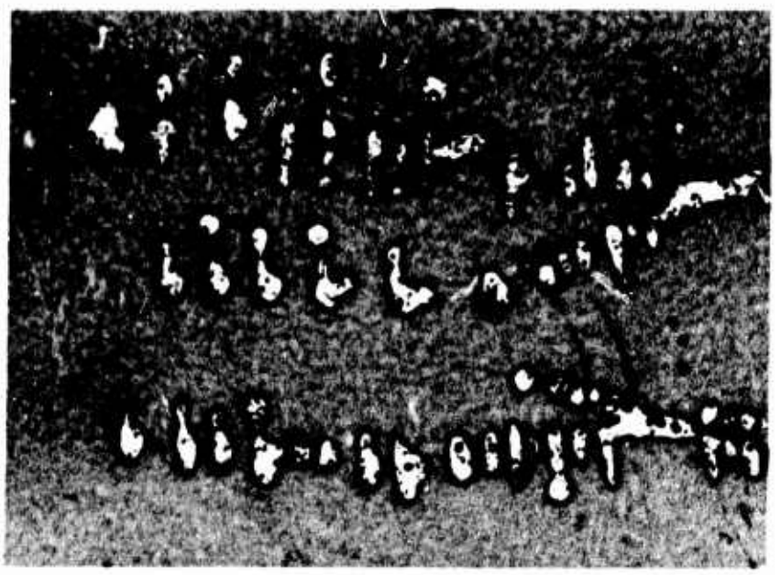

Figure 18. Zr-Si-C: 56/33/11, Arc-Melted, Quenched from Approximately 2400°C. X1000

Carbide Dendrites (White, Etch Stained) in $D8_8$ Matrix.

X-ray films of the molten portions of melting point samples from the central portion of the ternary region indicated that a basic change in the equilibrium, as determined at 1300°C, occurs at a higher temperature — probably quite close to the melting regions. Debye-Scherrer powder diagrams showed that $ZrSi_2$ was in equilibrium with ZrC_{1-x}. In other words, at a temperature between 1300°C and about 1600°C a four-phase reaction plane:

$$ZrSi\ (B\text{-}27) + SiC \leftrightharpoons ZrSi_2 + ZrC_{1-x}$$

occurs. Since no differential thermal analysis experiments were run, the exact temperature of this four phase plane was not more closely determined.

Interpretations of the complex behavior of the high temperature regions involving equilibria with the SiC phase were practically impossible. It was quite evident that SiC decomposes into silicon vapor and graphite at temperatures in the range of about 2000°-2700°C in ternary

samples. After each of the Pirani melting point experiments with ternary samples containing the SiC phase, the cooler inside parts of the melting point furnace were covered with a brownish-grey and sometimes slightly yellow (SiO) dust layer. The remaining specimens themselves were quite porous so that no metallography was possible; furthermore, small bits of material, identifiable to the naked eye as graphite, were seen on the surfaces of the sample. Subsequent examination of X-ray powder patterns of these samples showed free silicon and in cases where the concentration was high enough, free carbon. It seems as though the temperature of the peritectic-like or eutectic-like decomposition of SiC as proposed by Nowotny[24] and co-workers is depressed considerably in ternary zirconium carbide and zirconium silicide containing samples.

Both lattice parameter measurements and examination of metallographic sections of specimens quenched from the molten state indicate that there is no solubility into the ternary region by either the ZrSi(B-27) or $ZrSi_2$ phases. The lattice parameters were the same as those of binary samples, and no signs of precipitation from the silicide phases were seen metallographically.

The following metallographic pictures depict the representative findings from the central portion of the Zr-Si-C system as well as from the ternary region near the Zr-Si binary side. Although the lattice parameters of the ZrC_{1-x} phase in the ternary region in equilibrium with the extreme carbon defect end of the ZrC_{1-x} homogeneous range showed a very slight increase over the corresponding pure binary carbide phase (4.68_5 Å vs 4.68_7 Å), metallographic examination showed no signs of silicide precipitation from the carbide grains. There is virtually no silicide solubility in the ZrC_{1-x} phase, and no temperature dependent solubility even at high temperatures. Figures 22 and 23 show these metallographic findings.

The melting point results of the Zr-Si-C system are summarized in the following table (Table 9) which shows the minimum melting temperatures along various sections. In some instances the interface melting of some samples is governed by the melting points of the lower melting binary compound.

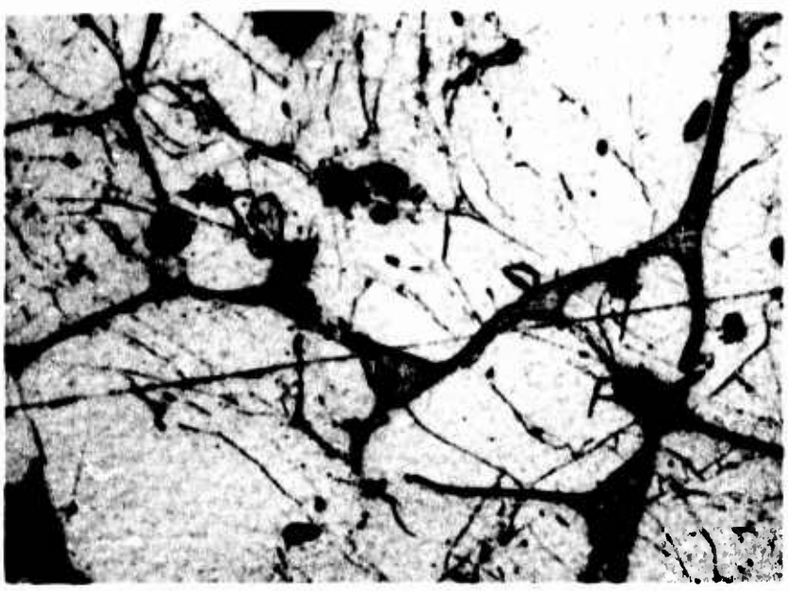

Figure 19. Zr-Si-C: 30/65/5 , Quenched from Approximately 1555°C. X1000

$ZrSi_2$ (Light Grey with Cracks) with Silicon Along Grain Boundaries. Small Amount of SiC Visible as Black Areas.

Figure 20. Zr-Si-C: 20/60/20, Quenched from Approximately 1571°C. X600

SiC (Black Clusters) and $ZrSi_2$ (White with Cracks) with Silicon Matrix (Grey).

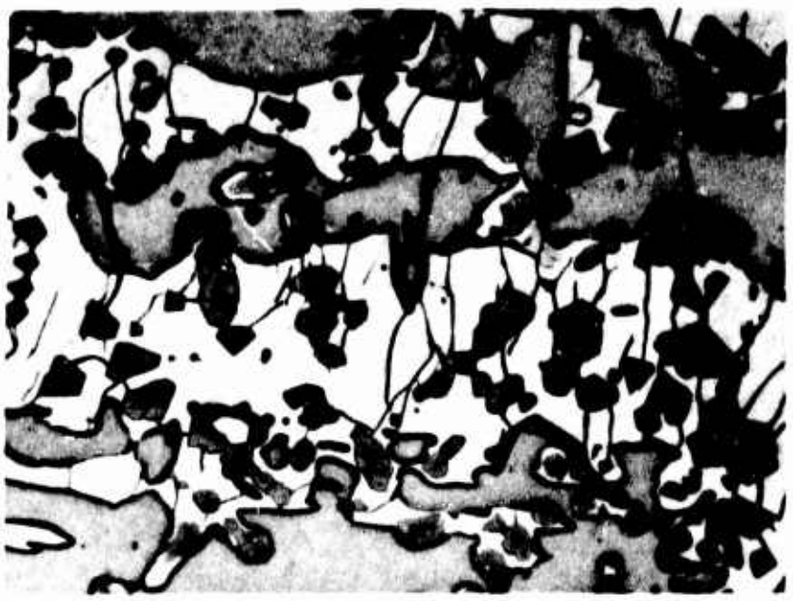

Figure 21. Zr-Si-C: 40/50/10, Quenched from Approximately 1750°C. X750

ZrC_{1-x} (Small Angular Grey Grains) and ZrSi ($ZrSi_{1-x}$) (Grey) in a $ZrSi_2$ Matrix (White with Cracks).

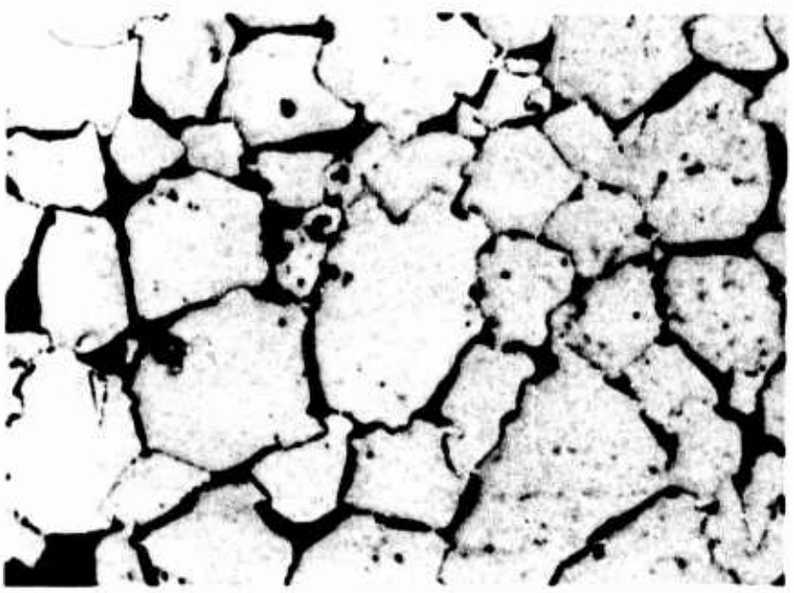

Figure 22. Zr-Si-C: 54/2/44, Quenched from Approximately 2800°C. X1000

Carbide Grains (White) with $D8_8$ Phase (Black) in Grain Boundaries.

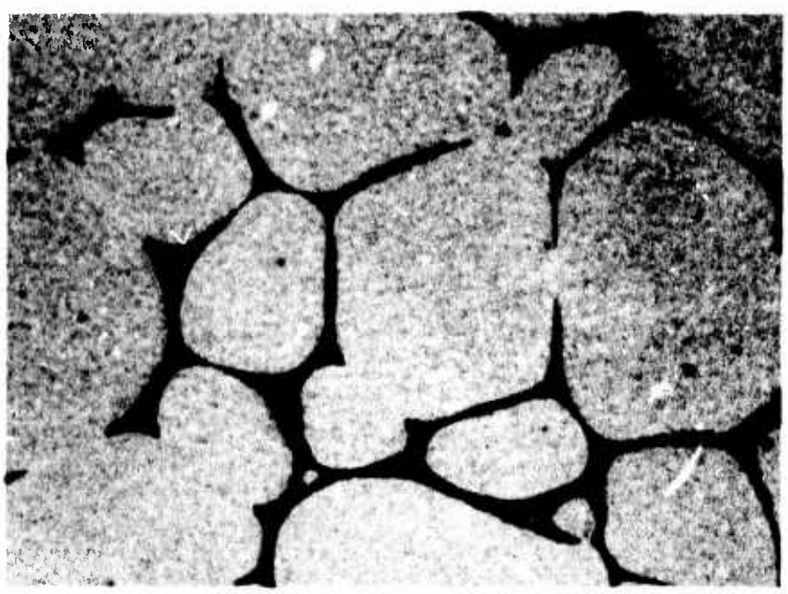

Figure 23. Zr-Si-C: 63/2/35, Quenched from Approximately 3300°C. X1000

Carbide Grains (White) with Zr Metal (Black) and Zr_2Si (Dark Grey) in Grain Boundaries.

Table 9. Minimum Melting Temperatures of Various Pseudo-binary Sections in the Zr-Si-C System

Section	Minimum Incipient Melting Temperature °Centigrade
$ZrSi_2$-ZrC_{1-x}	1526°
$ZrSi_2$-SiC	1520
ZrSi-SiC	1637°
ZrSi-ZrC_{1-x}	1658°
$D8_8$-ZrC_{1-x}	2385°
ZrC_{1-x}-SiC	2580°

An additional table (Table 10) displays the melting behavior and qualitative X-ray analysis of the ternary Zr-Si-C alloys examined.

Table 10. Melting Temperatures, Melting Behavior, and Qualitative X-ray Analysis of Zr-Si-C Alloys

Composition Atomic % Nominal			Melting Temperature °C		Type Melting	X-ray Analysis Phases Present
Zr	Si	C	Incipient	Collapse		
34	65	1	1490	1617	very heterog	$ZrSi_2$ + tr ZrSi (B-27)
32.5	66.5	1	1526	1559	heterogeneous	$ZrSi_2$ + tr Si + tr SiC
30	65	15	1520	1555	very heterog	$ZrSi_2$+little Si+tr SiC
26.5	63.5	10	1541	1541	heterogeneous	$ZrSi_2$ + little Si + SiC
23	65	15	1566	1617	very heterog	$ZrSi_2$ + Si + SiC
20	60	20	1561	1571	somewhat sharp	$ZrSi_2$ + Si + SiC
50	49	1	2230	2230	fairly sharp	ZrSi(B-27)+ZrSi(CrB)+$D8_8$
49	49	2	2230	2230	fairly sharp	ZrSi(B-27) + $ZrSi_2$
49	50	1	2225	2225	fairly sharp	ZrSi(B-27) + tr $ZrSi_2$
40	50	10	1719	1750	heterogeneous	ZrSi(B-27)+$ZrSi_2$ + ZrC
35	50	15	1677	1740	heterogeneous	$ZrSi_2$+ZrSi(B-27)+ZrC+little SiC
28	50	22	1719	1893	very heterog	$ZrSi_2$ + ZrC + SiC
50	40	10	2270	2270	somewhat sharp	ZrSi(B-27)+Zr+tr $ZrSi_2$
50	37	13	1785	2270	heterogeneous	ZrSi (B-27) + ZrC
50	33	17	<<2225	2290	very heterog	ZrSi (B-27) + ZrC
50	29	21	1802	2270	very heterog	ZrC + ZrSi (CrB)
18	32	50	2580	2765	heterogeneous	ZrC + SiC + tr C + little C49
25	25	50	2590	2646	very heterog	ZrC + SiC + C
31	20	49	2610	2688	very heterog	ZrC + $ZrSi_2$ + tr SiC
38	42	20	1678	1770	very heterog	ZrC + tr SiC + C
35	41	24	1688	1930	very heterog	ZrC + $ZrSi_2$ + SiC
40	35	25	1766	1857	very heterog	ZrC + $ZrSi_2$ + tr SiC
20	40	40	~2590	-	very heterog	ZrC + SiC + C + tr $ZrSi_2$
42	22	36	1751	2306	very heterog	ZrC + little SiC + $ZrSi_2$
60	37	3	2420	2420	fairly sharp	$D8_8$ + tr $ZrSi_2$ + tr ZrSi(CrB)
54	2	44	~2300	-	very heterog	ZrC + very slight tr?
63	2	35	3342	-	heterogeneous	ZrC + tr ?
90	7	3	1602	1602	sharp melting	Zr + ZrC + Zr_2Si
94	3	3	1630	1650	somewhat sharp	Zr + ZrC + tr Zr_2Si

2. The Hafnium-Silicon-Carbon System

Over 50 samples were prepared in the ternary Hf-Si-C and binary Hf-Si systems together; these specimens for solid state investigations at 1300°C were prepared by hot pressing and subsequent heat treatment.

Figure 24 shows the compositional location and qualitative X-ray analysis of the 1300°C samples.

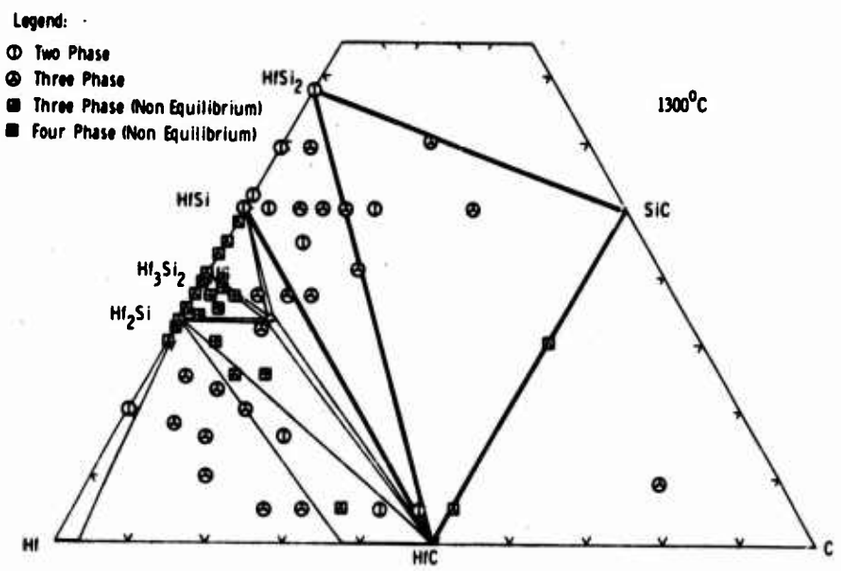

Figure 24. Hf-Si-C: Location and Qualitative X-ray Analysis of 1300°C Samples.

a. The Hf-Si System

The results of the binary Hf-Si samples heat treated at 1300°C showed that the hafnium-silicon system is less complex, as far as the number of appearing phases is concerned, than its sister system zirconium-silicon. The following phases and crystal structures were observed and confirmed (lattice parameters in parenthesis): $HfSi_2$, orthorhombic, C49 type ($a = 3.67_4$ Å, $b = 14.56$ Å, $c = 3.63_1$ Å); HfSi, orthorhombic, B-27 type ($a = 6.87_3$ Å, $b = 3.76_8$ Å, $c = 5.22_4$ Å), Hf_3Si_2, tetragonal, U_3Si_2-type

(a = 6.98_2 Å, c = 3.66_3 Å); and Hf_2Si, tetragonal, C 16 type (a = 6.55_3 Å, c = 5.18_8 Å).

No evidence whatsoever was found which would indicate the presence of a Hf_6Si_5 or $HfSi_{1-x}$ phase with a CrB-type structure similar to that in the Zr-Si system.

Barest traces of an unidentifiable phase in the vicinity of 45 At.% silicon were seen; this pattern probably is the phase recently observed[2] by H. Nowotny and co-workers. The diffraction lines of this U-1 designated phase were far too weak to permit measurement of the Debye-Scherrer powder photograph. In support of evidence[79] pointing to the fact that a $D8_8$-Nowotny phase is not present in the true binary Hf-Si system, it can be said that this crystal structure was not observed in Hf-Si binary samples which were heat treated at 1300°C. However, almost all the samples in the range of 30 to 48 At.% silicon, as well as those in this intermediate vicinity in the ternary Hf-Si-C region, did not attain complete equilibrium at 1300°C. This is evidenced by the observance of all four phases, Hf_2Si, Hf_5Si_2, traces of U-1, and HfSi in all X-ray films throughout this region.

At 1300°C in sintered samples from the binary Hf-Si system, as well as in ternary Hf-Si-C samples near the Hf-Si binary, no signs of a possible Hf_4Si or Hf_3Si were observed.

b. The Hf-Si-C Equilibria at 1300°C

The Hf-Si system is characterized by the formation of a ternary, $D8_8$-Nowotny phase with but a small homogeneous range at 1300°C.

This phase is located at a composition of $Hf_{55}Si_{33}C_{12}$ at 1300°C. Because of its rather small homogeneous range and the fact that at 1300°C complete equilibrium was not established in this region — even after the long time heat treatment — , the phase was never obtained as a

2. The Hafnium-Silicon-Carbon System

Over 50 samples were prepared in the ternary Hf-Si-C and binary Hf-Si systems together; these specimens for solid state investigations at 1300°C were prepared by hot pressing and subsequent heat treatment.

Figure 24 shows the compositional location and qualitative X-ray analysis of the 1300°C samples.

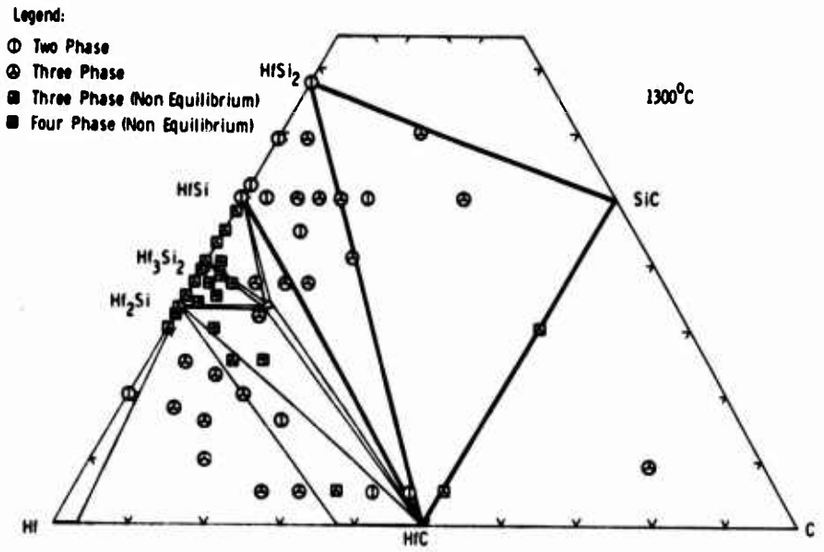

Figure 24. Hf-Si-C: Location and Qualitative X-ray Analysis of 1300°C Samples.

a. The Hf-Si System

The results of the binary Hf-Si samples heat treated at 1300°C showed that the hafnium-silicon system is less complex, as far as the number of appearing phases is concerned, than its sister system zirconium-silicon. The following phases and crystal structures were observed and confirmed (lattice parameters in parenthesis): $HfSi_2$, orthorhombic, C49 type ($a = 3.67_4$ Å, $b = 14.56$ Å, $c = 3.63_1$ Å); HfSi, orthorhombic, B-27 type ($a = 6.87_3$ Å, $b = 3.76_8$ Å, $c = 5.22_4$ Å), Hf_3Si_2, tetragonal, U_3Si_2-type

($a = 6.98_2$ Å, $c = 3.66_3$ Å); and Hf_2Si, tetragonal, C 16 type ($a = 6.55_3$ Å, $c = 5.18_8$ Å).

No evidence whatsoever was found which would indicate the presence of a Hf_6Si_5 or $HfSi_{1-x}$ phase with a CrB-type structure similar to that in the Zr-Si system.

Barest traces of an unidentifiable phase in the vicinity of 45 At.% silicon were seen; this pattern probably is the phase recently observed[2] by H. Nowotny and co-workers. The diffraction lines of this U-1 designated phase were far too weak to permit measurement of the Debye-Scherrer powder photograph. In support of evidence[79] pointing to the fact that a $D8_8$-Nowotny phase is not present in the true binary Hf-Si system, it can be said that this crystal structure was not observed in Hf-Si binary samples which were heat treated at 1300°C. However, almost all the samples in the range of 30 to 48 At.% silicon, as well as those in this intermediate vicinity in the ternary Hf-Si-C region, did not attain complete equilibrium at 1300°C. This is evidenced by the observance of all four phases, Hf_2Si, Hf_5Si_2, traces of U-1, and HfSi in all X-ray films throughout this region.

At 1300°C in sintered samples from the binary Hf-Si system, as well as in ternary Hf-Si-C samples near the Hf-Si binary, no signs of a possible Hf_4Si or Hf_3Si were observed.

b. The Hf-Si-C Equilibria at 1300°C

The Hf-Si system is characterized by the formation of a ternary, $D8_8$-Nowotny phase with but a small homogeneous range at 1300°C.

This phase is located at a composition of $Hf_{55}Si_{33}C_{12}$ at 1300°C. Because of its rather small homogeneous range and the fact that at 1300°C complete equilibrium was not established in this region — even after the long time heat treatment — , the phase was never obtained as a

single-phased alloy. The $D8_8$ phase forms two-phase equilibria with HfSi, H_3Si_2, Hf_2Si, and HfC_{1-x}; the best measurable lattice parameters of the $D8_8$ phase taken from a multiphase Hf-Si-C: 48/37/15 X-ray powder photograph were: a = 7.83$_2$ Å and c = 5.54$_2$ Å.

The HfC_{1-x} phase, which is the most stable phase in the ternary Hf-Si-C system, forms two phase equilibria with all other binary phases excepting Hf_3Si_2.

Figure 25 depicts the equilibrium of the Hf-Si-C system at 1300°C.

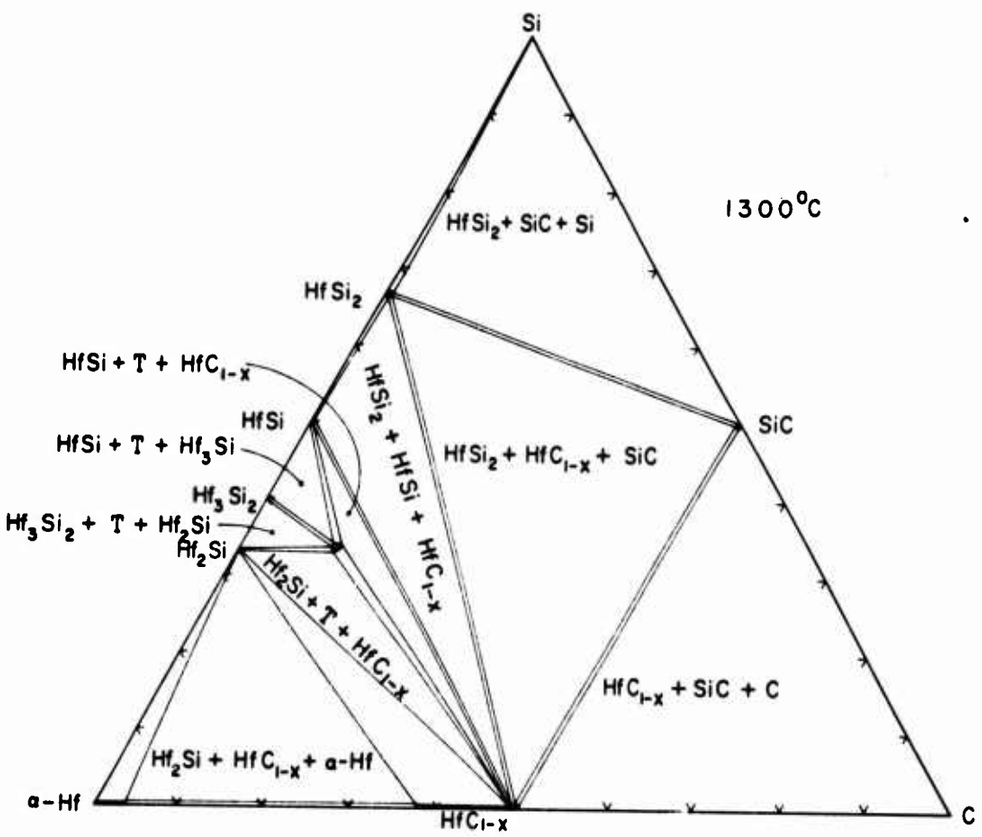

Figure 25. Hf-Si-C: Section at 1300°C.

The mutual solubilities of the binary silicide and carbide phases of the Hf-Si-C system are exceedingly small and in some cases, nonexistant at 1300°C. Lattice parameter measurements of the $HfSi_2$ phase show a slight enlargement of the orthorhombic unit cell pointing to a slight interstitial solubility probably of the order of 1/2 - 3/4 of an atomic percent carbon. The binary $HfSi_2$ values of a = 3.67_4 Å, b = 14.56 Å, c = 3.63_1 Å enlarge to a = 3.67_5 Å, b = 14.57 Å, and c = 3.63_8 Å. These values were obtained from a Hf-Si-C: 21/60/19 sample which contained the $HfSi_2$ phase in equilibrium with SiC.

The HfSi structure distorts slightly, showing a trace solubility for carbon. The binary lattice parameters of a = 6.87_3 Å, b = 3.76_8 Å, c = 5.22_4 Å change to a = 6.86_8 Å, b = 3.77_9 Å, and c = 5.22_4 Å in a Hf-Si-C: 40/50/10 ternary sample.

Due to the nonequilibrium conditions leading to quite diffuse Hf_3Si_2 patterns no measurement of the Hf_3Si_2 phase, which occurred in the ternary region, was possible. However, visual examination of the X-ray powder patterns indicated that the Hf_3Si_2 phase has no solubility into the ternary field.

There is no change in the crystal dimensions of the Hf_2Si phase in carbon containing ternary samples, and therefore no carbon solubility in the tetragonal Hf_2Si phase. In a similar manner, no solubility was observed in β-SiC, whose lattice parameter remained unchanged compared to the binary value at 4.35_8 Å in ternary, hafnium containing specimens. Qualitative evaluation of the X-ray, Debye-Scherrer powder photographs of various ternary alloys containing the cubic HfC_{1-x} phase, as well as precise lattice parameter measurements, have shown that all silicon containing phases, except Hf_2Si, which are in equilibrium with HfC_{1-x}, coexist with a HfC_{1-x} of a practically stoichiometric composition. In addition, it is noted that there is but a barest solubility — probably not greater than 1/2 an atomic percent silicon — shown by the more carbon defect end of the HfC_{1-x} homogeneous range. The lattice parameters of the HfC_{1-x} homogeneous range available from a previous investigation[11] were obtained from material containing 4.1 At%

zirconium. The hafnium used in these studies contained 6 At.% zirconium, and the respective lattice parameters are expected to be slightly larger but not so much larger so as to confuse interpretation of the solubilities in the Hf-Si-C system. The lattice parameter of the HfC_{1-x} phase taken from a Hf-Si-C:16/9/75 sample in the SiC-HfC_{1-x}-C region was 4.64_2 Å compared to 4.64_0 Å[11] in a binary Hf-C alloy with 2.1 At.% less zirconium and a carbon content of 50 At.%. By the same token, an alloy from the α-Hf-Hf_2Si-HfC_{1-x} three-phase region had an HfC_{1-x} lattice parameter of 4.62_4 Å, whereas the lattice parameter of the corresponding binary HfC_{1-x} phase[11] with less zirconium showed 4.61_9 Å. These results indicate an extremely slight — if any — solubility of silicon in the extreme carbon defect end of the HfC_{1-x} phase.

c. Melting Point Investigations

Figure 26 shows the compositional location of the melting point samples of the Hf-Si-C ternary and Hf-Si binary systems.

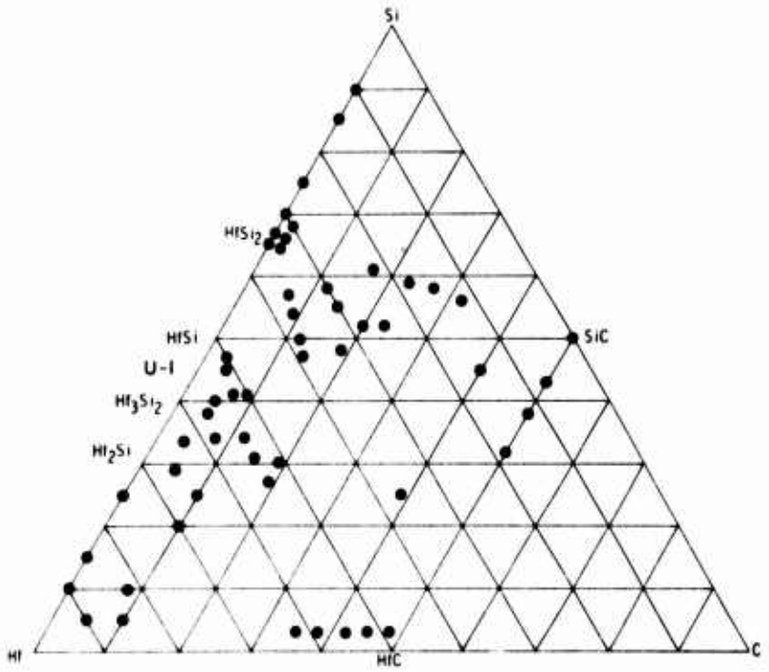

Figure 26. Hf-Si-C: Location of Melting Point Samples.

Partial investigations in the Hf-Si binary system have shown that a eutectic exists between $HfSi_2$ and silicon. Results with the Pirani hole technique indicate the eutectic temperature to be between 1322° and 1340°C. Incipient melting temperatures varied somewhat due to electrical contact difficulties encountered with the semiconductor silicon. Subsequent metallography showed the eutectic point to be at approximately 9 At.% Hf.

Figures 27 and 28 show the metallographic structures obtained from this region of the Hf-Si binary system.

Figure 27. Hf-Si: 15/85, Quenched from 1340°C. X250
Primary $HfSi_2$ (White Grains with Cracks) in $HfSi_2$-Si Matrix.

The melting point of $HfSi_2$ was determined to be 1571°C; the individual melting behavior of samples from the disilicide region as well as other binary and ternary Hf-Si-C alloys are listed in Table 13 at the end of this section.

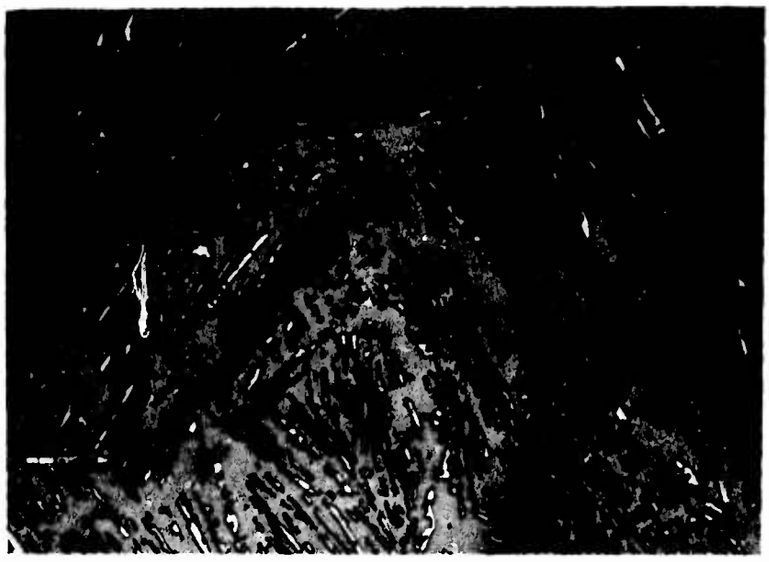

Figure 28. Hf-Si: 10/90, Quenched from 1340°C X400
$HfSi_2$-Si Eutectic Structure (Slightly Silicon-Rich)

A eutectic was also observed between β-Hf and Hf_2Si. The eutectic temperature was determined as 1806°C. Although the exact location of the β-Hf-Hf_2Si eutectic was not determined, the eutectic point probably lies between about 12 and 16 At.% silicon. Figure 29 shows the β-Hf-Hf_2Si eutectic with primary metal phase.

In the binary Hf-C there is a eutectic between β-Hf and HfC_{1-x} at about 1.5 At.% C[11]. In the ternary area, the three-phases present in this region, β-Hf, Hf_2Si, and HfC_{1-x} probably form a ternary eutectic close to the Hf-Si side in the hafnium corner although no HfC_{1-x} could be detected metallographically due to the small percentage of carbide which would be present in this eutectic. Furthermore, no decided minimum in melting temperatures was observed from the melting point samples in this region. This behavior indicates again that the ternary eutectic lies quite close to the Hf-Si binary; the ternary eutectic temperature probably is not much lower than the β-Hf-Hf_2Si eutectic temperature of 1806°C. The melting points and melting behavior of alloys from this region are shown in Table 13.

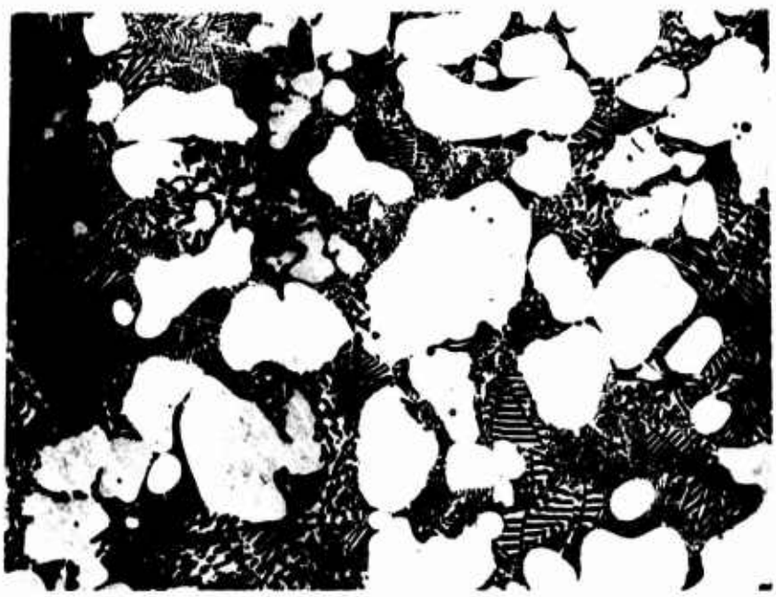

Figure 29. Hf-Si: 90/10, Quenched from Approximately 1830°C. X400

Primary β-Hf (White Grains) in a β-Hf-Hf_2Si Eutectic Matrix

Figure 30 shows primary β(transformed)-Hf with the eutectic structure observed in this region.

Powder X-ray diagrams of the molten portions of samples from the ternary region near the $D8_8$ phase showed that the homogeneous region of this phase increases with increasing temperature similar to the behavior of the $D8_8$ phase in the Zr-Si-C system. The homogeneous region of this phase at temperatures near melting is Hf: 62-55, Si: 33-37, and C: 3-11 atomic percent; this homogeneous region is not as large as that observed with the $D8_8$ phase in the Zr-Si-C system. The $D8_8$ phase melts with a broat maximum in the ternary region; the highest incipient melting temperature observed for the $D8_8$ phase was 2467°C in a Hf-Si-C:62/35/3 sample.

As in the analogous Zr-Si-C system, the $D8_8$ phase most probably forms a eutectic with HfC_{1-x}; because, however, of the great difference in melting points of these two compounds, the eutectic point lies quite close to the $D8_8$ phase, and a eutectic which would contain a relatively

small amount of HfC_{1-x} was not observed metallographically. Figure 31 shows a two-phased HfC_{1-x}-$D8_8$ alloy.

Figure 30. Hf-Si-C: 90/5/5, Quenched from 1908°C. X680

Primary β-Hf (Transformed) (Dark Grey Grains) with β-Hf-Hf_2Si Eutectic on Grain Boundaries (Small Amount of HfC_{1-x} not Resolved).

Lattice parameter measurements as well as metallographic examination of ternary alloys near the HfC_{1-x} homogeneous range in the binary Hf-C system showed that the solubility of silicon in the HfC_{1-x} phase is not increased at higher temperatures. Metallography showed carbide grains with the silicide phases on the grain boundaries; there were no signs of silicide precipitation from the carbide grains. The following metallographic pictures (Figures 32 and 33) depict the findings from the area near HfC_{1-x} in the ternary Hf-Si-C system.

The measured lattice parameters also show that virtually no silicon is taken into solid solution. Table 11 compares the lattice

Figure 31. Hf-Si-C: 54/27/19, Quenched from >2600°C. X1000

Primary HfC_{1-x} Dendrites (Light, Heavily Etch Stained) in $D8_8$ Matrix (Grey with Cracks).

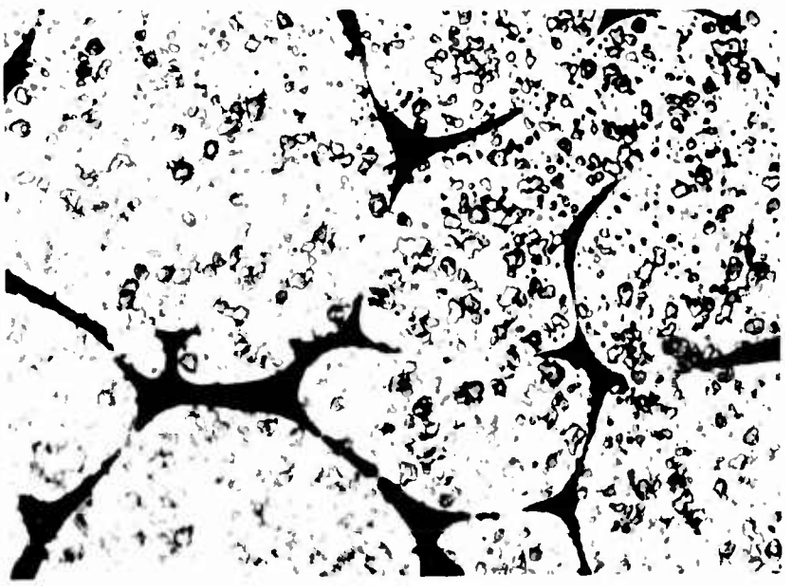

Figure 32. Hf-Si-C: 59/3/38, Quenched from 3581°C. X750

HfC_{1-x} (Large White Grains, Heavily Etch Stained) With Hf_2Si in Grain Boundaries.

parameters of the HfC_{1-x} phase of ternary silicon containing alloys with those of the corresponding silicon-free binary Hf-C alloys.

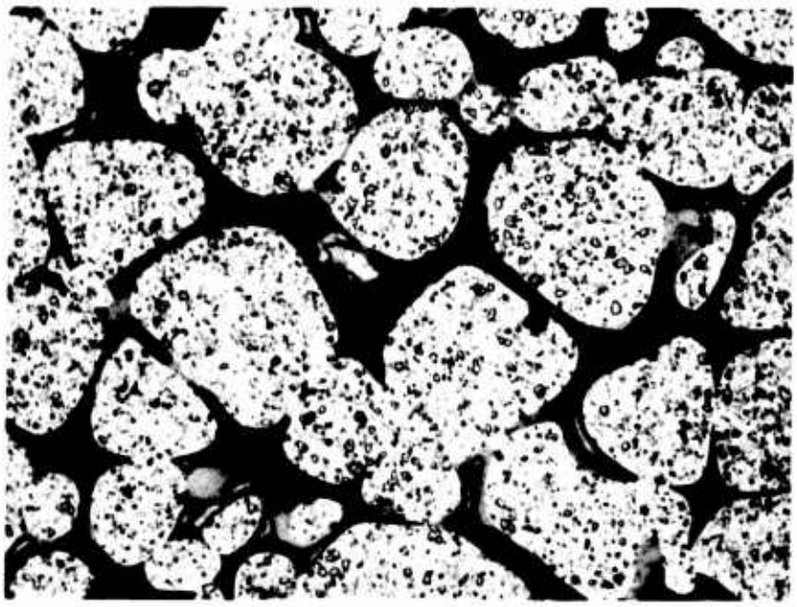

Figure 33. Hf-Si-C: 62/3/35, Quenched from 3302°C X600
HfC_{1-x} (Large White Grains, Heavily Etch Stained) With Hf_2Si (With Cracks) in Grain Boundaries. Lighter Grey Areas Preferentially More Lightly Etched.

Table 11. Lattice Parameters of the Cubic HfC_{1-x} Phase in Both Silicon-Containing and Silicon-Free Alloys

Nominal Composition in At.%			Lattice Parameter in Å	Corresponding Si-Free Alloys		Lattice Parameter in Å
Hf	Si	C		Hf	C	
18	32	50	4.63_8	51	49	4.64_0
49	3	48	4.63_9	51	49	4.64_0
59	3	38	4.62_9	58.5	41.5	4.62_8

The remnants of the silicon carbide from ternary Hf-containing samples, which had not decomposed upon heating to high temperatures, showed no change in lattice parameter compared with the pure binary

β-SiC: there is no high temperature solubility of hafnium silicides or carbide in silicon carbide.

The hafnium silicides present in ternary alloys which had been molten showed no changes in lattice parameters beyond those small changes noted in ternary samples at 1300°C; in addition, metallographic studies did not reveal any carbide precipitations from the silicide grains. These results lead to the conclusion that, as at lower temperatures, there is virtually no carbide solubility in the hafnium silicides at high temperatures.

The melting point samples in the regions of the ternary Hf-Si-C system containing the SiC phase in equilibrium with either $HfSi_2$ or HfC_{1-x} behaved in the same manner as those samples from the Zr-Si-C system. Decomposition of the SiC phase occurred, and samples suitable for metallographic examination were not obtained.

Similar to the results in the Zr-Si-C system, most interphase melting temperatures along various pseudo-binary sections in the ternary Hf-Si-C system are governed by the lowest melting component. Table 12 shows the minimum melting temperatures along several pseudo-binary sections in the ternary Hf-Si-C system. In addition, Table 13 lists the melting temperatures, melting behavior, and qualitative X-ray analysis of the Hf-Si-C samples studied.

Table 12. Minimum Melting Temperatures of Various Pseudo-Binary Sections in the Hf-Si-C System.

Section	Lowest Incipient Melting Temperature in °C
$HfSi_2$-SiC	1422°
$HfSi_2$-HfC_{1-x}	1521°
HfSi-HfC_{1-x}	1611°
$D8_8$(ternary)-HfC_{1-x}	2189°
Hf_2Si-HfC_{1-x}	2148°
HfC_{1-x}-SiC	2662°

Table 13. Melting Temperatures, Melting Behavior and Qualitative X-ray Analysis of Hf-Si-C alloys

Nominal Compositions in At.%			Melting Temperatures °Centigrade			Phases Present Qualitative
Hf	Si	C	Incipient	Collapsing	Melting Behavior	X-ray Analysis
10	90	0	1322	1322	quite sharp	Si + $HfSi_2$
15	85	0	1340	1340	somewhat heterog.	Si + $HfSi_2$
30	70	0	1373	1477	very heterogeneous	$HfSi_2$ + l. Si
33.3	66.7	0	1371	1571	quite heterogeneous	$HfSi_2$ + tr Si + tr HfSi
35	65	0	1561	1587	quite heterogeneous	$HfSi_2$ + Hf-Si + tr Si
75	25	0	2086	2132	very heterogeneous	Hf_2Si + Hf
85	15	0	1806	1816	quite heterogeneous	Hf + Hf_2Si
90	10	0	1806	-	quite heterogeneous	Hf + Hf_2Si
90	5	5	1832	1908	quite heterogeneous	Hf + Hf_2Si + tr HfC
82	10	8	1837	1847	heterogeneous	Hf + Hf_2Si + HfC
62	3	35	1966	3302	extremely heterog	HfC + Hf_2Si
59	3	38	2157	3581	extremely heterog	HfC + Hf_2Si
55	3	42	-	3784	extremely heterog	HfC + tr $D8_8$
52	3	45	-	3716	extremely heterog	HfC + tr ?
49	3	48	-	3643	very heterogeneous	HfC + tr ?
70	20	10	2005	2066	very heterogeneous	Hf_2Si + Hf + HfC
65	25	10	2148	2270	very heterogeneous	Hf_2Si + l. Hf + tr $D8_8$
66	29	5	2230	2255	heterogeneous	$D8_8$ + Hf_2Si + HfC
54	27	19	2322	2600	very heterogeneous	$D8_8$ + HfC + l. HfSi
54	31	15	2189	2367	very heterogeneous	HfC + $D8_8$ + HfSi
51	30	19	2138	2210	very heterogeneous	HfC + HfSi + tr $D8_8$

Table 13 (continued)

Nominal Compositions in At.%			Melting Temperatures °Centigrade			
Hf	Si	C	Incipient	Collapsing	Melting Behavior	Phases Present Qualitative X-ray Analysis
15	45	40	2556	2598	very heterog decompo	HfC + $HfSi_2$ + SiC + Si
36	25	39	1516	2505	very heterog decompo	HfC + tr $HfSi_2$
18	32	50	-	2564	very heterog.decompo	HfC + SiC + l. $HfSi_2$
12	38	50	2662	2900	very heterog decompo	HfC + SiC + $HfSi_2$
54	34	12	2230	2240	very heterogeneous	$D8_8$ + HfC + l. HfSi
58	34	8	2312	2518	heterogeneous	$D8_8$ + l. HfC
62.5	33.5	4	2467	2518	heterogeneous	$D8_8$ + tr HfC
57	38	5	2271	2496	very heterogeneous	$D8_8$ + tr HfC
55	40	5	2312	2508	very heterogeneous	$D8_8$ + tr HfC
52	41	7	2196	2353	very heterogeneous	$D8_8$ + l. HfC + l. HfSi
50	41	9	2179	2416	very heterogeneous	$D8_8$ + HfSi + HfC
51	45	4	2189	2231	very heterogeneous	HfSi + HfC + $D8_8$
50	47	3	1611	2211	quite heterogeneous	HfSi + l. $D8_8$ + l. HfC
39	47	14	1582	1668	quite heterogeneous	HfC + $HfSi_2$ + l. HfSi
38	50	12	1587	1687	quite heterogeneous	HfC + $HfSi_2$ + l. HfSi
37	54	9	1559	1581	quite heterogeneous	$HfSi_2$ + HfC
36	57	7	1567	1585	heterogeneous	$HfSi_2$ + HfC
30	68.5	15	1381	1487	heterogeneous	$HfSi_2$ + Si + tr HfC
32	66	2	1516	1560	heterogeneous	$HfSi_2$ + Si + l. HfC
33.5	64.5	2	1521	1567	heterogeneous	$HfSi_2$ + tr Si + l. HfC
22	61	17	1422	1596	heterogeneous	HfC + $HfSi_2$ + l. Si + l. SiC
18	59	23	1426	-		$HfSi_2$ + SiC + l. Si + HfC
15	58	27	1436	2387	very heterogen	SiC + Si + HfC + $HfSi_2$
30	58	12	1494	1516	very heterogeneo	$HfSi_2$ + HfC + tr Si

Table 13 (continued)

Nominal Compositions in At.%			Melting Temperatures • Centigrade			
Hf	Si	C	Incipient	Collapsing	Melting Behavior	Phases Present Qualitative X-ray Analysis
30	55	15	1467	1513	heterogeneous	$HfSi_2$ + HfC + 1.SiC + Si
28	52	20	1475	1486	heterogeneous	$HfSi_2$ + HfC + 1.SiC + Si
25	52	23	1463	-	heterogeneous	$HfSi_2$ + HfC + 1.SiC + Si
33	48	19	1467	1643	heterogeneous	HfC + $HfSi_2$ + tr. SiC

3. The Zirconium-Silicon-Boron System

E. Parthe and J.T. Norton[6] have made a comprehensive study of the Zr-Si-B system at 1400° (Figure 12), and it was deemed not necessary to repeat this phase of the investigations.

a. Melting Point Results and High Temperature Mutual Solubilities

Figure 34 shows the compositional location of the Zr-Si-B alloys on which melting point studies were made; again, because of electrical contact difficulties with the extremely silicon and boron-rich alloys, as well as the limited knowledge available on the Si-B binary system, the investigations in this ternary system were mainly concerned with the high temperature solubilities and melting temperatures of the metal-rich areas near the Zr-Si binary as well as those regions near ZrB_2.

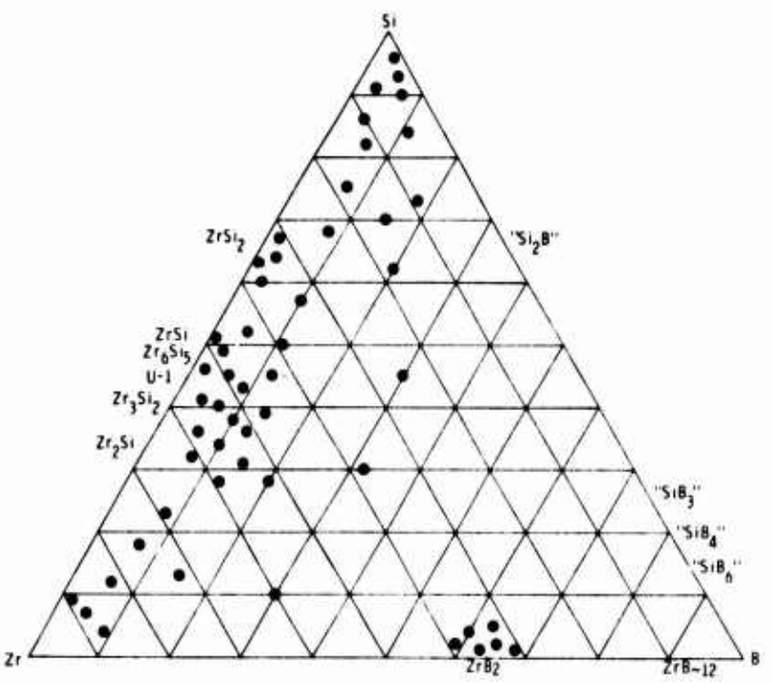

Figure 34. Zr-Si-B: Location of Melting Point Samples.

There is a eutectic in the binary Zr-B system at 12% B[28] which consists of ZrB_2 and β-Zr; the eutectic temperature is 1660°C; this eutectic, coupled with the eutectic in the Zr-Si binary between β-Zr and Zr_2Si at approximately 9 At.% Si[3] ($T_{eut.}$ = 1630°C)[3] gives rise to a ternary eutectic consisting of β-Zr, Zr_2Si, and ZrB_2. This ternary eutectic lies near Zr-Si-B: 65/12/23. The ternary eutectic melts at 1536°C, close to 100°C lower than the eutectic in the binary Zr-Si and Zr-B systems.

Figures 35 and 36 show the metallographic findings in the zirconium-portion of the Zr-Si-B system.

Figure 35. Zr-Si-B: 60/10/30, Arc Melted X300

Primary ZrB_2 (Large White Spears) in Ternary ZrB_2-β-Zr-Zr_2Si Eutectic (ZrB_2-Worm-Like Slivers,) Zr_2Si (Dark Grey Grains), and β-Zr (Transformed) (White Grains).

In analogy to the ternary phase in the Zr-Si-C system, the ternary $D8_8$ phase in the Zr-Si-B system increases its homogeneous range at higher temperatures; as evidenced by X-ray powder photographs of the molten portions of samples in this region, the $D8_8$ phase encompasses the

range Zr: 63-55, Si: 30-38, B: 5-11 At.%. The lattice parameters of this phase in a Zr-Si-B 54/31/15 sample were: a = 7.96$_0$ Å c = 5.60$_0$Å; these values show the increase in homogeneous range of the $D8_8$ phase, for Parthe[6] reports 7.94 Å and 5.57 Å as the lattice parameters of this phase at 1400°C.

Figure 36. Zr-Si-B: 72/13/15, Arc Melted. X1000

Primary Zr_2Si (Gray Grains in β-Zr(Transformed) (White)-ZrB_2 (Light Grey, Worm-Like) Eutectic.

Melting point results, which are tabulated in Table 15 show that the $D8_8$ phase melts with a rather large, flat maximum at temperatures varying from 2242° to 2343°C. The maximum melting point of the $D8_8$ phase was obtained in a sample of the composition Zr-Si-B: 62/32/6.

A eutectic exists between the ternary $D8_8$ phase and ZrB_2. As to be expected, the eutectic point lies rather close to the $D8_8$ homogeneous range. With the aid of metallography, the eutectic was located

at a composition quite close to Zr-Si-B: 54/31/15. The following photomicrograph shows this eutectic (Figure 37).

Figure 37. Zr-Si-B: 54/31/15, Arc Melted. X400

$D8_8$ (Ternary Phase)-ZrB_2 Eutectic.

ZrB_2 (White Spears) in $D8_8$ Matrix (Dark Grey with Cracks) with Small Amounts of ZrSi (B-27)(Light-Grey-White Patches).

In the region of the ternary system between the $D8_8$ phase and the binary ZrSi (B-27) phase, as well as on the ZrSi(B-27)- ZrB_2 section, high temperature liquid-solid reactions were virtually impossible to interpret. This difficulty stems to a great deal from the fact that the characteristics of the binary Zr-Si system in this area are not completely known and are indeed quite complicated. It must be said, however, that the monosilicide or Zr_6Si_5 phase with the CrB-type structure predominated in X-ray patterns of melted samples from this region. The indication is present, as in the Zr-Si-C system, that the silicide with CrB-type structure is either only a high temperature phase in the Zr-Si binary, or actually a ternary crystal structure stabilized by carbon and/or boron. The lattice parameters of the CrB-type crystal structure were found to be slightly different in two ternary samples:

Zr-Si-B: 48/43/9; a = 3.74_1 Å, b = 9.91_3 Å, c = 3.73_8 Å and Zr-Si-B: 49/48/3; a = 3.74_7 Å, b = 9.92_0 Å, and c = 3.74_4 Å. At this time a decision cannot be reached as to whether these changes are from a slight ternary homogeneous range or from a Zr_6Si_5 homogeneous range in the Zr-Si binary. Clarification of area of the Zr-Si-B system must await specific elucidation of the binary Zr-Si system.

Lattice parameter measurements of the melted areas of alloys containing ZrSi (B-27) and $ZrSi_2$ phases in ternary samples containing boron showed that there was no change whatsoever in the lattice parameters when compared with those of the pure binary silicides. Metallographically, faint traces of ZrB_2 were visible on the grain boundaries, and in the silicon phase there were no signs of boride precipitations from the silicide grains. These results indicate that there is no high temperature solubility of borides in the silicides ZrSi and $ZrSi_2$. Figure 38 shows a typical photomicrograph of alloys in the immediate vicinity of the binary $ZrSi_2$.

Figure 38. Zr-Si-B: 31/67/2, Quenched from Approximately 1630°C. X1000

$ZrSi_2$ (Large Light Grey Grains with Cracks) with Silicon (Dark Grey) Containing Minute Traces of ZrB_2 (Faint White Spots).

Along the section ZrB_2-Si there is a pseudo-binary eutectic very close to the silicon corner. The large difference in melting points between the diboride and silicon led, in the majority of cases, to a coagulation of the small amount of ZrB_2 present on the silicon grain boundaries. Only in isolated parts of the melted samples, where the quenching rate was exceedingly rapid, was the typical worm-like diboride-silicon eutectic obtained. The following two microphotographs (Figures 39 and 40) depict the findings along the ZrB_2-Si section.

Figure 39. Zr-Si-B: 9/73/18, Quenched from 1374°C X500

ZrB_2 (Dark Angular Grains) Along with Small Amounts of $ZrSi_2$ (White Grains) in Silicon Matrix (Grey).

Melting point results of the alloys along this section showed that the eutectic temperature is 1374°C; the eutectic point lies at a concentration of less than about 9 Mol.% ZrB_2.

The small contraction of the lattice parameter of silicon, which was noticed, (5.41$_9$ Å vs 5.43$_0$ Å for pure Si) is attributed to a small solubility of boron in silicon[6].

The ZrB_2 phase showed no solubility for silicon or silicides; the lattice parameters of the diboride phase were the same in both ternary, silicon-containing alloys and binary ZrB_2 specimens: a = 3.16_7 Å and c = 3.53_0 Å.

Metallographically, no evidence of solubility or a temperature dependent solubility (precipitations) curve for silicon was observed.

The following figures (Figures 41 and 42) show the metallographic findings in the vicinity of the ZrB_2 phase.

Figure 40. Zr-Si-B: 3/90/7, Quenched from 1374°C X600

ZrB_2-Si Eutectic; Trace Amounts of $ZrSi_2$ (White Grains).

Table 14 lists the minimum melting temperatures of various pseudo-binary sections in the Zr-Si-B system; in Table 15 the melting temperatures and behavior, as well as the qualitative X-ray analysis of the Zr-Si-B alloys examined are tabulated.

Figure 41. Zr-Si-B: 36/4/60, Quenched from 2847°C X400

ZrB_2 (Large White Grains) with $D8_8$ (Ternary Silicoboride), ZrSi, and Traces of Zirconium Metal in Grain Boundaries.

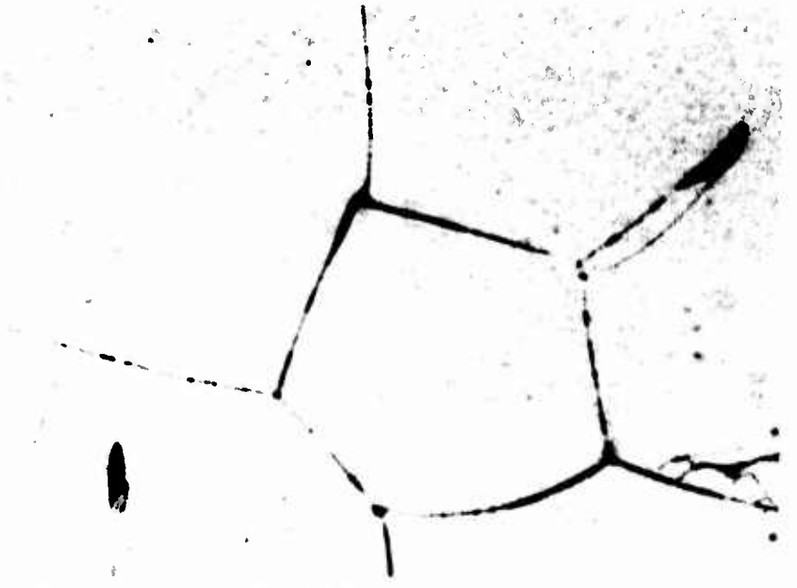

Figure 42. Zr-Si-B: 31/1/68, Quenched from 3012°C X1000

ZrB_2 with Traces of Silicon and/or a Silicoboride on Grain Boundaries.

Table 14. Minimum Melting Temperatures of Various Pseudo-Binary Sections in the Zr-Si-B System.

Section	Minimum Incipient Melting Temperature, °C
ZrB_2-Si	1374°
ZrB_2-$ZrSi_2$	1587°*
ZrB_2-ZrSi	2215°*
ZrB_2-$D8_8$(ternary)	2312°*
ZrB_2-Zr_2Si	2312°*

* Probably slightly lower — binary Zr-Si not investigated.

4. The Hafnium-Silicon-Boron System

a. Solid State Investigations

Figure 43 shows the compositional locations and qualitative X-ray analysis of the Hf-Si-B alloys heat-treated at 1300°C.

At 1300°C the predominate feature of this ternary system is the formation of a ternary $D8_8$-Nowotny phase at a composition of $Hf_{52}Si_{38}B_{10}$. The homogeneous range of this ternary phase is quite small, and inspection of the Debye-Scherrer films of alloys from this region indicate that the phase is stabilized less easily than those analogous phases in the Zr-Si-C, Zr-Si-B, and Hf-Si-C systems. No single-phased alloy of the $D8_8$ phase was obtained. The lattice parameters of the $D8_8$ phase at various compositions are listed in Table 16. Alloys lying in the region bounded by approximately Hf_2Si, Hf_3Si_2, and the ternary $D8_8$ phase were found not to have attained complete equilibrium, even after the long time heat treatment at 1300°C. Four phases were always present in varying amounts: Hf_2Si, Hf_3Si_2, HfB_2,

Table 15. Melting Temperatures, Melting Behavior and Qualitative X-ray Analysis of Zr-Si-B Alloys

Nominal Compositions in At.%			Melting Temperatures °Centigrade			
Zr	Si	B	Incipient	Collapse	Melting Behavior	Phases Present Qualitative X-ray Analysis
87	4	9	1587	1597	somewhat heterog.	Zr + v.l. Zr_2Si + v.l. ZrB_2
88	7	5	1567	1567	heterogeneous	Zr + tr ZrB_2 + tr Zr_2Si
89	9	2	1582	1582	somewhat sharp	Zr + tr ZrB_2 + tr Zr_2Si
82	12	6	1546	1546	somewhat heterog.	Zr + v.l. ZrB_2 + l. Zr_2Si
75	18	7	1597	1597	somewhat heterog	Zr_2Si + ZrB_2 + tr Zr
72	13	13	1546	1546	somewhat sharply	Zr_2Si + l. ZrB_2 + tr Zr
60	10	30	~1536	1536	heterogeneous	Zr + Zr_2Si + l. ZrB_2
69	23	8	~1924	-	very heterogeneous	Zr_2Si + $D8_8$ + l. ZrB_2 + tr Zr
59	28	13	1883	2312	heterogeneous	$D8_8$ + l. ZrB_2
54	31	15	2333	2333	fairly sharp	$D8_8$ + l. ZrB_2
38	30	32	2149	2200	very heterog.	ZrB_2 + $ZrSi_2$ + Zr_6Si_5
61	32	7	2343	2343	somewhat sharp	$D8_8$ + v.l. ZrB_2 + tr Zr_2Si
58	36	6	2242	2312	heterogeneous	$D8_8$ + l. ZrB_2
56	34	10	2323	2323	somewhat sharp	$D8_8$ + l. ZrB_2
51	36	13	2230	2240	somewhat sharp	$D8_8$ + ZrB_2 + l. Zr_6Si_5
47	39	14	2230	2261	heterogeneous	ZrB_2 + $D8_8$ + Zr_6Si_5
52	38	10	2250	2271	heterogeneous	$D8_8$ + ZrB_2 + l. Zr_6Si_5
56	40	7	2250	2261	somewhat heterog	Zr_6Si_5 + $D8_8$ + l. ZrB_2
52	46	2	2260	2260	somewhat sharp	$D8_8$ + Zr_6Si_5 + tr ZrB_2
49	48	3	2215	2215	fairly sharp	Zr_6Si_5 + tr $ZrSi_2$ + tr ZrB_2
49	45	6	2215	2215	somewhat sharp	ZrSi + tr. $ZrSi_2$ + l. ZrB_2 + l Zr_6Si_5

Table 15 (continued)

Nominal Compositions in At.%			Melting Temperatures °Centigrade			Phases Present Qualitative
Zr	Si	B	Incipient	Collapse	Melting Behavior	X-ray Analysis
48	43	9	2230	2240	heterogeneous	Zr_6Si_5 + l. ZrB_2 + tr $ZrSi_2$
43	45	12	1678	1923	very heterogeneous	ZrSi + ZrB_2 + tr $ZrSi_2$
39	50	11	1663	1740	quite heterogeneous	$ZrSi_2$ + ZrSi + l. ZrB_2
25	45	30	1566	1648	very heterogeneous	$ZrSi_2$ + ZrB_2 + tr Si
43	52	5	1668	1832	very heterogeneous	ZrSi + $ZrSi_2$ + l. ZrB_2
27	60	3	1622	1658	quite heterogeneous	$ZrSi_2$ + tr ZrB_2 + ZrSi
33	57	10	1617	1638	heterogeneous	$ZrSi_2$ + ZrB_2
18	62	20	~1374	1394	rather heterogeneous	$ZrSi_2$ + ZrB_2 + Si
24	68	8	1384	1384	quite heterogeneous	$ZrSi_2$ + ZrB_2 + Si
15	70	15	1465	1465	somewhat sharp	$ZrSi_2$ + Si + ZrB_2
10	86	4	1364	1364	somewhat sharp	Si + $ZrSi_2$
6	91	3	1360	1380	heterogeneous	Si + ZrSi + tr ZrB_2
1	96	3	1389	-	heterogeneous	Si + tr $ZrSi_2$ + tr. ZrB_2
3	90	7	~1374	-	somewhat heterog.	Si + ZrB_2 + l. $ZrSi_2$
5	84	11	1379	1379	heterogeneous	Si + $ZrSi_2$ + l. ZrB_2
9	73	18	1374	-	somewhat heterog	Si + $ZrSi_2$ + l. ZrB_2
48	51	1	1628	1678	heterogeneous	ZrSi + l. $ZrSi_2$ + l. ZrB_2
32	5	63	≈2179	-	extremely heterog.	ZrB_2 + tr ?
36	4	60	~2282	2847	extremely heterog	ZrB_2 + v.l. $D8_8$ + tr "ZrB"(B1)
39	2	59	~2261	2909	extremely heterog	ZrB_2 + tr Zr + tr"ZrB"(B1)
36	1	63	~2476	3033	extremely heterog	ZrB_2 + tr "ZrB"(B1)
33	2	65	~2538	3048	extremely heterog	ZrB_2 + tr ?
31	1	68	~2384	3012	very heterogeneous	ZrB_2 + tr ?
36	63	1	~1617	1653	heterogeneous	$ZrSi_2$ + ZrSi + tr. ZrB_2 + tr Si
33	64	3	1587	1648	very heterogeneous	$ZrSi_2$ + ZrSi + tr. ZrB_2 + tr Si
31	67	2	1617	1617	heterogeneous	$ZrSi_2$ + v.l. ZrB_2 + tr Si+tr ZrSi

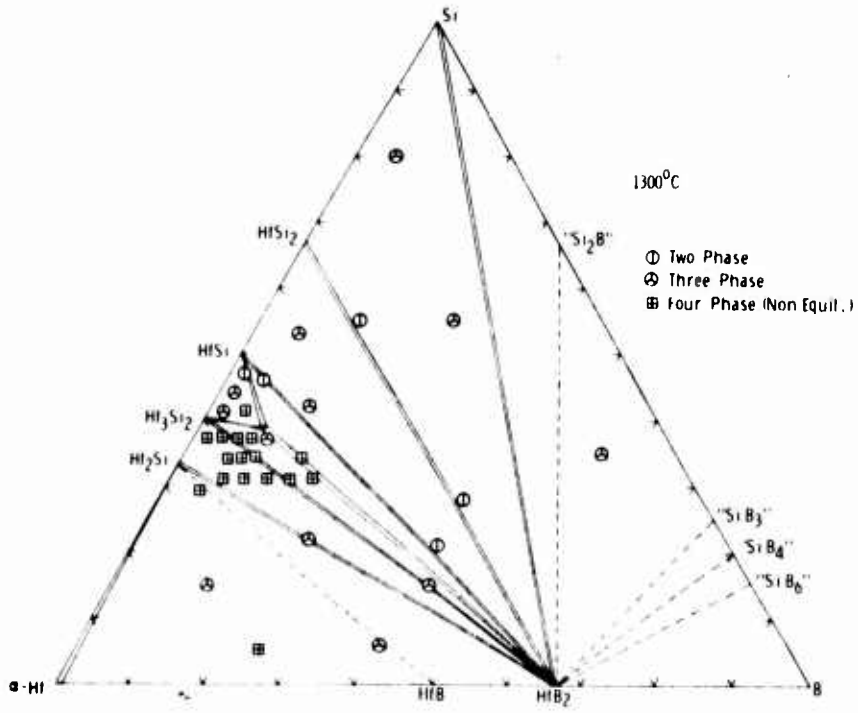

Figure 43. Hf-Si-B: Location and Qualitative X-ray Analysis of 1300°C Samples.

Table 16. Lattice Parameters of the Hf-Si-B $D8_8$ Phase

Composition in At.%			Lattice Parameters in Angstroms	
Hf	Si	B	a	c
57	41	2	7.79_5	5.52_2
53	37	10	7.79_2	5.50_7
50	34	16	7.80_6	5.52_3

and the $D8_8$-ternary phase. In spite of this difficulty, it was concluded that the equilibrium Hf_3Si_2-HfB_2 exists rather than the Hf_2Si-$D8_8$ (ternary) at 1300°C.

In contrast to its sister system, Zr-Si-B, the Hf-Si-B ternary does not show any evidence of the formation of a CrB-type crystal structure in the vicinity of the binary Hf-Si system. It must be said, however, that very faint traces of an unknown pattern, presumably the recently discovered[2] U-1,σ-similar,phase in the Hf-Si binary, were observed in the vicinity of 40-45 At.% Si in the Debye-Scherrer powder patterns of alloys containing up to 5 At.% boron. Since this pattern did not manifest itself with any degree of intensity, no indication of the possible equilibria formed with this phase is given in the isothermal section . In fact, confirmation of this phase and establishment of the exact characteristics of the binary Hf-Si system must await future studies on this binary system.

Figure 44 shows the isothermal section of the Hf-Si-B system at 1300°C.

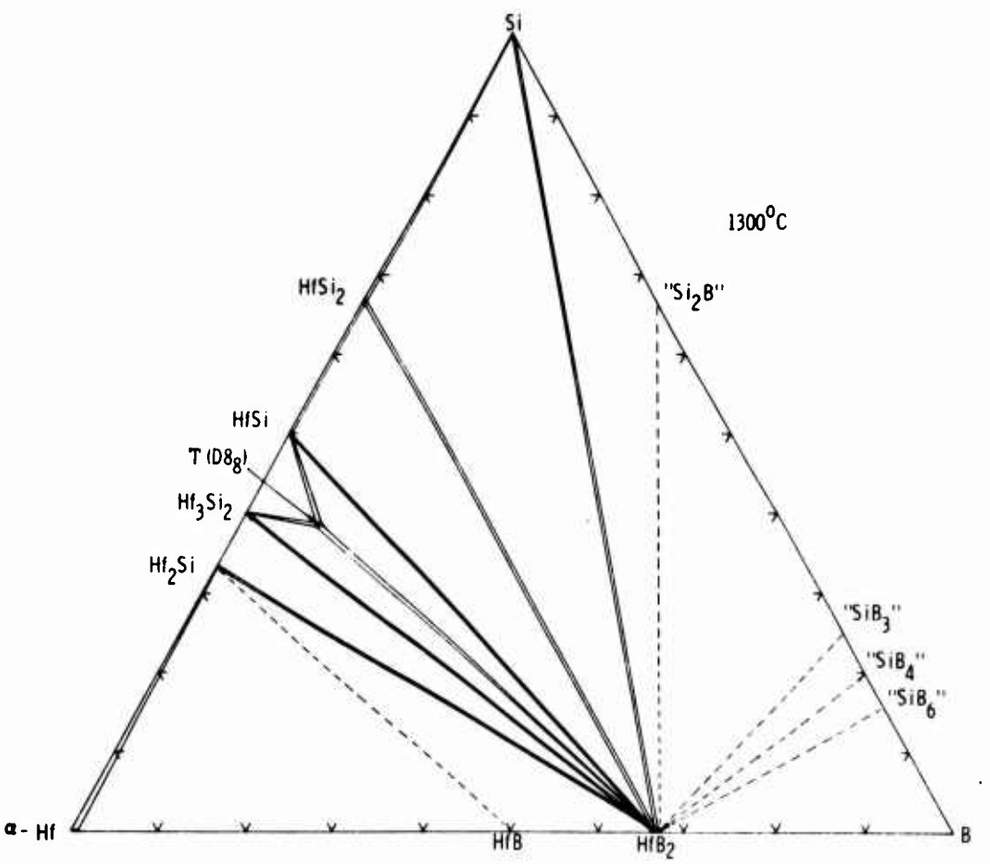

Figure 44. Hf-Si-B: Section at 1300°C.

HfB_2, the most stable phase in this system, forms two-phase equilibria with all the hafnium silicides and silicon as well.

E. Rudy[49] has indicated that hafnium monoboride may decompose in a very slow reaction to hafnium metal and diboride at a temperature near 1250°C. Only one of the ternary samples in the Hf-Si-B solid state studies gave any evidence of the presence of the HfB phase; the X-ray film of this one sample, Zr-Si-B: 70/5/25, showed slight traces of the B-27 type structure along with major quantities of Hf_2Si, HfB_2, and hafnium metal. In accord with previous findings[49], it seems that the formation of the HfB phase takes place very slowly, especially in the presence of the extremely stable diboride. Owing to the uncertainty of the stability of the HfB near the 1300°C[49] the equilibrium of HfB with Hf_2Si can be indicated only with uncertainty in Figure 44.

The mutual solubilities of the hafnium silicides and hafnium diboride are exceedingly small at 1300°C; lattice parameter measurements of the binary phases in ternary samples indicate that the solubilities are minimal and probably not greater than about 1/2 an atomic percent. Table 17 compares the lattice parameters of the pure binary compounds with those measured in ternary alloys.

Table 17. Lattice Parameters of Binary Hf-Si and Hf-B Phases Measured in Binary and Ternary Alloys

Phase	Lattice Parameters in Angstroms					
	Binary			Ternary		
	a	b	c	a	b	c
$HfSi_2$	3.67_4	14.56	3.63_1	3.67_3	14.56	3.64_3
HfSi	6.87_3	3.76_8	5.22_4	6.87_7	3.77_1	5.23_3
Hf_2Si	6.55_3	-	5.18_8	6.54_4	-	5.18_1
HfB_2	3.14_2	-	3.47_7	3.13_8	-	3.48_1

Accurate lattice parameter measurements were not able to be made on the Hf_3Si_2 phase in ternary boron containing alloys due to the quite diffuse nature of the Debye-Scherrer photographs; however, visual inspection of these films indicates no ternary solubility in this phase.

The dashed lines, showing possible equilibria with the suspected Si-B phases, are depicted only to indicate these possibilities. An X-ray film of samples in this region of the ternary system showed mainly the lines of HfB_2 and Si; other faint lines were attributed to amorphous boron and/or possibly one or more of the uncertain silicoborides.

b. Melting Point Results and High Temperature Solubilities

Figure 45 shows the compositional locations of the Hf-Si-B melting point samples. Again, due to the poor conductivity of the more silicon and boron-rich alloys, the investigations were limited to the region bounded by the Hf-HfB_2-Si triangle.

The eutectic in the hafnium-silicon binary between β-hafnium and Hf_2Si at approximately 12-16 At.% Si and the eutectic in the hafnium-boron binary between β-hafnium and HfB give rise to a ternary eutectic consisting of β-Hf, Hf_2Si, and HfB. Metallographic evidence and melting point results showed the ternary eutectic is located close to the composition Hf-Si-B: 75/10/15. The eutectic temperature is about 1841°C. Due to the rapid agglomeration of the boride on the grain boundaries of the Hf_2Si and Hf phases, no typical eutectic structure was observed in this area; the closest approach to a eutectic-like structure is shown in one of the following pictures. Figures 46 - 48 show the typical metallographic findings in the metal-rich portion of the Hf-Si-B ternary.

Qualitative X-ray analysis and metallography of both arc-melted and melting point samples from the vicinity of the ternary $D8_8$ phase show that the homogeneous range of the ternary phase enlarges somewhat at higher temperatures; the single phase region is not, however, as

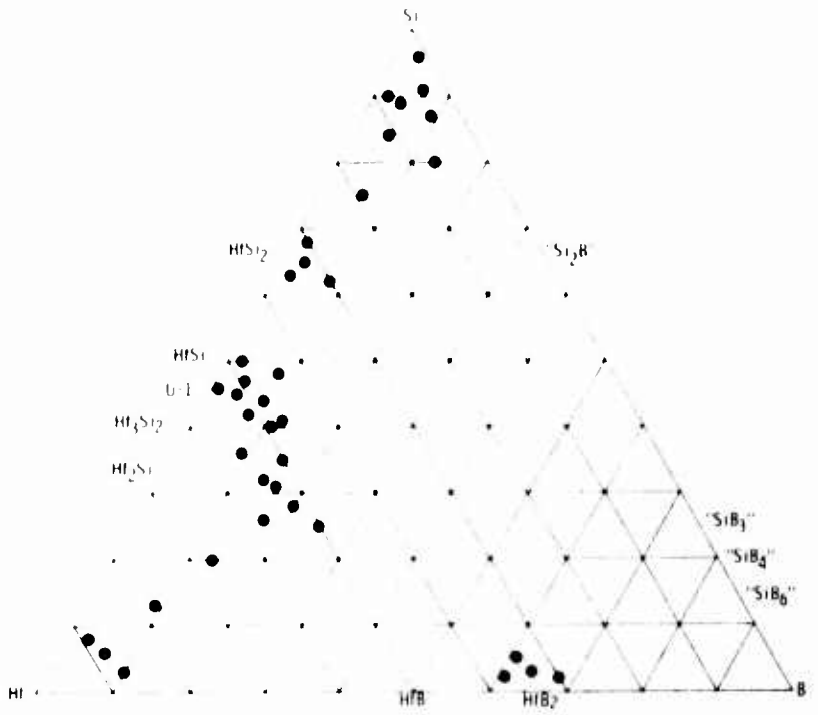

Figure 45. Hf-Si-B: Location of Melting Point Samples.

Figure 46. Hf-Si-B: 67/20/13, Arc Melted. X400

Hf_2Si (Grey Grains) with β-Hf(Transformed) in Between Grains, and Small Amount of HfB (White Grains).

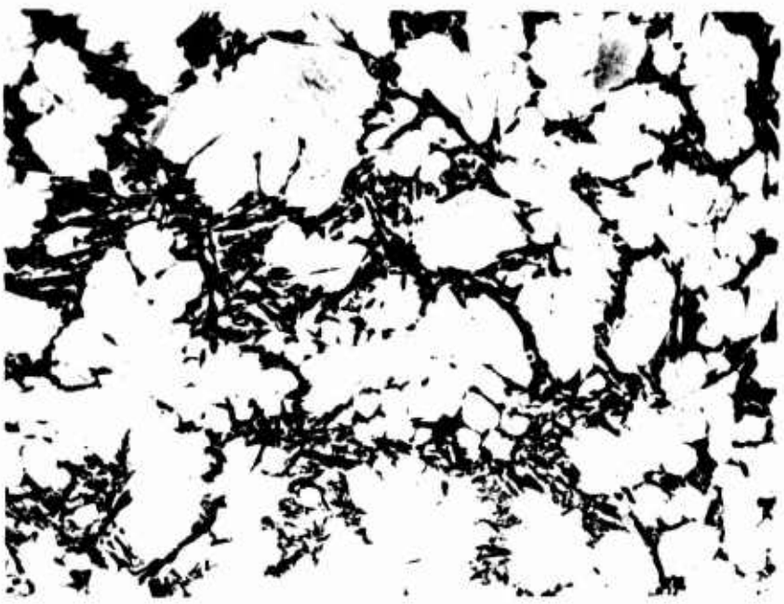

Figure 47. Hf-Si-B: 87/3/10, Arc Melted. X400

Primary β-Hf(Transformed)(Light Grains) with HfB Spears (Dark)(Partially Agglomerated) and Hf_2Si-β-Hf Eutectic on Grain Boundaries

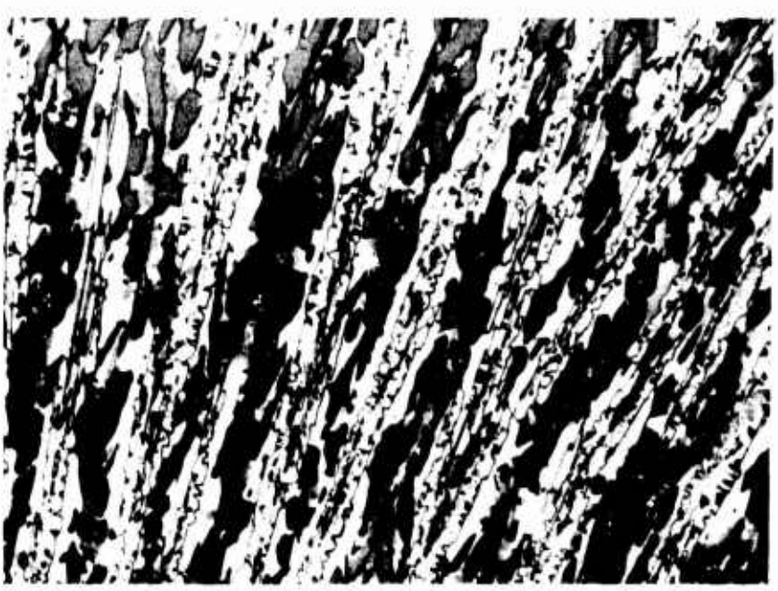

Figure 48. Hf-Si-B: 54/6/40, Arc Melted. X680

HfB (Light Mottled Grains)-Hf_2Si(Dark Grey Grains)-β-Hf(Transformed)(Light Grey). Partially Agglomerated Eutectic.

large as those corresponding single phase regions of the $D8_8$ phase in the other systems investigated herein. The Hf-Si-B $D8_8$ region assumes the following dimensions at temperatures near melting: Hf: 60-67, Si: 32-37, B: 6-13. The ternary phase melts with a flat maximum; the highest recorded melting temperature for the $D8_8$-phase was 2425°C, and the largest lattice parameters were: $a = 7.81_4$ Å and $c = 5.516_6$ Å.

The $D8_8$ phase forms a eutectic with HfB_2; the eutectic point lies quite close to the ternary phase, probably quite near the composition Hf-Si-B: 54/32/14. The eutectic temperature was determined to be close to 2380°C. The following two photomicrographs depict the eutectic structure observed in this area.

Figure 49. Hf-Si-B: 52/28/20. Arc Melted X325

Primary HfB_2 (Light) Spears in HfB_2-$D8_8$ (Ternary) Eutectic.

Figure 50. Hf-Si-B: 52/28/20, Arc Melted. X1000
HfB_2-$D8_8$ Eutectic. (from Eutectic Portion of Sample)

There is also a eutectic formed between HfB_2 and silicon; this eutectic is very silicon-rich and is located at less than 10 mole percent HfB_2 along the HfB_2-Si section. The eutectic temperature as determined on several samples from this pseudo-binary section is 1388°C. The extreme difference in melting points between HfB_2 and silicon made it quite difficult to obtain a eutectic structure from this silicon-rich region. A small portion of one sample ,which apparently cooled quite rapidly,produced the following photomicrograph (Figure 51).

The slight contraction observed in the lattice parameter of silicon is attributed to a small solubility of boron in silicon[6].

Similar to the findings in the Hf-Si-C system, no phase with the chromium monoboride-type crystal structure was observed in melting point samples from the Hf-Si-B system. It is apparent that this

crystal structure is not stabilized in either boron or carbon containing hafnium silicon ternary systems; this observation leaves reason to suspect that the reported $ZrSi_{1-x}$ or Zr_6Si_5 (CrB-type) is a ternary crystal structure and not a true binary compound.

Figure 51. Hf-Si-B: 3/91/6, Quenched from Approximately 1400°C. X600

HfB_2-Si Eutectic, HfB_2-Dark Spears, Traces of $HfSi_2$ (White Grains) Visible.

Lattice parameter measurements on the silicide phases, measured in boron-containing samples, showed that there was no change in the crystal dimensions beyond those slight changes noted in 1300°C solid state samples when compared to the pure binary phases. Figure 52 shows the presence of small quantities of HfB_2 in the immediate vicinity of the $HfSi_2$ phase. As also noted in part "a" of the Hf-Si-B section, no accurate lattice parameter measurements were possible on the Hf_3Si_2 phase due to the diffuse Debye-Scherrer patterns of this crystal structure; however, visual comparison of the patterns available with those of the pure binary indicate that no solubility for borides is present at high temperatures.

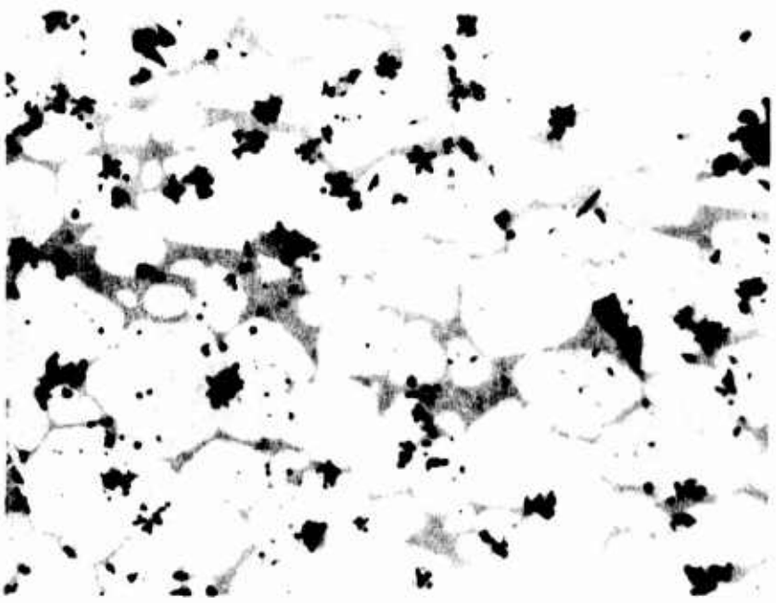

Figure 52. Hf-Si-B: 30/68/2, Quenched from Approximately 1571°C. X750

$HfSi_2$ (Large White Grains), Si (Grey) Matrix, and Clusters of HfB_2 on Grain Boundaries.

Figure 53 shows a microphotograph of a ternary alloy in the vicinity of the HfB_2 binary phase. The silicide on the grain boundaries is plainly visible and no precipitations in the boride grains are seen. This observation, as well as the fact that the lattice parameters of the diboride phase in alloys which were held at high temperatures showed no change over those values of similar samples held at 1300°C, indicates that there is no high temperature solubility of silicon or silicides in HfB_2.

Table 18 lists the minimum melting temperatures of various pseudo-binary sections in the Hf-Si-B ternary system, and Table 19 lists the melting behavior and temperatures as well as the qualitative X-ray analysis of the Hf-Si-B melting point samples.

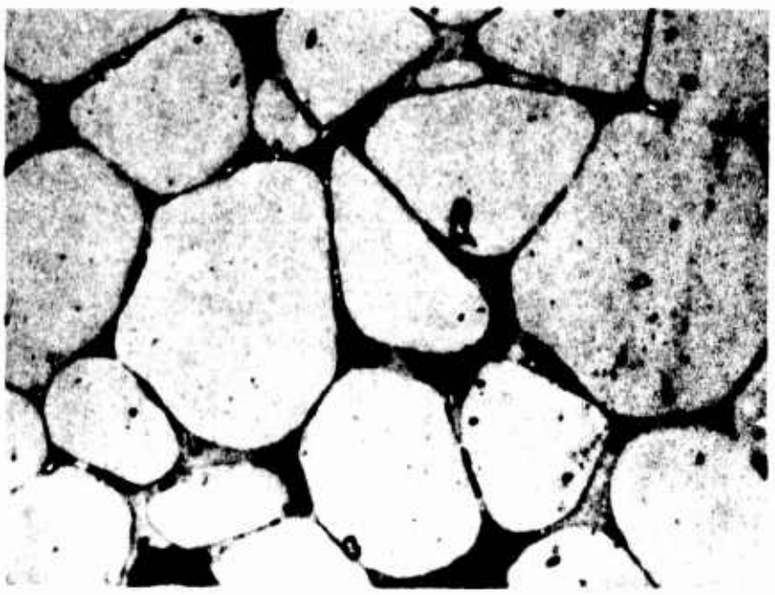

Figure 53. Hf-Si-B: 34/5/61, Quenched from Approximately 2800°C. X1000

HfB_2 (Large Grey Grains) with Hf_2Si and β-Hf in Between Grains.

Table 18. Minimum Melting Temperatures of Various Pseudo-Binary Sections in the Hf-Si-B System.

Section	Minimum Incipient Melting Temperature, °C
HfB_2Si	1388°
HfB_2-$HfSi_2$	1576°*
HfB_2-HfSi	1627°*
HfB-Hf_2Si	1806°*
HfB_2-$D8_8$(ternary)	2380°

* Binary Hf-Si not yet accurately known

Table 19. Melting Temperatures, Melting Behavior, and Qualitative X-ray Analysis of Hf-Si-B Alloys

Nominal Composition in At.%			Melting Temperatures °Centigrade			
Hf	Si	B	Incipient	Collapse	Type of Melting	Phases Present Qualitative X-ray Analysis
3	91	6	1388	1388	somewhat sharp	Si + l. HfB_2 + v.l. $HfSi_2$
4	87	9	1388	1388	somewhat heterog	Si + l. HfB_2 + l. $HfSi_2$
7	80	13	1383	1383	slightly heterog	Si + l. HfB_2 + l. $HfSi_2$
8	90	2	1319	1319	sharp	Si + $HfSi_2$
11	84	5	1352	1363	heterogeneous	Si + $HfSi_2$ + tr. HfB_2
19	75	6	1352	1383	heterogeneous	$HfSi_2$ + Si + tr. HfB_2
30	68	2	1433-1453	1571	heterogeneous	$HfSi_2$ + Si + tr HfB_2
32	65	3	1474	1576	heterogeneous	$HfSi_2$ + l. Si
35	63	2	1576	1612	heterogeneous	$HfSi_2$ + tr. Si + tr HfB_2
30	62	8	1545	1566	heterogeneous	$HfSi_2$ + tr. HfB_2
48	50	2	1657	2127	very heterogeneous	HfSi + v.l. D8 + tr. HfB_2
44	48	8	1637	1910	very heterogeneous	HfSi + HfB_2 + tr. $D8_8$
49	47	4	1637	2157	very heterogeneous	HfSi + $D8_8$ + HfB_2
51	45	4	1668	2230	very heterogeneous	$D8_8$ + HfSi + HfB_2
53	46	1	1637	2210	very heterogeneous	$D8_8$ + HfSi
48	44	8	1627	2127	very heterogeneous	$D8_8$ + HfSi + HfB_2
51	42	7	1637	2207	heterogeneous	$D8_8$ + v.l. HfSi + v.l. HfB_2
49	40	11	1642	2227	heterogeneous	$D8_8$ + v.l. HfSi + HfB_2
47	41	12	1657	2166	very heterogeneous	HfSi + $D8_8$ + HfB_2
57	34	9	2425	2425	somewhat sharp	$D8_8$ + l. HfB_2
50	35	15	1667	2280	heterogeneous	$D8_8$ + tr HfB_2 + tr HfSi

Table 19 (continued)

Nominal Composition in At. %			Melting Temperatures °Centigrade			
Hf	Si	B	Incipient	Collapse	Type of Melting	Phases Present Qualitative X-ray Analysis
54	32	14	1688	2415	heterogeneous	$D8_8 + HfB_2$
53	31	16	2310	2415	heterogeneous	$D8_8 + HfB_2$
52	28	20	2394	2394	sharp	$D8_8 + HfB_2$
50	25	25	2370	2415	somewhat heterog	$D8_8 + HfB_2$
57	26	17	2310	2385	quite heterogeneous	$D8_8$ + 1. HfB_2 + tr (HfB(B1)
67	20	13	2015	2087	heterogeneous	$Hf_2Si + HfB_2$ + tr Hf
78	13	9	1841	1841	quite heterogeneous	Hf_2Si + Hf
89	8	3	1821	1821	somewhat heterog	Hf + 1. Hf_2Si
88	6	6	1790	1805	heterogeneous	Hf + Hf_2Si
87	3	10	1852	1862	heterogeneous	Hf + tr Hf_2Si + tr HfB (B1)
34	5	61	1769	2800	very heterogeneous	HfB_2 + tr HfB (B1) + tr ?
37	2	61	2435	-	very heterogeneous	HfB_2 + 1. $D8_8$ + tr. HfB (B1)
33	3	64	2147	-	very heterogeneous	HfB_2 + tr HfB (B1) + tr ?
30	2	68	2096-2177	-	very, very heterog	HfB_2 + tr ?
60	19	21	1954	2015	heterogeneous	HfB + Hf_2Si + Hf + tr HfB_2
70	10	20	1913	1923	heterogeneous	HfB + Hf_2Si + Hf + tr HfB_2
62	10	28	1949	2005	heterogeneous	HfB + Hf_2Si + Hf + tr HfB_2

IV. DISCUSSION

The purpose of these investigations into the phase equilibria and maximum solidus regions of the four ternary systems studied is to present general guidelines and specific temperature limitations for feasible application possibilities of composite materials involving combinations of hafnium-silicon-carbon, hafnium-silicon-boron, zirconium-silicon-carbon, and zirconium-silicon-boron. In addition to the presentation of the general high temperature characteristics of these ternary systems, it would have been beneficial to have been able to provide detailed descriptions of the complex liquid-solid equilibrium; however, until the necessary information concerning the exact characteristics of the binary systems Hf-Si, Zr-Si, Si-C, and Si-B becomes available, a thorough interpretation and description of the liquid-solid regions of the ternary systems Hf-Si-C, Hf-Si-B, Zr-Si-C, and Zr-Si-B is not possible.

Since many of the silicides of the refractory metals exhibit high temperature oxidation resistance, although the modes of protection are different for various silicides, it is of basic interest to know how these silicides behave at higher temperatures in the presence of other materials such as carbides and borides. Hafnium and zirconium diboride, themselves, exhibit high temperature oxidation resistance, and even with the possibility of great mutual solubilities between silicides and diborides or carbides ruled out by reason of crystal structural energetical considerations; a proven small solubility of silicon in the diborides or carbides might have increased the innate oxidation resistance of the diborides or carbides. The results of these investigations show, however, that in all cases the mutual solubilities of silicides with borides and carbides at low as well as at high temperatures are practically nil; increased oxidation resistance of borides and carbides is not to be found by attempting to incorporate silicon or silicides into the diboride or carbide crystal lattices.

In addition to the fact that there is virtually no silicon or silicide solubility in the diborides and carbides, it is seen from the results of melting point investigations that composites of silicides — in particular hafnium and

zirconium silicides — with borides and carbides are limited in high temperature application. In general, the interphase melting temperatures between silicides and borides or carbides are strongly governed by the much lower melting silicides. The exceptions to this low melting behavior in the systems studied is to be found along the sections $D8_8$ (ternary phase) — refractory-metal carbide or refractory-metal diboride as well as the sections HfC-SiC and ZrC-SiC.

From the phase diagrams of the two silicocarbide systems investigated, Hf-Si-C and Zr-Si-C, it is seen that no silicide is in equilibrium with graphite, and any attempts to combine a hafnium or zirconium silicide with graphite for high temperature use such as in an oxidation protective scheme for graphite would lead to rapid failure not only at the lower melting points of the silicides, but at even lower temperatures due to interphase reactions predicted by the phase equilibria of the ternary systems.

In this matter, as noted previously[24], the only refractory-metal silicide — actually a silicocarbide — of all refractory metal-silicon-carbon systems studied, which is in equilibrium with graphite is the ternary $D8_8$ phase in the Mo-Si-C[24] system.

Of all the pseudo-binary sections investigated in this study of the four ternary systems, the two sections HfC-SiC and ZrC-SiC appear to be promising for moderately high temperature applications if such a combination is ever desired. However, it must be said that the compounds HfC, ZrC, and SiC individually behave far more favorably with their higher melting points than pseudo-binary combinations; the melting or decomposition point of these pseudo-binary mixtures containing SiC is depressed-several hundred degrees below that of pure SiC. It was unfortunate that the region bounded by the refractory metal carbide-SiC-C was not able to be investigated for ternary eutectics due to the decomposition of SiC as well as difficulties due to the nonavailability of DTA container materials; nonetheless, it may be assumed that in the presence of a possible ternary eutectic in this region, the high temperature capabilities of such refractory carbide-SiC combinations in contact with graphite would be limited to temperatures probably

not much higher than about 2100°C. These temperatures are considerably lower than the possible application temperatures of a refractory metal carbide graphite mixture.

REFERENCES

1. H. Nowotny, B. Lux, and H. Kudielka: Mh. Chem. 87 (1956), 447.
2. O. Schob, H. Nowotny, and F. Benesovsky: Planseeber, 10 (1962), 65.
3. C. E. Lundin, D.J. McPherson, and M. Hansen: Trans.ASM. 45 (1953)901
4. K. Schubert, H.G. Meissner, and W. Rossteutscher: Naturewiss, 21 (1964) 506.
5. O. Schob, H. Nowotny, and F. Benesovsky: Mh.Chem. 92 (1961) 1218.
6. E. Parthe and J.T. Norton: Mh. Chem. 91 (1960) 1127.
7. E. Rudy, D.P. Harmon, and C.E. Brukl: AFML-TR-65-2, Part I, Volume II (May 1965).
8. R. Kieffer and F. Benesovsky: Hartstoffe, Springer-Verlag, Vienna, 1963, pg. 101.
9. R.V. Sara, C.E. Lowell, and R.T. Dolloff: WADD-TR-60-143, Part IV (1963).
10. R.V. Sara: J.Amer. Ceram. Soc. 48 (1965), 243.
11. E. Rudy: AFML-TR-65-2, Part I, Volume IV (Sept 1965).
12. A.E. Van Arkel: Physica, 4 (1924) 286.
13. J. Farr: Unpublished Work Quoted by E.K.Storms: LAMS-2674 (1962).
14. J. Farr: Data reported by E.K.Storms: Critical Review of Refractories, A.E.C., L.A. 2942 (March, 1964)
15. F. Benesovsky and E. Rudy: Planseeber Pulvermet., 8 (1960), 66.
16. C. Agte and H. Alterthum: Z. Tech. Physik, 11 (1930), 182.
17. K. Portnoi, Y.Levinski, and W. Fadejeva: Akad.ezvest. Nauk, SSSR, ezvest.Tekhn.Nauk, Metallurgija i Topliov 2 (1961) 147.
18. D. Cotter and J. Kohn: J. Amer. Ceram. Soc., 37 (1954), 441.
19. K. Becker and F. Ebert: Z.Physik, 31 (1925), 368.
20. R. Sara and C.E. Lowell: WADD TDR-60-143, Part V (1964).
21. N.H. Krikorian: lit. cit. ref. #13.

REFERENCES (Cont'd)

22. M. Hansen: Constitution of Binary Alloys, McGraw-Hill, 1958, pg 378.

23. N. Thibault: Amer. Min. 29 (1944) 249 and 327.

24. H. Nowotny, E. Parthe, R. Kieffer, and F. Benesovsky: Mh.Chem. 85

25. O. Ruff: Trans. Elektrochem. Soc., 68 (1935) 87.

26. R. Scarce and G. Slack: J. Chem. Phys. 30 (1959), 1551.

27. R.T. Dolloff: WADD-TR-60-143, Part I, (1960).

28. E. Rudy and St. Windisch: AFML-TR-65-2, Part I, Vol.VIII, Jan 1966.

29. P.M. McKenna: Ind. Eng. Che. 28 (1936) 767.

30. R. Kiessling: Acta Chem. Scand. 3 (1949) 90.

31. E. Rudy and F. Benesovsky: Mh. Chem. 92 (1961) 415.

32. K. Moers: Z. anorg. allg. Chem. 198 (1931) 262.

33. C. Agte: Thesis, Technische Hochschule Berlin, 1931.

34. F. Glaser and B. Post: Trans. AIME 197 (1953) 1117.

35. P. Schwarzkoph and F. Glaser: Z.Metallkunde 44 (1953) 353.

36. B. Post and F. Glaser: J. Chem. Phys. 20 (1952) 1050.

37. F.W. Glaser: Trans. AIME 194 (1952) 391.

38. W. Schedler: Thesis, Technische Hochschule Graz, Austria (1951)

39. L. Brewer, D. Sawyer, D. Templeton, and C. Dauben: J. Am.Cearm. Soc., 34 (1951) 173.

40. Op. Cit. Ref. #8, pg. 387.

41. F. Glaser, D. Moskowitz, and B. Post: J. Metals 5 (1953), 1119.

42. C. Agte and K. Moers: Z. anorg. allg. Chem. 198 (1931) 233.

43. R. Kieffer, F. Benesovsky, and E. Honak: Z. anorg. allg. Chem. 268 (1952) 191.

44. E. Rudy and F. Benesovsky: Mh. Chem. 92, (1961) 415.

REFERENCES (Cont'd)

45. H. Nowotny, F. Braun and F. Benesovsky: Radex-Rundsch (1960) 367.

46. E. R: ' 'hesis, Technische Hochschule, Vienna (1960).

47. L. Kaufman and E. Clougherty: RTD-TDR-63-4096 Part II, Feb. 1965.

48. Op. Cit. Ref. #8, pg. 396.

49. E. Rudy and St. Windisch: AFML-TR-65-2, Part I, Vol. IX., January 1966.

50. H. Moissan and A. Stock: Compt. Rend. 31 (1900) 139.

51. G.V. Samsonov and V.P. Latysheva: DAN SSSR 105 (1955) 483.

52. R. Adamsky: Acta. Cryst. 11 (1958) 744.

53. C. Cline: J. Electrochem.Soc. 106 (1959) 322.

54. C. Cline and D.E. Sands: Nature 185 (1960) 456.

55. E. Colton: J. Amer. Chem. Soc. 82 (1960) 1002.

56. V. Matkovich: Acta. Cryst., 13 (1960) 679.

57. H. Rizzo, B. Weber, and M. Schwartz: J.Amer.Ceram. Soc. 43 (1960), 497.

58. C. Brosset and B. Mangnusson: Nature 187 (1960) 54.

59. L. Brewer, D. Sawyer, D. Templeton, and C. Dauben: J.Amer.Ceram. Soc., 34 (1951), 173.

60. V. Sleptsov and G.V. Samsonov: Dopovidi Akad. Nauk.Ukr. RSR, (1959), 982.

61. W. Knarr: Dissertation, Univ. of Kansas (1959).

62. G. Samsonov and V. Sleptsov: Akad. Nauk. Ukr. RSR, Dopovidi 8 (1962), 1066

63. R. Elliott: Constitution of Binary Alloys, First Supplement, McGraw-Hill, 1965

64. H. Seyfarth: Z. Krist. 67 (1928), 295.

65. St. v. Naray-Szabo: Z. Krist. A97 (1937), 223.

66. G. Brauer and A. Mitius: Z. anorg. Chem. 249 (1942), 338.

REFERENCES (Cont'd)

67. G. Brauer and H. Haag: unpublished work quoted by Ref. 68 .

68. H. Schachner, H. Nowotny, and H. Kudielka: Mh.Chem. 85 (1954), 1140.

69. H. Schachner, H. Nowotny, and R. Machenschalk: Mh.Chem. 84 (1953), 677.

70. P. Pietrokowsky: Acta Cryst. 7 (1954), 435.

71. L. Brewer and O. Krikorian: A.E.C. Publ. UCRL-2544 (1954).

72. R. Kieffer, F. Benesovsky, and R. Machenschalk: Z. Metallkunde 45 (1954) 493.

73. L. Brewer and O. Krikorian: J. Electrochem. Soc. 103 (1956) 38.

74. P. Pietrokowsky: Quoted by Ref. #73.

75. C. H. Dauben: J. Electrochem. Soc. 104 (1957), 521.

76. Lit. Cit. Ref. #8, pg. 474 .

77. B. Post, F. Glaser, and D. Moskowitz: J. Chem. Phys., 22 (1954), 1264.

78. J.F. Smith and D.M. Bailey: Acta Cryst. 10 (1957), 341.

79. H. Nowotny, E. Laube, R. Kieffer, and F. Benesovsky: Mh. Chem. 89 (1958) 701.

80. Lit. Cit. Ref. #8 pg. 478.

81. E. Rudy, St. Windisch, and Y.A. Chang: AFML-TR-65-2, Part I, Vol. I. (1965).

DOCUMENT CONTROL DATA - R&D

(Security classification of title, body of abstract and indexing annotation must be entered when the overall report is classified)

1 ORIGINATING ACTIVITY (Corporate author)	2a REPORT SECURITY CLASSIFICATION
Aerojet-General Corporation Materials Research Laboratory Sacramento, California	Unclassified
	2b GROUP N.A.

3 REPORT TITLE

Ternary Phase Equilibria in Transition Metal-Boron-Carbon-Silicon Systems

Part II. Ternary Systems, Volume X. The Zr-Si-C, Hf-Si-C, Zr-Si-B, and Hf-Si-B Systems

4 DESCRIPTIVE NOTES (Type of report and inclusive dates)

RTD Technical Report

5 AUTHOR(S) (Last name, first name, initial)

Brukl, C. E.

6 REPORT DATE	7a TOTAL NO. OF PAGES	7b NO. OF REFS
September 1966	95	81

8a CONTRACT OR GRANT NO. AF 33(615)-1249 b PROJECT NO. 7350 c Task No. 735001 d	9a ORIGINATOR'S REPORT NUMBER(S) AFML-TR-65-2 Part II, Vol. X. 9b OTHER REPORT NO(S) (Any other numbers that may be assigned this report) N.A.

10 AVAILABILITY/LIMITATION NOTICES

This document is subject to special export controls, and each transmittal to foreign governments or foreign nationals may be made only with prior approval of Metals & Ceramics Div., AF Materials Laboratory, Wright-Patterson, AFB, Ohio.

11 SUPPLEMENTARY NOTES	12 SPONSORING MILITARY ACTIVITY
	AFML (MAMC) Wright-Patterson AFB, Ohio 45433

13 ABSTRACT

Phase equilibria and mutual solubilities in the Zr-Si-C, Hf-Si-C, and Hf-Si-B ternary systems have been determined at 1300°C. The general melting behavior and high temperature mutual solubilities in the Zr-Si-C, Hf-Si-C, Zr-Si-B, and Hf-Si-B systems have been studied; minimum melting temperatures along various pseudo-binary sections are given. All four systems are characterized by the formation of a ternary $D8_8$-Nowotny phase.

Most melting temperatures in the ternary systems are governed by the lower melting binary silicide compounds. Guidelines for feasible high temperature applications are given.

DD FORM 1 JAN 64 1473

Unclassified
Security Classification

14 KEY WORDS	LINK A		LINK B		LINK C	
	ROLE	WT	ROLE	WT	ROLE	WT
High Temperature Melting Points Phase Equilibria Silicocarbides Silicoborides Zirconium-Silicon-Carbon Hafnium-Silicon-Carbon Zirconium-Silicon-Boron Hafnium-Silicon-Boron						

INSTRUCTIONS

1. ORIGINATING ACTIVITY: Enter the name and address of the contractor, subcontractor, grantee, Department of Defense activity or other organization *(corporate author)* issuing the report.

2*a*. REPORT SECURITY CLASSIFICATION: Enter the overall security classification of the report. Indicate whether "Restricted Data" is included. Marking is to be in accordance with appropriate security regulations.

2*b*. GROUP: Automatic downgrading is specified in DoD Directive 5200.10 and Armed Forces Industrial Manual. Enter the group number. Also, when applicable, show that optional markings have been used for Group 3 and Group 4 as authorized.

3. REPORT TITLE: Enter the complete report title in all capital letters. Titles in all cases should be unclassified. If a meaningful title cannot be selected without classification, show title classification in all capitals in parenthesis immediately following the title.

4. DESCRIPTIVE NOTES: If appropriate, enter the type of report, e.g., interim, progress, summary, annual, or final. Give the inclusive dates when a specific reporting period is covered.

5. AUTHOR(S): Enter the name(s) of author(s) as shown on or in the report. Enter last name, first name, middle initial. If military, show rank and branch of service. The name of the principal author is an absolute minimum requirement.

6. REPORT DATE: Enter the date of the report as day, month, year, or month, year. If more than one date appears on the report, use date of publication.

7*a*. TOTAL NUMBER OF PAGES: The total page count should follow normal pagination procedures, i.e., enter the number of pages containing information.

7*b*. NUMBER OF REFERENCES: Enter the total number of references cited in the report.

8*a*. CONTRACT OR GRANT NUMBER: If appropriate, enter the applicable number of the contract or grant under which the report was written.

8*b*, 8*c*, & 8*d*. PROJECT NUMBER: Enter the appropriate military department identification, such as project number, subproject number, system numbers, task number, etc.

9*a*. ORIGINATOR'S REPORT NUMBER(S): Enter the official report number by which the document will be identified and controlled by the originating activity. This number must be unique to this report.

9*b*. OTHER REPORT NUMBER(S): If the report has been assigned any other report numbers *(either by the originator or by the sponsor)*, also enter this number(s).

10. AVAILABILITY/LIMITATION NOTICES: Enter any limitations on further dissemination of the report, other than those imposed by security classification, using standard statements such as:

(1) "Qualified requesters may obtain copies of this report from DDC."

(2) "Foreign announcement and dissemination of this report by DDC is not authorized."

(3) "U. S. Government agencies may obtain copies of this report directly from DDC. Other qualified DDC users shall request through

_____."

(4) "U. S. military agencies may obtain copies of this report directly from DDC. Other qualified users shall request through

_____."

(5) "All distribution of this report is controlled. Qualified DDC users shall request through

_____."

If the report has been furnished to the Office of Technical Services, Department of Commerce, for sale to the public, indicate this fact and enter the price, if known.

11. SUPPLEMENTARY NOTES: Use for additional explanatory notes.

12. SPONSORING MILITARY ACTIVITY: Enter the name of the departmental project office or laboratory sponsoring *(paying for)* the research and development. Include address.

13. ABSTRACT: Enter an abstract giving a brief and factual summary of the document indicative of the report, even though it may also appear elsewhere in the body of the technical report. If additional space is required, a continuation sheet shall be attached.

It is highly desirable that the abstract of classified reports be unclassified. Each paragraph of the abstract shall end with an indication of the military security classification of the information in the paragraph, represented as *(TS)*, *(S)*, *(C)*, or *(U)*

There is no limitation on the length of the abstract. However, the suggested length is from 150 to 225 words.

14. KEY WORDS: Key words are technically meaningful terms or short phrases that characterize a report and may be used as index entries for cataloging the report. Key words must be selected so that no security classification is required. Identifiers, such as equipment model designation, trade name, military project code name, geographic location, may be used as key words but will be followed by an indication of technical context. The assignment of links, rules, and weights is optional.